UNIVERSITY OF LONDON

Imperial College of Science and Technology

Physics Department

Applied Optics Section

THE DESIGN OF OPTICAL SYSTEMS WITH EXTENDED DEPTH OF FOCUS

by

FINKLER RAMI M.Sc., D.I.C.

Thesis submitted for the degree of Doctor of Philosophy of the University of London

1978

THE DESIGN OF OPTICAL SYSTEMS WITH EXTENDED DEPTH OF FOCUS

by

FINKLER RAMI

A B S T R A C T

In the design of some optical systems, depth of focus is considered to be the most important criterion of performance. For industrial lenses of the type used in copying machines, a large depth of focus is useful because it permits copying machine to be manufactured with reasonable mechanical tolerances. In cases such as this, the focal depth is determined by the longitudinal focal range maintaining a given MTF value. Typically, the cut-off frequency is of the order of 6 cycles/mm, and the required MTF is no more than 50%. Such systems are not diffraction limited and their design requires special optimisation techniques.

Previous studies of the effect of aberrations on the OTF suggest that aberration balance has a major effect on the depth of focus. The reduction of aberrations does not necessarily produce an improved depth of focus. Therefore, normal optical optimisation, which is based on the damped least squares method and incorporates a merit function which is the sum of properly weighted squared aberrations, may be found inadequate.

Possible optimisation methods for larger depths of focus may be classified into two major groups. Two stage optimisation in which a primary program is used to provide essential information such as possible target values which would be used, as a second stage, in an optimisation program. Alternatively, single stage optimisation can be carried out, either by normal optimisation, where the weighting of aberrations in the merit function is changed in an empirical way or by optimisation with a merit function which indicates directly the focal depth of the system.

This work suggests a direct optimisation technique which uses the geometrical MTF values in two defocussed image planes as a merit function. The SLAMS version 14 program is modified to perform this direct optimisation. This technique is then compared with a single plane geometrical MTF optimisation in the design of copying and reducing lenses for monochromatic and polychromatic cases.

The results are discussed and assessed in a way which indicates in which circumstances a particular technique should be used. The practical results are also compared with the theoretical cases described in earlier publications. Some suggestions are put forward as to possible further improvements in specific cases with special additional conditions.

CONTENTS

ACKNOWLEDGEMENTS

I wish to thank Dr. M.J. Kidger for supervising this work.

I would also like to acknowledge Mrs. P.M.J.H. Wormell for her invaluable guidance through the programs of the optical design group at Imperial College , for many helpful discussions and for her assistance in the writing of this thesis.

Finally, I wish to acknowledge the financial support from the B'nai B'rith, Leo Baeck (LONDON) Lodge, Scholarship Fund.

CHAPTER 1

OPTIMISATION METHODS IN OPTICAL DESIGN AND THE SLAMS PROGRAMS

1.1 Introduction to Optical Optimisation

Perfect optical systems, without aberrations, are never possible in practice. Therefore, an optimum optical design is searched for, using an optimisation program. This program changes the parameters of the lens data such as curvature separation and glasses to improve the performance of the system. The performance of the system in the optimisation program, can be judged by several methods.

Hopkins and McCarthy (1955) were concerned with the seven primary aberrations. The performance of a system was measured by the values of these aberrations, which was a simple task bearing in mind the limited number of design parameters that had been used. The main disadvantage of this method is that higher order aberrations or criteria other than primary aberrations are, sometimes, of great significance.

Glatzel (1961) used aberration tolerances as an optimum target which was detailed by Glatzel and Wilson (1968), but this method has not been widely adopted.

The most common approach is to define a "merit function" which normally is some function of the aberrations of the system, weighted according to their importance. The optimisation program actually becomes a minimisation program where the "merit function" is minimised. It follows that the merit function is very critical to the optimisation and its form is still discussed by

optical designers. Even a simple merit function will improve a system in the early stages of a design, steering the system into a region with sufficiently small aberrations. The further stages of the design need a more advanced merit function. The following section deals with some published merit functions and discusses their use in optical design.

1.2 The Merit Function

The earliest version of the SLAMS program, Wynne (1959), used a merit function, ψ, constructed from the finite ray aberrations. Calculation of ray aberrations is a relatively simple task since raytracing being a repetitive and simple algorithm is suitable for computer techniques and has been used in England by Wynne as early as 1949. The merit function is given by;

$$\Psi = \sum_i (X_i - X_{o_i})^2 W_i^2 \qquad (1\text{-}1)$$

where X_i is the aberration of the i^{th} ray, X_{o_i} is the target value for this particular aberration and W_i is the corresponding weighting factor. The two obvious limitations of this merit function are:-

a) production of good aberration balance requires considerable experience since it is dependent on the choice of aberrations and weighting factors.

b) The merit function, should be considered from the point of view of image formation, and must consist of terms directly related to the image.

However, with some experience and by trial and error, this merit function was studied and improved and the later versions of the SLAMS programs used them quite successfully.

The mathematical methods used in the optimisation procedure are clearly related to the form of the merit function.

In the literature one finds different kinds of criteria for merit functions, Gostick (1974) discussed some of them, not all of which are independent, and compared their properties in conjunction with optimisation. The considered merit functions were the following,

a) Root-mean-square image spot size

b) Minimum image spot size

c) Mean square value of the wave aberrations

d) Marèchal approximation to the Strehl ratio

e) The diffraction OTF

f) The geometrical OTF

g) Hopkins' approximation to the diffraction OTF

h) Hopkins' approximation to the geometrical OTF

The relations between the wavefront aberrations $w(x,y)$ and the transverse ray aberrations $\delta\xi$, $\delta\eta$ are given by;

$$\delta G = n \sin\alpha\, \delta\xi = -\partial w/\partial x \text{ and } \delta H = n \sin\alpha\, \delta\eta = -\partial w/\partial y \qquad (1\text{-}2)$$

where α is the semi-aperture angle. We may define γ as;

$$\gamma^2 = \delta G^2 + \delta H^2 \qquad (1\text{-}3)$$

which gives the r-m-s image spot size

$$\langle r^2 \rangle = \frac{1}{A} \iint_A \gamma^2 dA \qquad (1\text{-}4)$$

where A is the area of the pupil. The mean square of the wavefront aberrations is given by;

$$\overline{W}^2 = \frac{1}{A} \iint_A W^2\, dA \qquad (1\text{-}5)$$

and the Marèchal approximation to the strehl ratio is given by;

$$E = \overline{W}^2 - (\overline{W})^2 = \frac{1}{A} \iint_A W^2\, dA - \left(\frac{1}{A} \iint_A W\, dA\right)^2 \qquad (1\text{-}6)$$

The r-m-s spot size criterion provides an image consisting of a bright central region surrounded by a diffused halo. The minimisation is a reduction of the distance between the largest positive and negative transverse aberration. The maximum and minimum occur when $\partial^2 w/\partial \rho^2 = 0$, where ρ is the polar co-ordinate of the aperture. Since $\rho = 1$ at the edge of the aperture, the aberrations value will be larger, without being a differential extremum.

It has been found that criterion a does not take into account diffraction effect and therefore is restricted to cases of large aberrations relative to the wavelength λ. Criterion b is difficult to incorporate into an automatic minimisation program because of the value of the aberrations when $\rho = 1$. Criterion c has the same limitations as b, eventhough both were used in early optimisation programs. Criterion d is actually the variance of the wavefront aberration, in the Marèchal approximation the accuracy is considered sufficient for systems with strehl ratio greater than 0.8. King (1968) concluded that the approximation was valid for systems with strehl intensity greater than 0.5. Gostick (1974) shows that if used as an OTF optimising criterion Marèchals approximation is valid for systems with 20 wavelengths of high order aberrations. The diffraction and geometrical OTF were found to be valid and useful over a large range of frequencies. Both functions behave in a similar way, reaching a maximum at the same frequency. Hopkins' approximations were found to be valid only for low frequencies. This comparison is shown graphically in figure 1a.

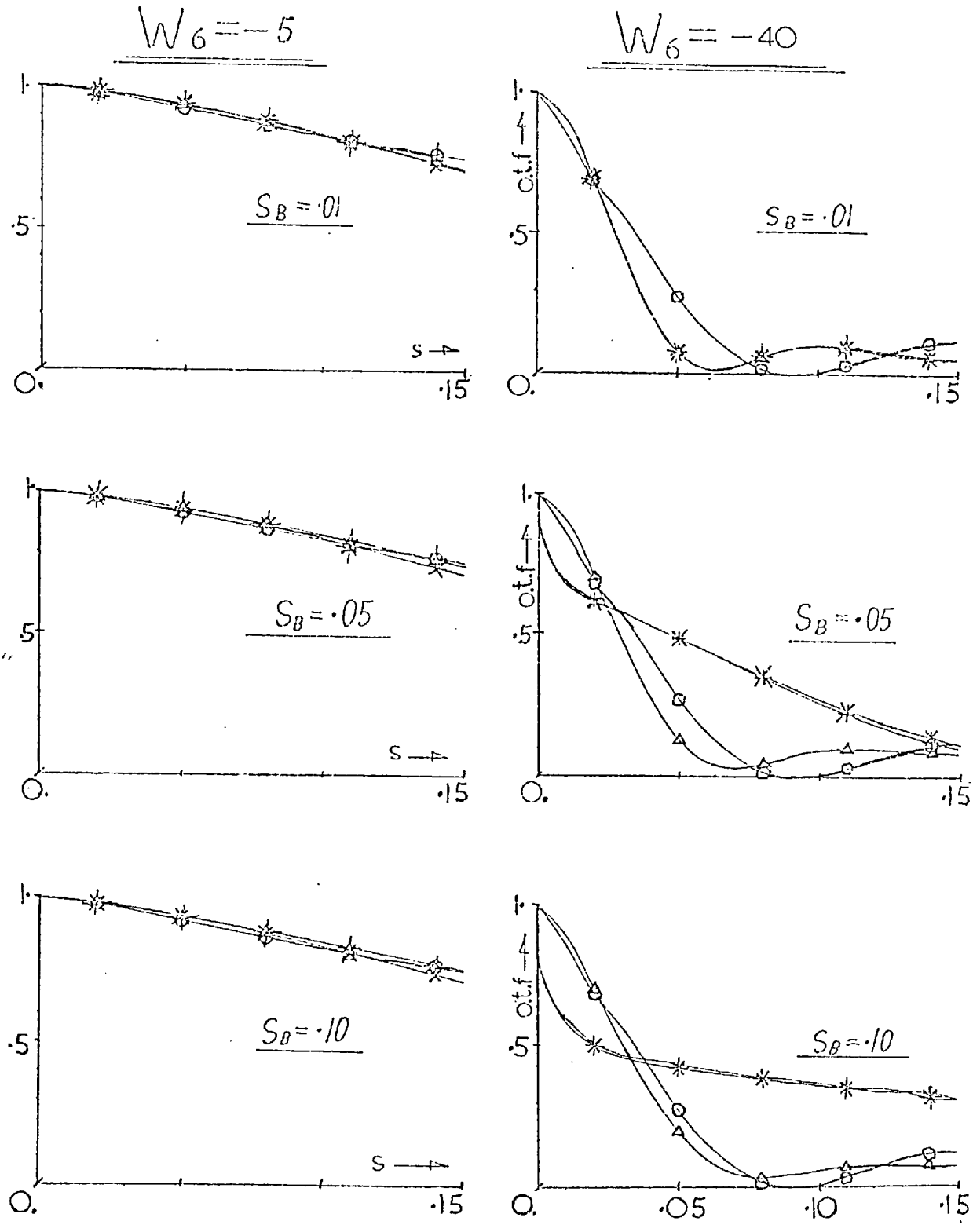

1.a 0 - Strehl ratio . ∇-Hopkins approximation

\+ - diffraction OTF , X - geometrical OTF

Comparison between the Strehl ratio, Hopkins' approximation, diffraction and geometrical OTF criteriens.

(GOSTICK 1974)

1.3 The Problem of Optical Optimisation

As described above, the optimisation process is actually the minimisation of a merit function, which is itself a sum of expressions of all the design parameters. It is assumed, in most practical cases, that over a sufficiently small range of parameter changes, the aberrations will be a linear function of the design parameters.

In a simple case of two parameters, the contour map of the merit function is as illustrated below in figure 1.b, with a minimum at point P_o and a starting point P;

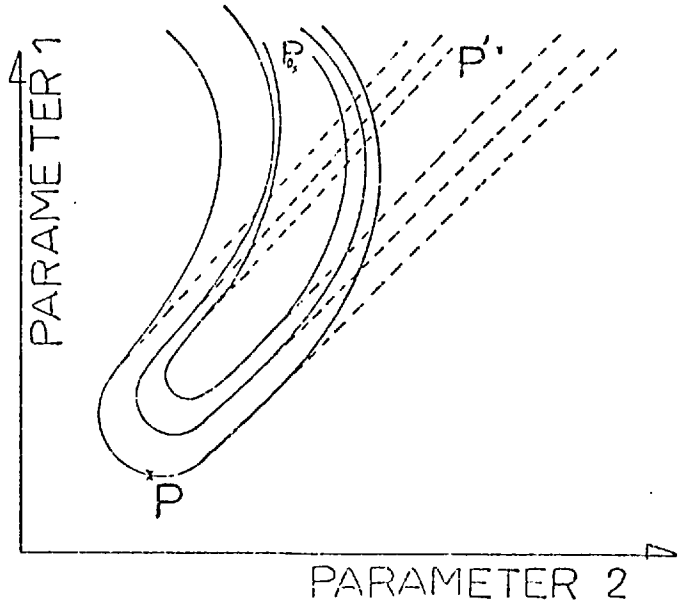

1b. Contour map of a simple merit function.

Knowledge of the aberrations and their derivatives with respect to the system parameters makes it possible to predict the shape of the contours of the merit function ψ, as shown by the dotted lines. The predicted contours suggest a minimum at P'which differs from the actual minimum at point P_o, this difference is due to non-linearities of the aberrations with respect to parameter changes, the primary aberrations make a large contribution to this non-linearity.

One of the earliest methods used in optical design optimisation was that of "steepest descent" which is basically the same as solving simultaneous equations suggested by Cauchy (1847) and which was discussed by Feder (1957,1962). If the initial design parameters are given by $x_1 \ldots\ldots x_n$ and the partial derivatives are given by $\partial\psi/\partial x_j$, then,

$$\text{grad } \psi = \left(\partial\psi/\partial x_1, \ldots \partial\psi/\partial x_n \right) \qquad (1\text{-}7)$$

A set of parameter changes $\Delta\underline{x}$ is taken, where $\Delta\underline{x}$ is a vector such that

$$\Delta\underline{x} = s \ (\text{grad } \psi) \qquad (1\text{-}8)$$

s is a scalar quantity, determining the step length. The merit function after the change is given by;

$$\psi' = \psi + \Delta\underline{x} \ (\text{grad } \psi) = \psi + s(\text{grad } \psi)^2 \qquad (1\text{-}9)$$

The parameter changes are assumed to be small enough for grad ψ to remain constant and S is chosen to reduce the merit function as much as possible, this process is repeated until the minimum is reached.

This method is ill-conditioned, since the normal to the contours will not usually point to the centre or the minimum, and because of the non-linearity, the convergence of this method is very slow. However, the steepest descent method can be modified, for example directions along a line joining alternative points can be taken, which will pass through the minimum. This method was used but without success.

The relaxation method described by Black (1955) minimises ψ with respect to one variable at a time, the poor convergence of this method was improved by using combinations of changes, but again was not successful.

The method of "least squares", first described in the context of optical design by Rosen and Eldert (1954) is of considerable interest. A set of parameter changes is computed which will, according to linear approximation, minimise ψ in one step, however, due to non-linearities as described above, it is obvious that in practical cases this will rarely happen. Rose and Eldert give an example in which the system was nearly corrected, so the required parameter changes were small, which accounts for the convergence found.

The least squares method is modified in the "Damped Least Squares" method, as described by Levenberg (1944), Wynne (1959), Wynne and Nunn (1959) and by Girard (1958). In this at each itteration the minimised quantity is given by;

$$\psi + p^2 \sum_{j=1}^{n} (x_j)^2 \qquad (1\text{-}10)$$

where x_j are the parameter changes and p is a damping factor. A minimisation program calculates parameter changes which are proportional to the reciprocal of P. In regions with high linearity, this will

approach the ordinary least squares methods; on the other hand, in non-linear regions the p value will be larger, limiting the parameter changes to small values.

Modification of the damped least squares method is possible by using the Lagrange multipliers and combined minimisation technique as described by Hopkins RE (1961) and Spencer (1963). Using this it is possible simultaneously to minimise the sum of the squares of one set of aberrations and to correct a second set of aberrations to target values. This suggests a way of controlling the boundary conditions of a system, such as edge thickness of elements, available refractive indices and v-values of glasses, which is essential for production of practical systems.

1.4 The SLAMS Version 14 Program

The optical design group at Imperial College uses an optimisation program based on the damped least squares method, which uses the technique of Successive Linear Approximations at Maximum Step - SLAMS. The merit function, ψ, is taken as a sum of m weighted aberrations f_i, the n systems parameters are denoted by x_j. At the beginning of each iteration the program sets up a matrix of differentials, A, where

$$A_{ij} = \partial_{f_i}/\partial_{x_j} \qquad (1\text{-}11)$$

If the origin is set to the point $x_j = 0$ and the parameter changes x_j are applied within the linearity region, the aberrations f_i become f_i' where;

$$f_i' = f_i + \sum_{j=1}^{n} A_{ij}\, x_j \qquad (1\text{-}12)$$

or in the matrix notation $f' = f + A.X$.

Differentiation of ψ with respect to each of the parameters defines a vector g by;

$$g_K = \tfrac{1}{2}\,\partial^{\psi}/\partial x_K = \sum_1^n f_i\,\partial f_i/\partial x_K = \sum_1^n A_{iK}\,f_i \qquad (1\text{-}13)$$

or $g = \tilde{A}.f$ in matrix notation. At the minimum of ψ the gradient and the vector g may be set to zero.

$$g = \tilde{A}.A.X + \tilde{A}.f = 0 \qquad (1\text{-}14)$$

By including the necessary damping factor, as described above, we get:

$$g = \tilde{A}\,A\,X + p^2X + \tilde{A}\,f = 0 \qquad (1\text{-}15)$$

where p is the damping factor. The term p^2 is added to the diagonal of $\tilde{A}.A$ which controls the changes of the parameters x_j. The control of the step height in the original SLAMS program was described by Wynne (1963).

A detailed description of the SLAMS program with the features of version 11 is given by Kidger (1971). Version 14, largely written by Wormell of the IC design group is currently in use. The main improvements in version 12 and 13 were control of wavefront aberrations as well as transverse ray aberrations, boundary conditions calculations in all wavelengths and control of clear apertures. The calculation of ray aberrations in different wavelength and with glass changes, were included, in addition to the Conrady formula calculations.

Version 14 accepts systems with up to 50 surfaces including the image surface, the number of variable parameters allowed is 75 with a maximum of 50 rays. The maximum number of calculated aberrations is 150 but the maximum number of controlled aberrations and violations is 100. All surfaces may be aspherical, rotational symmetry of the system is assumed which prevents optimisation of systems with tilted or de-centred elements.

The boundary conditions include variation of focal lengths, magnification, throw, thickness, thickness of elements, asphericities, edge thickness etc. On demand a file "Punch" is produced, which has the final system parameters. Throughout this work the SLAMS version 14 is referred to as V14.

1.5 Modification Of V14 To Include MTF Values In The Merit Function

When OTF became a popular criterion for measuring the performance of optical systems, it was suggested that merit functions should include some form of OTF value but the complexity of the calculations involved prevented it from having any practical use, Kazuo Sayanagi(1961) suggested that a single figure of merit, based on the OTF , be included in the merit function, Gostick (1974) suggested adding the geometrical MTF values to the merit function, weighted as other aberrations.

The geometrical MTF was found to behave in the same way as the diffraction OTF, for systems with low aberrations in the later stages of optimisation. The real part of the geometrical OTF takes the value of $\Sigma \cos(2\pi F \delta\eta)$, where F is the spatial frequency and $\delta\eta$ the transverse ray aberration, therefore it is simple to include the geometrical MTF in the merit function. The assumptions made are that the sum is over a sufficiently large number of rays with the appropriate distribution over the pupil and that the imaginary part is negligible over the frequency interval in question so that the real part of the geometrical OTF is actually the geometrical MTF. Normally we assume that if the target values of transverse ray aberrations are zero we get;

$$\Psi = \sum_j W_i^2 f_i = \sum_i W_i^2 \delta\eta_i^2 \qquad (1\text{-}16)$$

but if instead of transverse ray aberrations we consider geometrical MTF components, we can replace $\delta\eta$ by Sin $(\pi F\delta\eta)$ in the region where $|\delta\eta| < \frac{1}{2F}$, and the modification to the existing program is minimal. By minimising a sufficiently large sum of Sin $(\pi F\delta\eta)$ terms we actually minimise the values of 2 Sin $^2(\pi F\delta\eta)$, while keeping $\delta\eta$ in the region defined above, since by simple trigonometry we get;

$$\Sigma\ 2\ \text{Sin}^2(\pi F\delta\eta) = \Sigma[1 - \text{Cos}(2\pi F\delta\eta)] \propto 1 - MTF_g \qquad (1\text{-}17)$$

where MTF_g denotes the geometrical MTF.

The theoretical maximum of the MTF is 1, hence minimisation of $1\text{-}MTF_g$ will actually maximise MTF_g, in other words the simple substitution of $\delta\eta$ by Sin $(\pi F\delta\eta)$ in the merit function maximises the geometrical MTF of the system, provided sufficient number of terms are included in the summation described by 1-17 and with the right distribution over the pupil area. Since the diffraction OTF behaves similarly to the geometrical MTF, in the above region of aberrations, the final design will have higher OTF values.

To enable V14 to accept this modification it was found necessary to increase the number of aberrations incorporated in the program to 300. The MTF is calculated using the aberrations of one half of the pupil, which was found to be sufficient due to the symmetry of the pupil MTF, and the summation described by 1-17 required the aberrations of 20 rays to give a reasonable approximation to (1-MTF). The principal ray aberrations and chromatic aberrations, as well as any aberration required by the designer, are not replaced by the MTF_g values.

The addition of the sine terms adds to the non linearity of the merit function, especially for cases where the aberrations product, $|F\ \delta\eta|$, approaches 0.5.

In such cases the derivatives with respect to any parameter become zero, the program therefore assumes that no parameter change will produce an improvement in the system. In practice one must be careful in the choice of the frequency value for optimisation, selecting a value such that the product of frequency and aberration is in the interval (-0.5;0.5). This may result in the need to run the program several times with a low frequency so as to satisfy the above condition, increasing the value gradually till the required frequency is reached. The value of the frequency chosen will depend on the maximum value of the aberrations $\delta\eta$.

In this way a direct OTF optimisation is possible, which is expensive as far as computer time is concerned, but requires less work on the part of the designer. Neglect of phase shift terms is accepted because of the fact that this program is only used in the final stages of design. Optimisation by V14 at the initial stages will result in low transverse ray aberrations which in turn keeps the phase shift fairly constant. In cases of small phase shift, the significance of the phase term of the OTF to the optical system is not fully understood.

This program which is referred to throughout this work as VGOTF, was tried on major types of lenses. This test was carried out by Gostick, who was able to improve existing designs produced by V14.

CHAPTER 2

EFFECT OF ABERRATIONS ON THE OPTICAL TRANSFER FUNCTION

2.1 The Optical Transfer Function

The Fourier analysis approach to optical imaging, initiated by Duffieux (1946), has been utilized by Hopkins (1953) to formulate a general diffraction theory of optical image formation In the case of incoherent illumination, the intensity distribution in the image of an extended source is obtained by summation of the intensity distribution in the diffraction image associated with each point in the object. If a point in the object plane has the cartesian co-ordinates (ξ,η) and α is the convergence angle of the marginal ray with the principal ray, the reduced co-ordinates of the point, u and v, are given by;

$$U = \frac{2\pi}{\lambda} n \text{ Sin } \alpha \, \xi \text{ and } V = \frac{2\pi}{\lambda} n \text{ Sin } \alpha\eta \qquad (2\text{-}1)$$

The intensity distribution of such a point is denoted by B(u,v), and primes denote the corresponding quantities in the image space. The diffraction intensity distribution is denoted by G(u'-u,v'-v) and the image intensity distribution due to the whole extended object is given by;

$$B'(u,'v') = \frac{1}{2\pi} \iint_{-\infty}^{\infty} B(u,v) \quad G(u'-u,\ v'-v)du\ dv \qquad (2\text{-}2)$$

where $\frac{\pi}{2}$ is a convenient photometric factor.

Now, G(u,'v') is given by the square modulus of the complex amplitude in the image of a point source at (0,0), that is to say

$$G(u,'v') = \left|F(u,'v')\right|^2 \qquad (2\text{-}3)$$

where

$$F(u,'v') = \frac{1}{2\pi} \iint_{-\infty}^{\infty} f(x_o,y_o) \ell^{i(u'x_o+v'y_o)} \, dx_o dy_o \qquad (2\text{-}4)$$

the function $f(x_o,y_o)$ is the pupil function, and (x_o,y_o) are the reduced co-ordinates of a point in the pupil.

If the radius of the entrance pupil is h, and a ray from an object point intersects a reference sphere, at the entrance pupil, at a point (a,b), then

$$x_o = \frac{a}{h} = \frac{a'}{h'} \quad \text{and} \quad y_o = \frac{b}{h} = \frac{b'}{h'} \qquad (2\text{-}5)$$

as illustrated in figure 2a below.

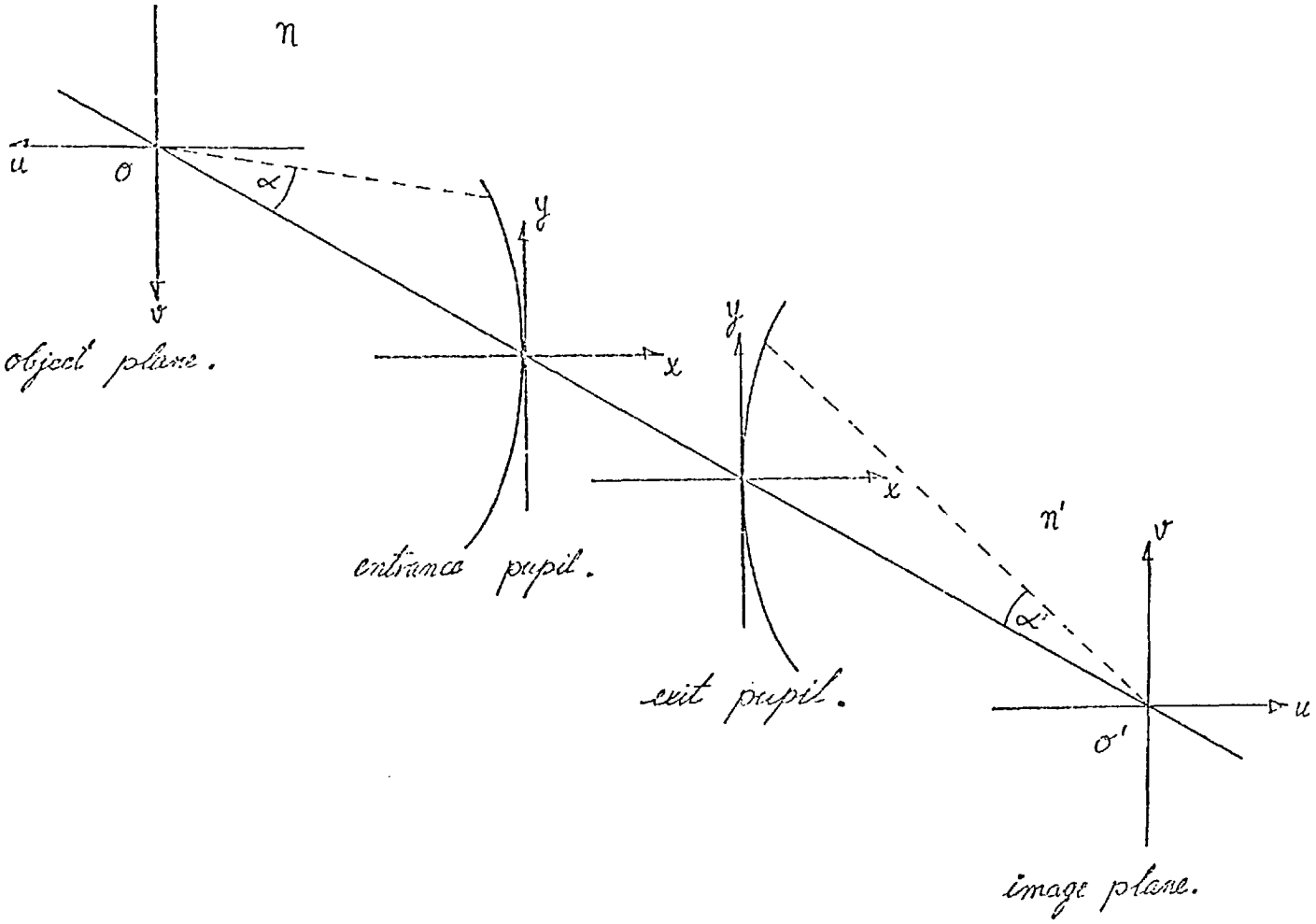

2a Co-ordinates of an optical system

The wavefront lying outside the circle $x_o^2 + y_o^2 = 1$, in the case of a circular pupil, will not be transmitted by the system, hence

$$f(x_o,y_o)=0 \quad \text{for} \quad x_o^2 + y_o^2 > 1 \tag{2-6}$$

If we represent the Fourier transform of G(u',v') by $g(s_o,t_o)$, s_o and t_o are spatial frequencies, and apply Parseval's theorm, we get;

$$g(s_o,t_o) = \frac{1}{2\pi} \int\int_{-\infty}^{\infty} f(x_o,y_o)\ f^*(x_o - s_o, y_o - t_o)\ dx_o dy_o \tag{2-7}$$

where f^* denotes the complex conjugate of f. A shift of the origin will reduce (2-7) to;

$$g(s_o,t_o) = \frac{1}{2\pi} \int\int_{-\infty}^{\infty} f\left(x_o + \frac{s_o}{2}, y_o + \frac{t_o}{2}\right) f^*\left(x_o - \frac{s_o}{2}, y_o - \frac{t_o}{2}\right) dx_o dy_o \tag{2-8}$$

If the Fourier transform of the object intensity function is denoted by $b(s_o,t_o)$, where (s_o,t_o) are the reduced spatial frequencies, we get by applying the convolution theorm,

$$b'(s_o,t_o) = b(s_o,t_o)\ g(s_o,t_o) \tag{2-9}$$

By virtue of the inverse transform relationship between B (u,v) and $b(s_o,t_o)$, the length of one period, u_o of the frequency s_o is given by $u_o s_o = 2\pi$, hence

$$u_o s_o = \frac{2\pi}{\lambda}\, n \sin\alpha\ \xi\ s_o = 2\pi \tag{2-10}$$

or

$$s_o = \frac{\lambda}{n \sin\alpha} R \tag{2-11}$$

where R is the resolution in the object.

The frequency response function $D(s_o,t_o)$ is given by;

$$D(s_o,t_o) = \frac{g(s_o,t_o)}{g(o,o)} = \frac{1}{A} \int\int_{-\infty}^{\infty} f\left(x_o + \frac{s_o}{2}, y_o + \frac{t_o}{2}\right) f^*\left(x_o - \frac{s_o}{2}, y_o - \frac{t_o}{2}\right) dx_o dy_o \tag{2-12}$$

where A=g(0,0) is a normalizing constant which gives $B(u,v)=1$ over the entire object. Throughout the above formulation isoplanatism of the optical system is assumed.

If the transparency of the pupil is uniform and the wavefront aberration function is denoted by W(x,y), the pupil function has the form

$$\begin{aligned} f(x,y) &= 0 \text{ if } X^2+y^2>1 \\ &= \exp[iKW(x,y)] \text{ if } X^2+y^2 \leq 1 \end{aligned} \qquad (2\text{-}13)$$

W(x,y) being the optical path length between the reference sphere and the emergent wavefront, KW(x,y) measures the phase advance at the point (x,y) of the reference sphere.

2.2 The Effect of Defocusing on the Transfer Function.

The effect of defocus on the transfer function, in the case of an aberration free system, was studied by Hopkins (1955). In the case of a circular aperture, the pupil function might be written as:

$$\begin{aligned} f(x,y) &= \exp[iKW_{20}(X^2+y^2)] \qquad X^2+y^2 \leq 1 \\ f(x,y) &= 0 \qquad\qquad\qquad\qquad\quad X^2+y^2 > 1 \end{aligned} \qquad (2\text{-}14)$$

The coefficient W_{20} measures the defocus by the optical path length of the intercept between the emergent wavefront and a reference sphere centred on the axial point O' of the defocused image plane, as illustrated in Figure 2.b below;

If $\delta z' = O'_o O'$, where O'_o is the true focal plane, the defocus is given by;

$$W_{20} = \tfrac{1}{2}\, n' \mathrm{Sin}^2\alpha' \cdot \delta z' \qquad (2\text{-}15)$$

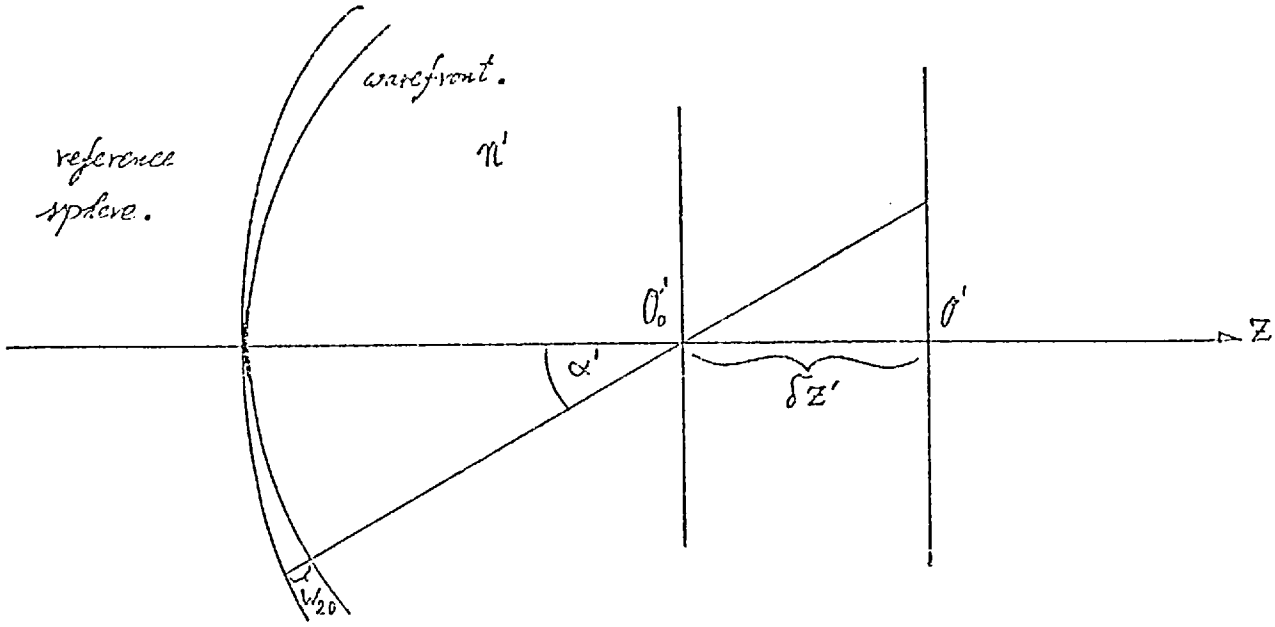

2.b - The effect of defocusing on the wavefront.

Due to the rotational symmetry in this problem, a line parallel to the v - axis was studied. B(u) and B'(u') will denote the object and image functions, their inverse transform becomes:

$$b(s) = \frac{1}{\sqrt{2\pi}} \int_{\infty}^{\infty} B(u) \cdot \exp(-ius)\,du \qquad (2\text{-}16)$$

the normalised frequency response is then given by;

$$D(s) = \frac{g(s,o)}{g(o,o)} \qquad (2\text{-}17)$$

For a normalised frequency s the integration is over the area common to two overlapping unit circles, centred at $(\pm\, {}^{s}/_{2}, 0)$, as shown in Figure 2.c below;

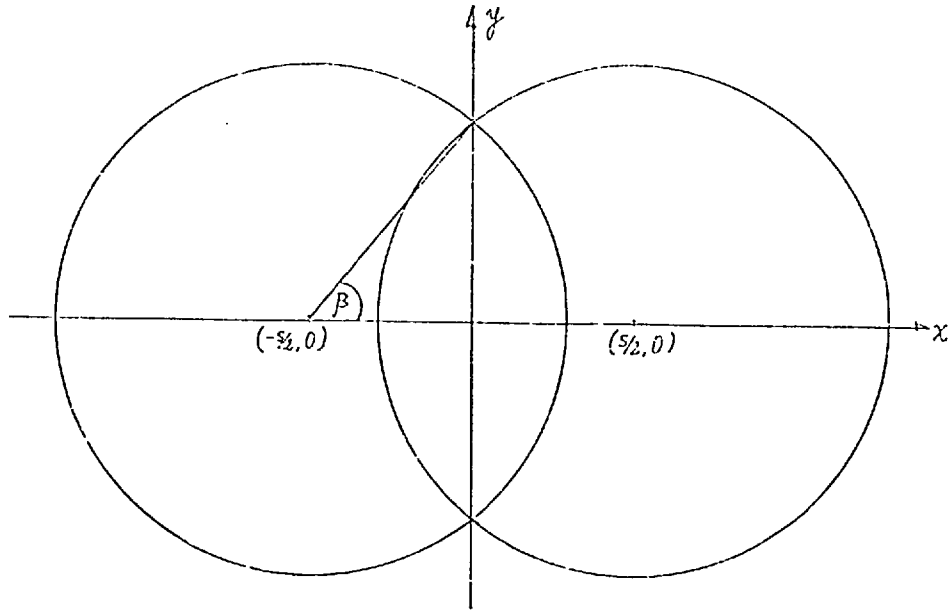

2.c - The integration area.

within which area the integration is given by;

$$\exp[iKW_{20}] \quad \{[(x + \frac{s}{2})^2 + y^2] - [(X-\frac{s}{2})^2 + y^2]\} = \exp(iax) \qquad (2\text{-}18)$$

where $a=2KW_{20}|s| = \frac{4\pi}{\lambda} \cdot W_{20}|s.|$, and therefore the frequency response function is given by;

$$D(s)= \frac{1}{\pi} \iint_{q} \exp(iax)dx\, dy \qquad (2\text{-}19)$$

where q denotes the integration area. Due to symmetry of the integration region, the integral reduces to:

$$D(s) = \frac{4}{\pi a} \int_{0}^{\sqrt{1-(\frac{s}{2})^2}} \text{Sin } a[\sqrt{1-y^2} - \frac{|s.|}{2}] \, dy \qquad (2\text{-}20)$$

By substituting $y_\beta = \sin\theta$, the integral may be expanded as follows:

$$D(s) = \frac{4}{\pi a}\cos\frac{a}{2}|s|\int_0^\beta \sin(a\cos\theta)\cos 0\,d\theta -$$

$$-\frac{4}{\pi a}\sin\frac{a}{2}|s|\int_0^\beta \cos(a\cos\theta)\,0\,d\theta \qquad (2\text{-}21)$$

By substituting $\alpha = \frac{4\pi}{\lambda} W_{20}|s|$ and β, and by expanding sin and cos in terms of Bessel functions, we get;

$$D(s)\ \frac{4}{\pi a}\cos\frac{a}{2}|s|\left\{\beta J_1(\alpha) + \frac{\sin 2\beta}{2}[J_1(\alpha) - J_3(\alpha)] - \frac{\sin 4\beta}{4}\cdot\right.$$

$$\left.\cdot[J_3(\alpha) - J_5(\alpha)] + \ldots\ldots\ldots\right\} -$$

$$-\frac{4}{\pi a}\sin\frac{a}{2}|s|\left\{\sin\beta\,[J_0(\alpha)-J_2(\alpha)] - \frac{\sin 3\beta}{3}[J_2(\alpha)-J_4(\alpha)] + \right.$$

$$\left.\frac{\sin 5\beta}{5}[J_4(\alpha)-J_6(\alpha)] \ldots\ldots\right\} \qquad (2\text{-}22)$$

These series are convergent and convenient for numerical evaluation.

Using the above sum, Hopkins calculated frequency response curves for defocus values of $W_{20} = \frac{N}{\pi}\lambda$, N taking values from o to 60. The largest N represents a defocus of $W_{20} = \pm 19.1\lambda$. The results were plotted as curves of the form shown in Figure 2.d.

Hopkins observed a rapid deterioration of the frequency response for higher frequencies with the introduction of a small defocus in excess of λ/π. Beyound the point $W_{20} = 3\lambda$ the effect of increasing defocus and the transmitted bandwidth, is by comparison very slow. For $W_{20} = 3\lambda$ the cut off frequency is $s = 0.10$.

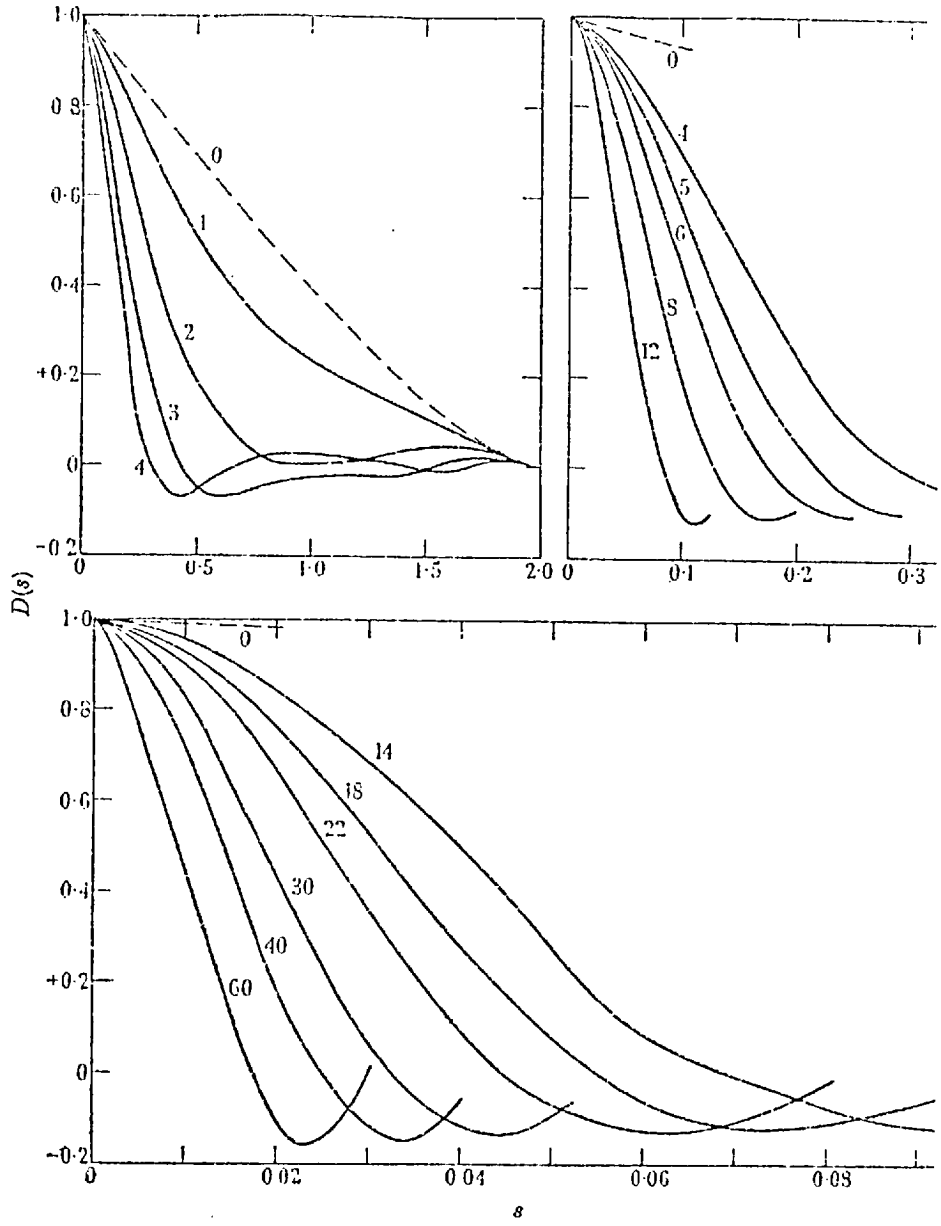

2.d. Out of focus MTF curves, the curve number relates to a defect of focus $W_{20} = n\,\lambda/\pi$. (Hopkins 1955)

The geometrical frequency response function, Dg, may be calculated with the geometrical approximations. Introduction of polar coordinates, (ρ,ψ), such that $\rho' = (u'^2 + v'^2)^{\frac{1}{2}}$ and $\Psi = \tan^{-1}(\frac{u'}{v'})$, and for $\rho' < \rho_o'$ where $\rho_o' = \frac{2\pi}{\lambda}\,(n'\sin\alpha')\,\delta\xi'\,\tan\alpha' = \frac{4\pi}{\lambda}\,W_{20}\,\sec\alpha'$, gives the following results;

$$D(s) = \frac{1}{2\pi} \int_0^{p'} \int_0^{2\pi} \exp(-ip's \sin \Psi) p' dp' d\Psi' \qquad (2\text{-}23)$$

which gives

$$Dg(s) = \frac{2 J_1(a)}{a} \qquad \text{where} \quad a = \frac{4\pi}{\lambda} W_{20}|s| \qquad (2\text{-}24)$$

this expression is valid for the region $\text{Sec}\alpha' = 1$. The first zero occurs at $a = 3.83$, giving the cut off frequency by:

$$S = \frac{0.30\lambda}{W_{20}} \qquad (2\text{-}25)$$

Hopkins compared frequency response values and cut off frequencies calculated by diffraction and geometrical formulas, as shown in Figure 2.e. below;

The error in the geometrical approximation did not exceed 2% providing $D(s) \geq 0.80$.

Hopkins gives tolerance formulas based on the above calculation. The modulation, M(s), is the ratio of the defocused and infocus frequency response values and for $M \geq 0.80$ the tolerance is given by:

$$\delta Z' = \pm \frac{0.20}{R' \sin\alpha'} \qquad (2\text{-}26)$$

Hopkins found his tolerances in good agreement with experimental results described by MacDonald (1951). He also stated that in the

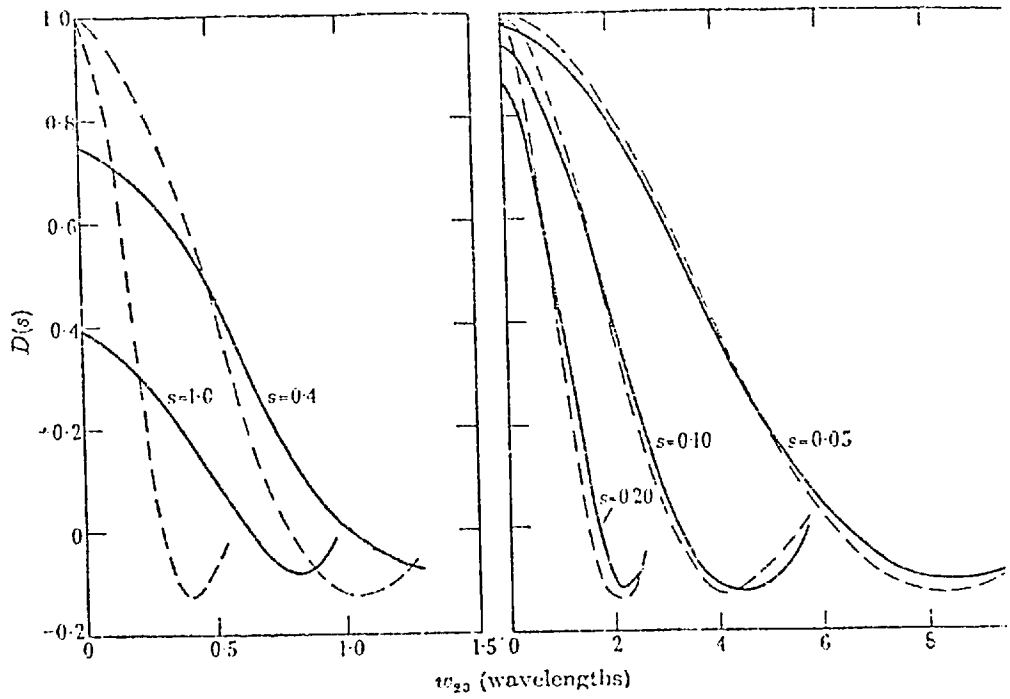

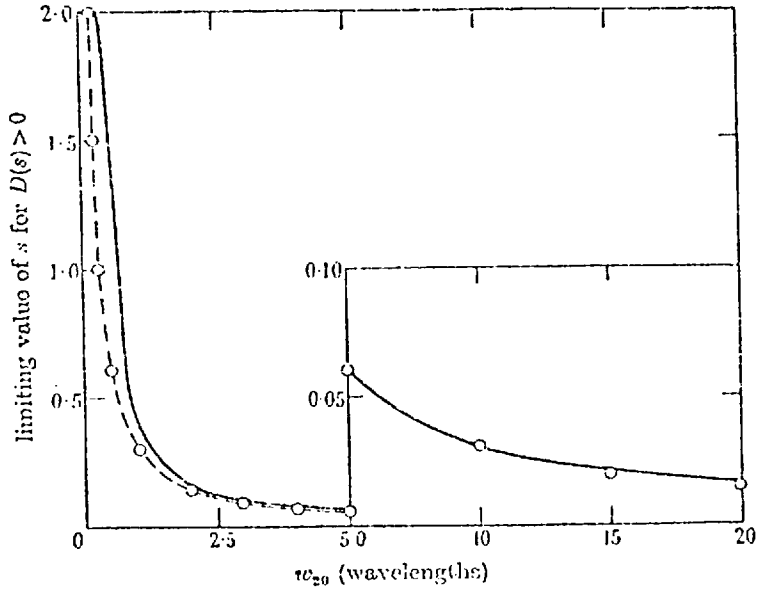

2.e - Comparison between diffraction (full line) and geometrical (dashed line) MTF and frequency band-width for the case of defocus (Hopkins 1955)

presence of aberrations the depth of focus is known to increase.

2.3 The Effect of Astigmatism on the Transfer Function.

De (1955) included astigmatism in the wavefront aberration function, in the following manner;

$$W(X_0,Y_0) = W_{20}X_0^2 + (W_{20}+W_{22})\ y_0^2 \qquad (2-27)$$

The integration area in this case is defined as the common area of two overlapping circles, as illustrated in Figure 2.f below;

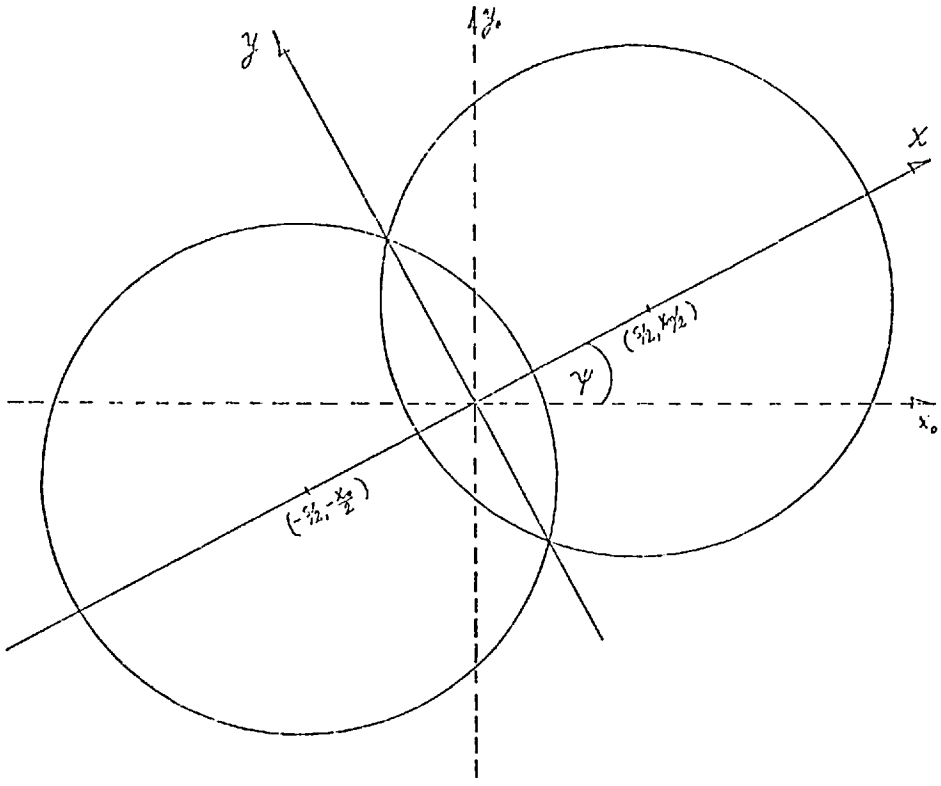

2.f The integration area.

By a similar treatment, to that of the case of defocus only, we get the following series which is convergent and suitable for numerical evaluations:

$$D(s,\Psi) = \frac{2}{P\pi}\sum_0^\infty E_n J_{2n}(q)\Big[\sum_{m=0}^\infty (-1)^m J_{2m+1}(p)\ \Big\{\frac{\sin(2m+2n+2)\beta}{2m+2n+2} + \frac{\sin(2m+2n)\beta}{2m+2n} +$$

$$+ \frac{\sin(2m-2n+2)\beta}{2m-2n+2} + \frac{\sin(2m-2n)\beta}{2m-2n}\Big\}\cos\left(\frac{ps}{2}\right) - \sum_0^\infty (-1)^m \frac{E_m}{2} J_{2m}(p)\Big\{\Big(\frac{\sin(2m+2n+2)\beta}{2m+2n+2} +$$

$$+ \frac{\sin(2m+2n)\beta}{2m+2n} + \frac{\sin(2m-2n+2)\beta}{2m-2n+2} + \frac{\sin(2m-2n)\beta}{2m-2n}\Big\}\sin\left(\frac{ps}{2}\right)\Big] \qquad (2-28)$$

where $E_0=1$ and $E_j = 2$ for $j \neq 0$, $p = 2Ks\ (W_{20} + W_{22}\ Sin^2\psi)$, $q=Ks\ Sin\ 2\Psi$ and $\beta=Cos^{-1}(\frac{s}{2})$. Transfer curves have been drawn out, for the image plane midway between the foci, for values of $W_{22}=N\frac{\lambda}{\pi}$ (N taking values between 0 and 60), as illustrated in Figure 2.g below;

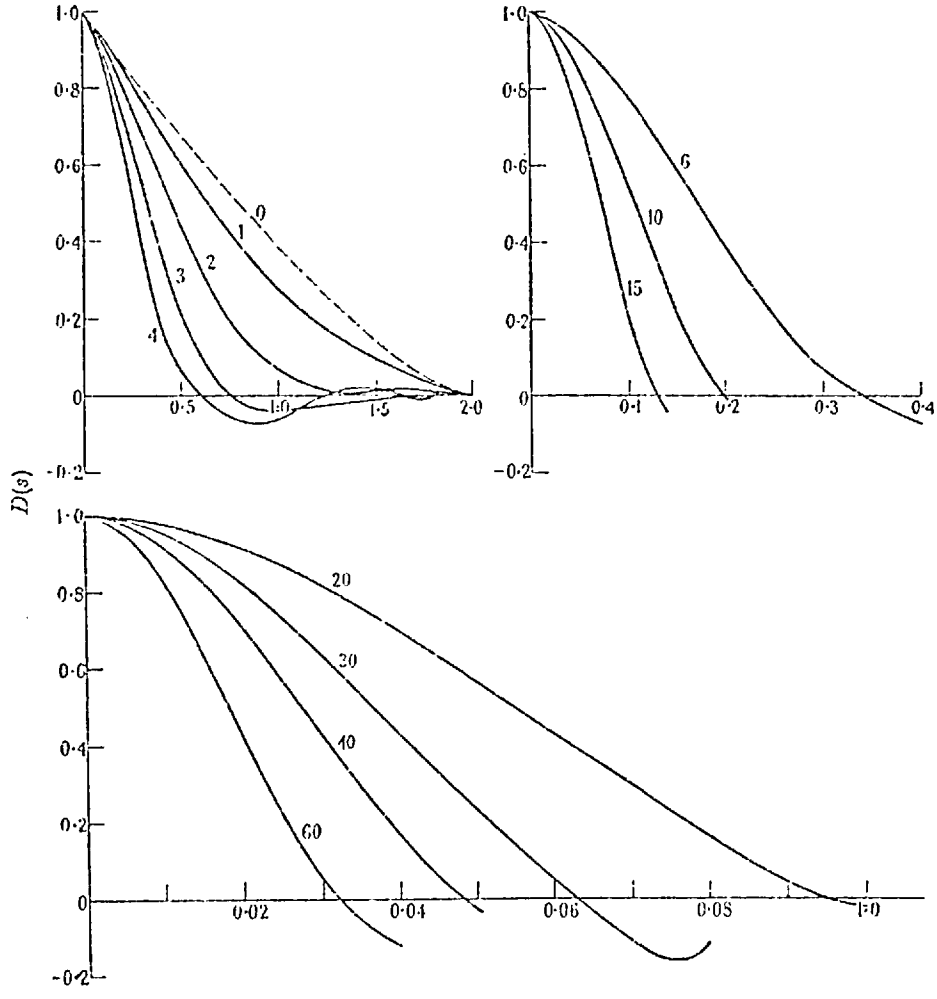

2.g - MTF MNF curves for image plane midway between sagittal and tangential foci, Curve number , n, relates to astigmatism $W_{22} = n\ \lambda/\pi$. (De 1955)

From the information produced by the above calculations, De concluded that for optical systems with S< 0.20, tests with line structures inclined at 45^0 to the tangential meridian will give

sufficient information regarding the performance of a system suffering from astigmatism.

In the same way as for the case of defocus only (Hopkins 1955), De formulates tolerances for astigmatic cases with $M(s) \geq 0.8$. The tolerance is given by;

$$\frac{2\pi}{\lambda^2}^2 \left(W_{20}^2 + \frac{1}{2} W_{22}^2 + W_{20}W_{22}\right)S^2 \leq 0.2 \qquad (2\text{-}29)$$

The above expression is maximum when $W_{20} = -\frac{1}{2} W_{22}$, which implies focusing on the mid-plane between the two foci. The tolerance in respect of this best focal plane, is then given by;

$$\frac{1}{2} \frac{\pi^2}{\lambda^2} W_{22}^2 S^2 = 0.2 \qquad \text{or by} \qquad |W_{22}| = \frac{0.20\ n' \sin\alpha'}{R'} \qquad (2\text{-}30)$$

Zeroing of Petzval curvature by astigmatism is a common practise. If S_{III} and S_{IV} are the aberration terms of astigmatism and curvature the following relations hold (Hopkins 1955);

$$W_{20} = \frac{1}{4}(S_{III} + S_{IV}) \quad \text{and} \quad W_{22} = \frac{1}{2} S_{III} \qquad (2\text{-}31)$$

Differentiating with respect to S_{III}, and equating the result to zero gives:

$$S_{III} = -\frac{2}{5} S_{IV} \quad \text{and} \quad W_{20} = -\frac{3}{4} W_{22} \qquad (2\text{-}32)$$

As in the previous cases, geometrical approximation is possible. If we define P by;

$$P = (2kW_{20})^2 S_0^2 + [2K(W_{20} + W_{22})t_0]^2$$

the geometrical transfer function becomes:

$$Dg(P, \Psi) = \frac{2 J_1(P)}{P} \qquad (2\text{-}33)$$

Comparison between diffraction and geometrical transfer functions is illustrated in Figure 2.h, below;

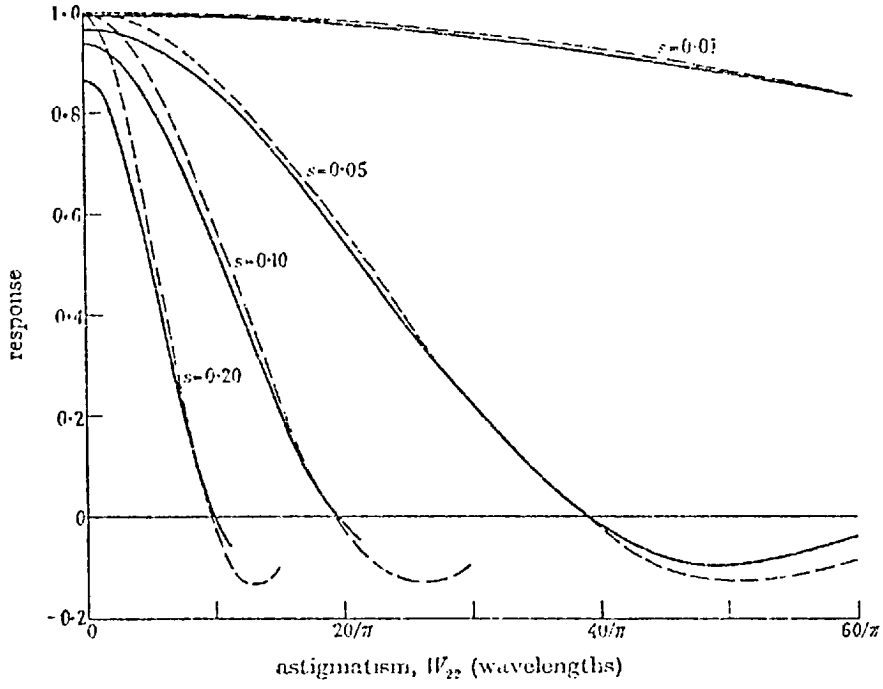

2.h - Comparison between diffraction (full line) and geometrical (dashed line) MTF curves in the case of astigmatism. (De 1955)

There is ~~no good~~ agreement between the diffraction and geometrical functions. For the case of S= 0.10, for example, the maximum deviation does not exceed 6%.

2.4. The Transfer Function in the Presence of Spherical Aberration.

Black and Linfoot (1956) studied the effect of spherical aberration on the information content of a photgraphic recording system. In this paper the effect of the aberration on the optical transfer function was studied for cases relevant to photography only. Goodbody (1958) studied the effect of a wavefront function of the form:

$$W(x,y)=W_{20}(X^2+y^2) + W_{40}(X^2+y^2)^2 + W_{60}(X^2+y^2)^3 \qquad (2\text{-}34)$$

The aberration coefficients ratio is defined as $\beta_2 = \frac{W_{20}}{W_{60}}$ and $\beta_4 = \frac{W_{40}}{W_{60}}$, where W_{60} is the secondary spherical aberration coefficient. Transfer functions were calculated for the cases where $W_{60} = -4\lambda$, -6λ, -9λ and -12λ, each with three different values of W_{40} given by $\beta_4=\beta_4'$, $\beta_4=\beta_4' \pm 0.5$, where β_2' and β_4' are the optimum values according to Hopkins (1957). The five focal planes used in this calculation were given by $\beta_2=\beta_2'$, $\beta_2' \pm 0.25$ and $\beta_2' \pm 0.5$, the results are given in series of graphs of the form shown in Figure 2.i;

Curves of the transfer function in the presence of primary and secondary aberrations were given, as shown in Figure 2.j.

Bromilow (1958) has given results based on a geometrical approximation, in which the frequency transfer is a function of SW_{60} or SW_{40} where no secondary aberrations are present, for given values of β_2 and β_4. The extent of agreement with diffraction theory can be seen from the curves, in Figure 2.k, calculated for optimum values of β_2 and β_4;

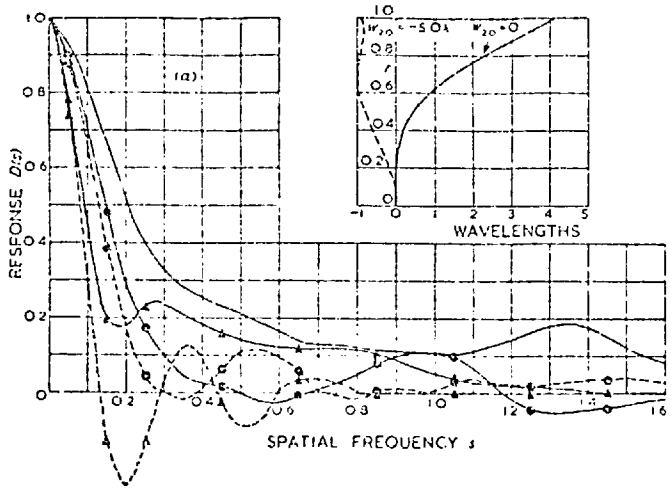

(a) $w_{60} = -4\lambda$, $\beta_4 = \beta_4' - 0{\cdot}5$.

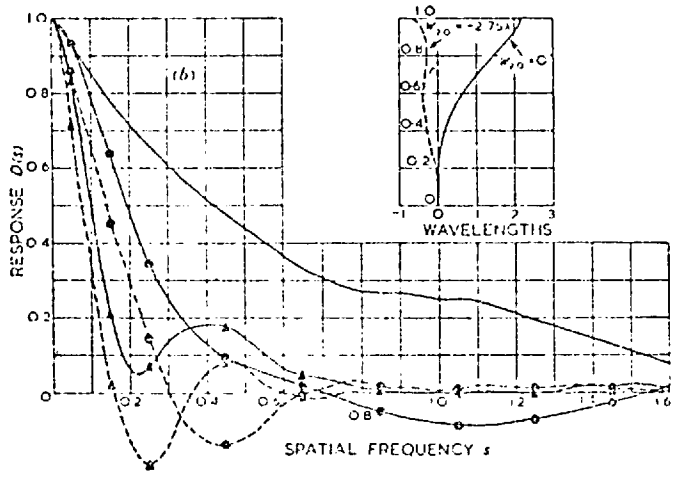

(b) $w_{60} = -4\lambda$, $\beta_4 = \beta_4'$.

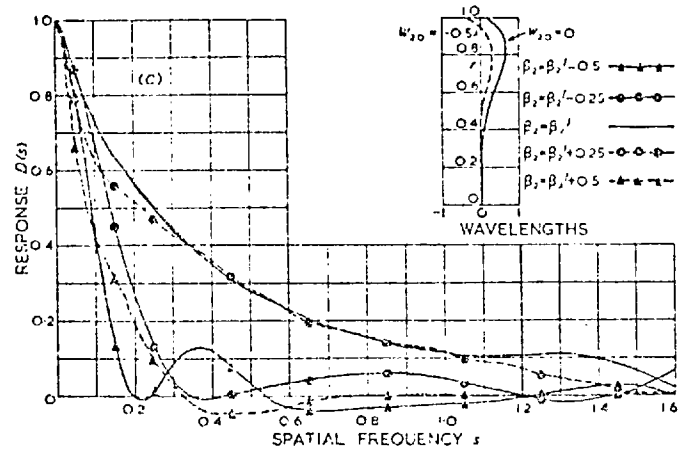

(c) $w_{60} = -4\lambda$, $\beta_4 = \beta_4' + 0{\cdot}5$.

2.i - OTF curves in the presence of spherical aberrations

(Linfoot 1956)

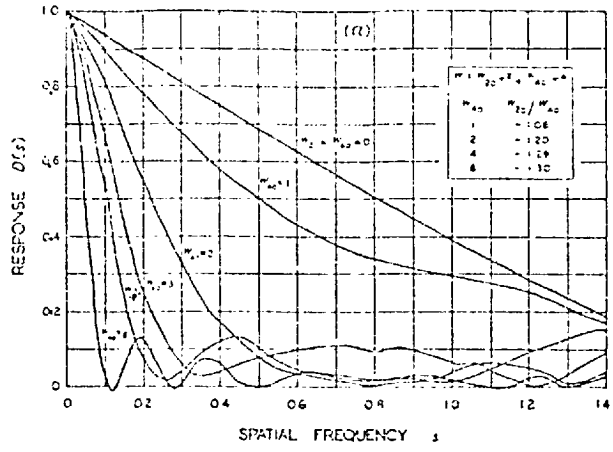

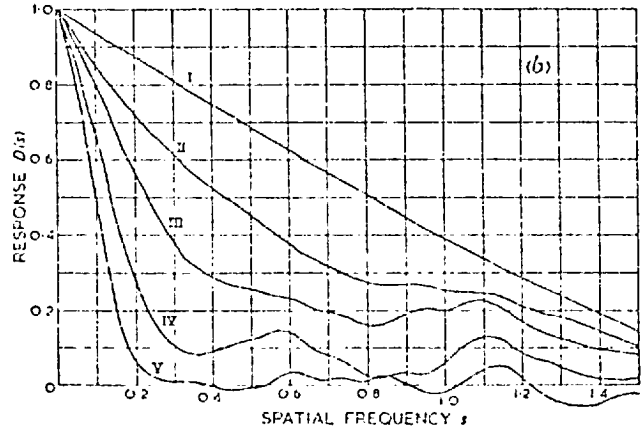

2.j - MTF curves in the best focal plane in the presence of spherical aberrations;

a. Primary spherical aberration

b. Primary and secondary spherical aberration

I $W_{60}=W_{40}=W_{20}=0$

II $W_{60}= -4; W_{40}=6.13; W_{20}= -2.75$

III $W_{60}= -6; W_{40}=9.78; W_{20}= -4.53$

IV $W_{60}= -9; W_{40}=15.24; W_{20}= -7.24$

V $W_{60}= -12.; W_{40}=20.66; W_{20}= -9.05$

(Linfoot 1956)

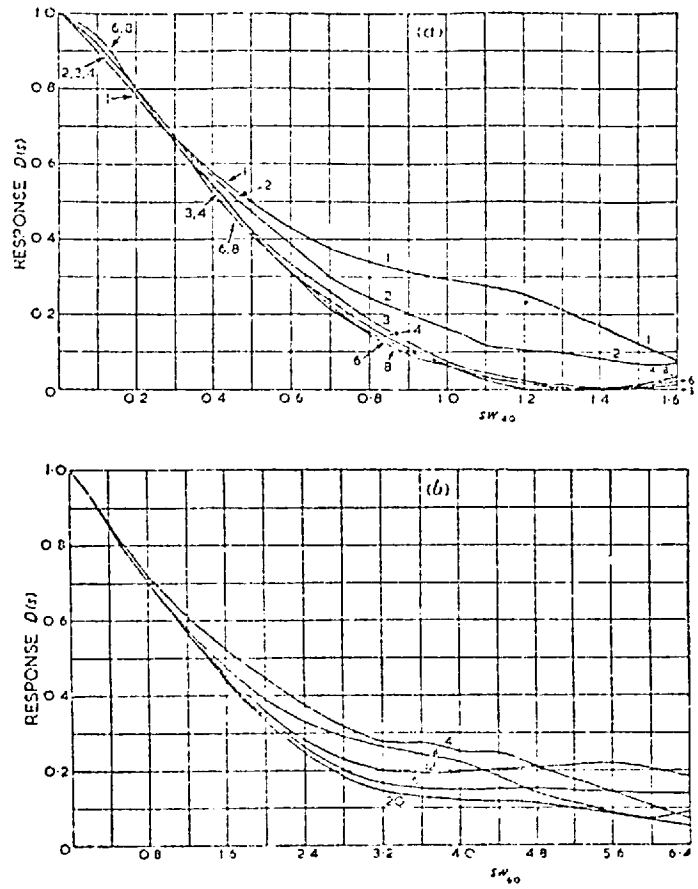

2.k - a. MTF in the presence of primary spherical aberration plotted as a function of SW_{40} - the number on the curve denotes the value of W_{20} in wavelength. W_{20}/W_{40} = 1.06.

b. MTF in the presence of primary and secondary spherical aberration plotted as a function of SW_{60}. β_2= 0.69 β_4= 1.53.

(Linfoot 1956)

2.5 Transfer Function for Optical Systems with Coma.

De and Nath (1958) calculated the frequency response function for systems with primary coma; comparison of the diffraction theory calculation which leads to a double series of Bessel functions with a geometrical approximation were given, in the form of curves of the

form shown in Figure 2.1 below;

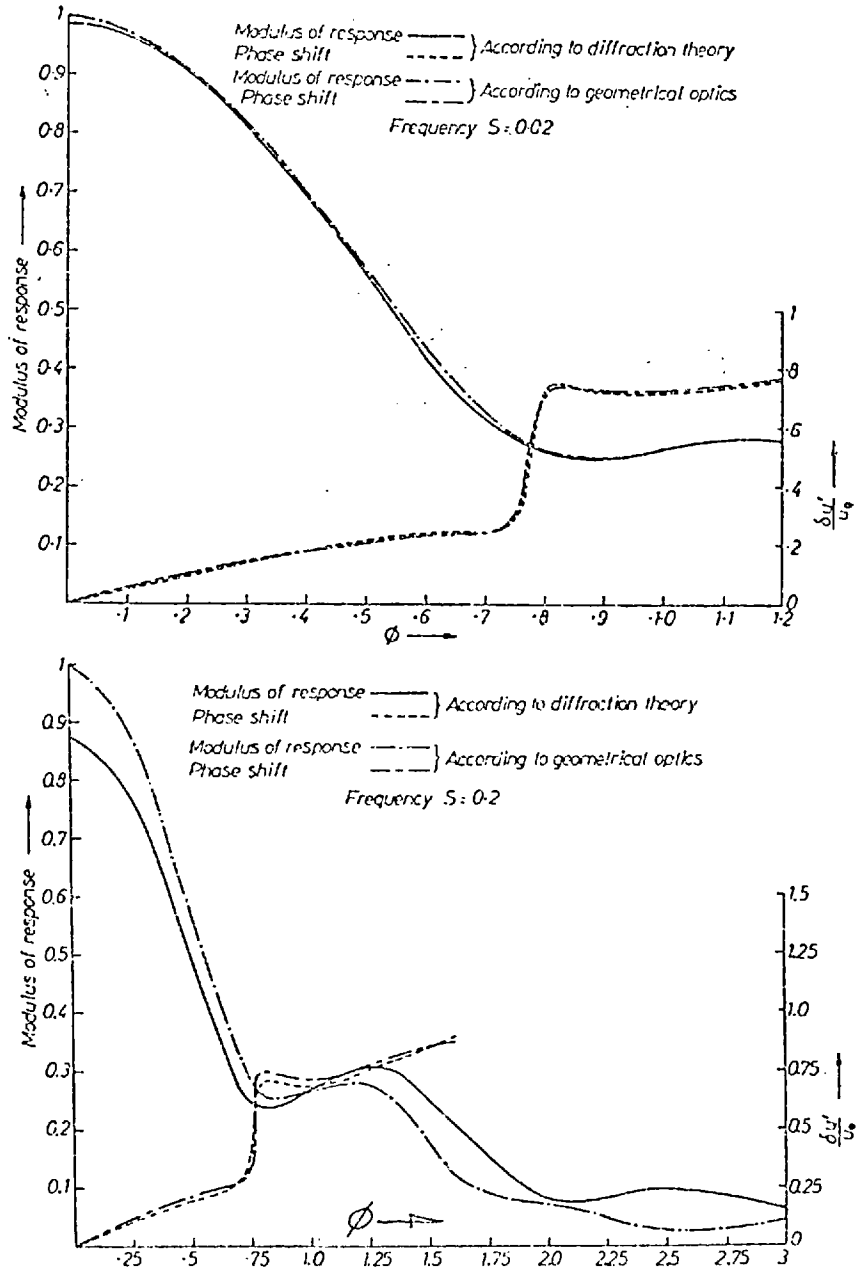

2.1 - Comparison between diffraction and geometrical OTF. (De and Nath 1958)

Goodbody (1959) studied the more general case where the wavefront aberration function included secondary coma, in the form;

$$W(x,y)=W_{20}(x^2+y^2)+W_{31}(x^2+y^2)(Y\cos\psi+X\sin\psi)+W_{51}(x^2+y^2)^2(Y\cos\psi+X\sin\psi) \quad (2\text{-}35)$$

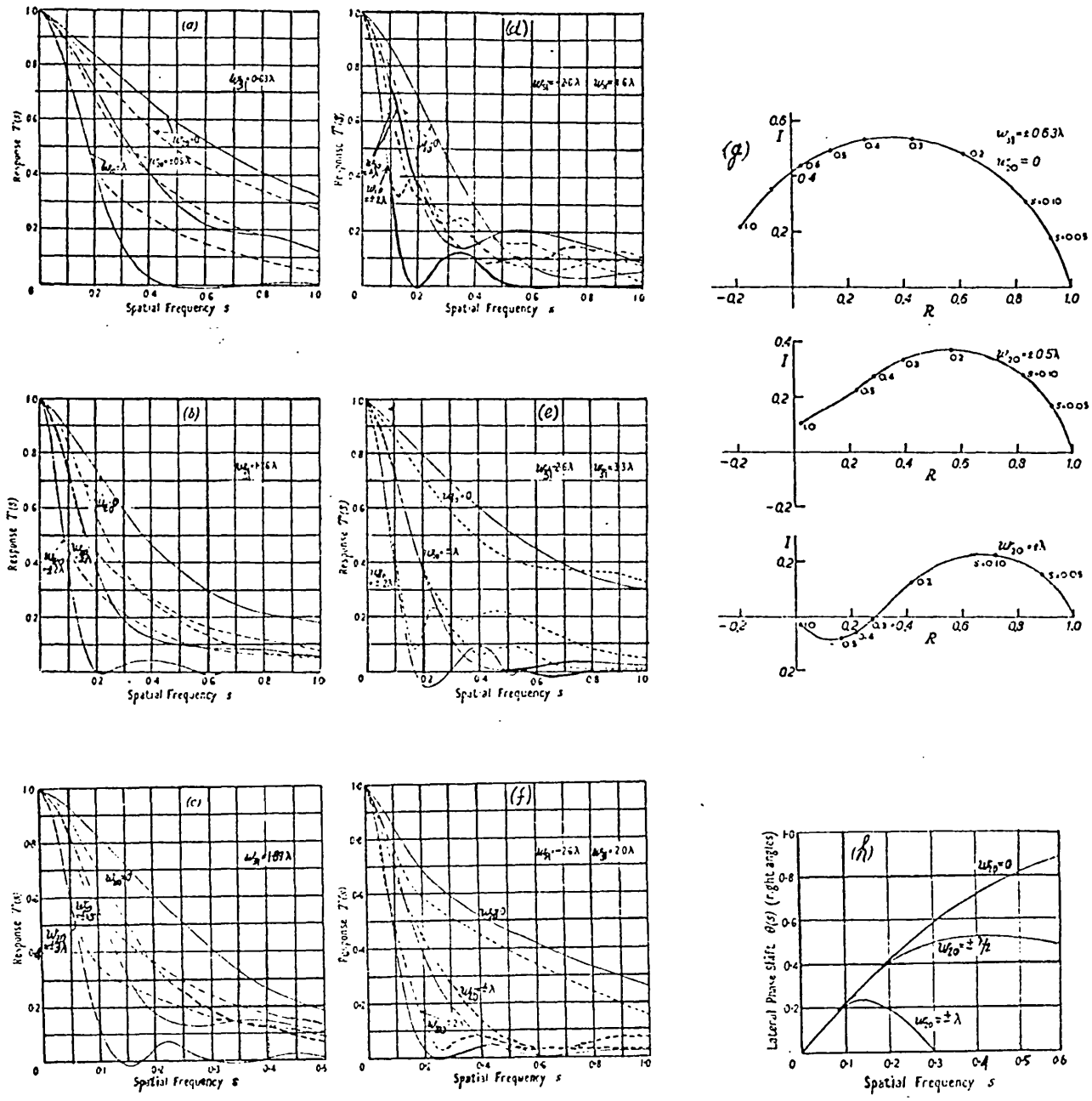

2.m - (a) - (f) MTF curves in the presence of coma, the full line corresponds to the sagittal azimuth and the dashed line to the tangential azimuth.

(g) shows the OTF on an Argand diagram, the numbers indicate the value of the spatial frequency s at the point.

(h) shows the lateral phase shift for W31=± .63λ

(Hopkins 1957)

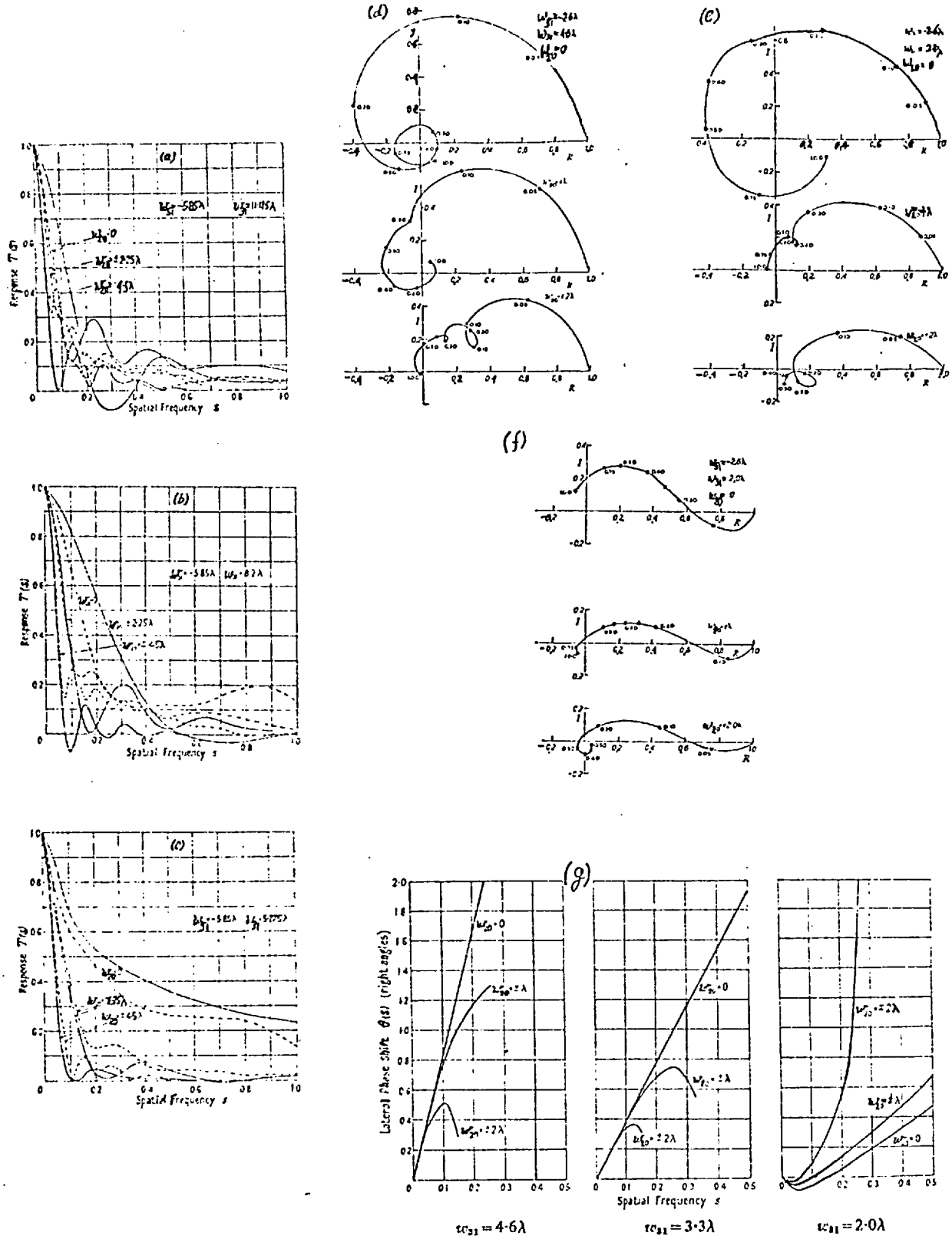

Figure 2.n - (a) - (c) MTF in the presence of primary and secondary comma, the full line corresonds to the sagittal azimuth and the dashed line to the tangential azimuth.

(d) - (f) OTF in the presence of comma, on the Argand diagram.

(g) The lateral phase shift for $W_{51} = 2.6$

(Hopkins, 1957)

where ψ is the angle of the line structure to the meridian plane of the optical system, giving the radial case when $\psi=0$ and the tangential case when $\psi = \pi/2$. The aberration coefficients were expressed by means of the ratios $\beta_{23}=\frac{W_{20}}{W_{31}}$, $\beta_{25}= \frac{W_{20}}{W_{51}}$ and $\beta_{35}= \frac{W_{31}}{W_{51}}$, the value of β_{35} corresponds to the optimum suggested by Hopkins (1957). Results for primary aberration alone, were represented in the form of graphs as shown here in Figure 2.m, ~~below~~;

For the cases where W_{51} was included the functions were of the form shown in Figure 2.n.

It was found that with negative values of W_{51} the relative phase shifting of frequency components within the image has no appreciable effect on the image quality in the cases considered when this negative secondary coma is compensated by a suitable, numerically large, positive primary coma ($W_{31}+ W_{51} > 0$).

CHAPTER 3

'DEPTH OF FOCUS' OF OPTICAL SYSTEMS

3.1 Definition of the 'Depth of Focus'.

The 'Optical Transfer Function', or the OTF, is a complex function, its modulus is known as the 'Modulation Transfer Function' or as the MTF. The arguemnt of the OTF is known as the phase transfer function.

The optical systems discussed in this work are not diffraction limited, and are designed for low frequencies, typically between 5 and 10 cycles per mm. The modulation of the image should be above a specified target value, being in the range 35 - 45 percent. For such systems, an MTF value of 80% has no advantage over an MTF value of 75%.

For optical systems of this nature we define the 'Depth of Focus' as the longitudinal defocus distance for which the MTF of the system is above the limiting target. At the same time, the OTF should remain larger than the target inside this focal range defined by the DOF ("Depth of Focus") of the system. The best way to investigate the DOF is to study the MTF as a function of normalised frequency and of defocus. For a given system it is much more convenient to study the MTF as a function of defocus, by freezing the frequency at its practical value of interest.

For a practical real optical system, one calculates different MTF functions for the sagittal and tangential planes. It follows that the DOF will be defined as the longitudinal defocus range for which both the sagittal and tangential MTF are simultaneously above the limiting value. In practice MTF values are calculated at several field angles, resulting in two separate MTF curves, for the two azimuths, for each field angle. If an optical system is to be used in more than one wavelength, the above process is repeated for each wavelength. The DOF is then defined as the longitudinal defocus range, for which the MTF in any field angle, direction of lines (normally only the sagittal and tangential directions are sufficient) and wavelength used by the system is above the limiting value.

The rest of this chapter describes the DOF for systems with limiting MTF values of 40%. Some of the results that follow have been obtained from the studies described in the previous chapter, the rest are from a previous work (Finkler, 1975) which studied optical systems with low frequencies and 40% MTF as the target value.

3.2 'Depth of Focus' of the Optical Systems in Chapter 2

In Chapter 2, the general discussion did not refer to specific systems, thus reduced or normalised frequencies were used. In this section the DOF is described for a particular optical system with the following properties. The numerical aperture of the system is 0.04464, the resolution is 10 line pairs per mm, and the wavelength is 0.0005 mm (a monochromatic system is considered). This system has a normalised frequency S=0.112 in air, as given by equation 2-11. The limiting MTF value is 40% and the magnification is unity. These are the characteristics of a copying lens with f/5.6, suitable for a typical office photocopying machine.

From Hopkins (1955), the effect of defocusing on an aberration free system can be obtained, as illustrated in Figure 3.a below;

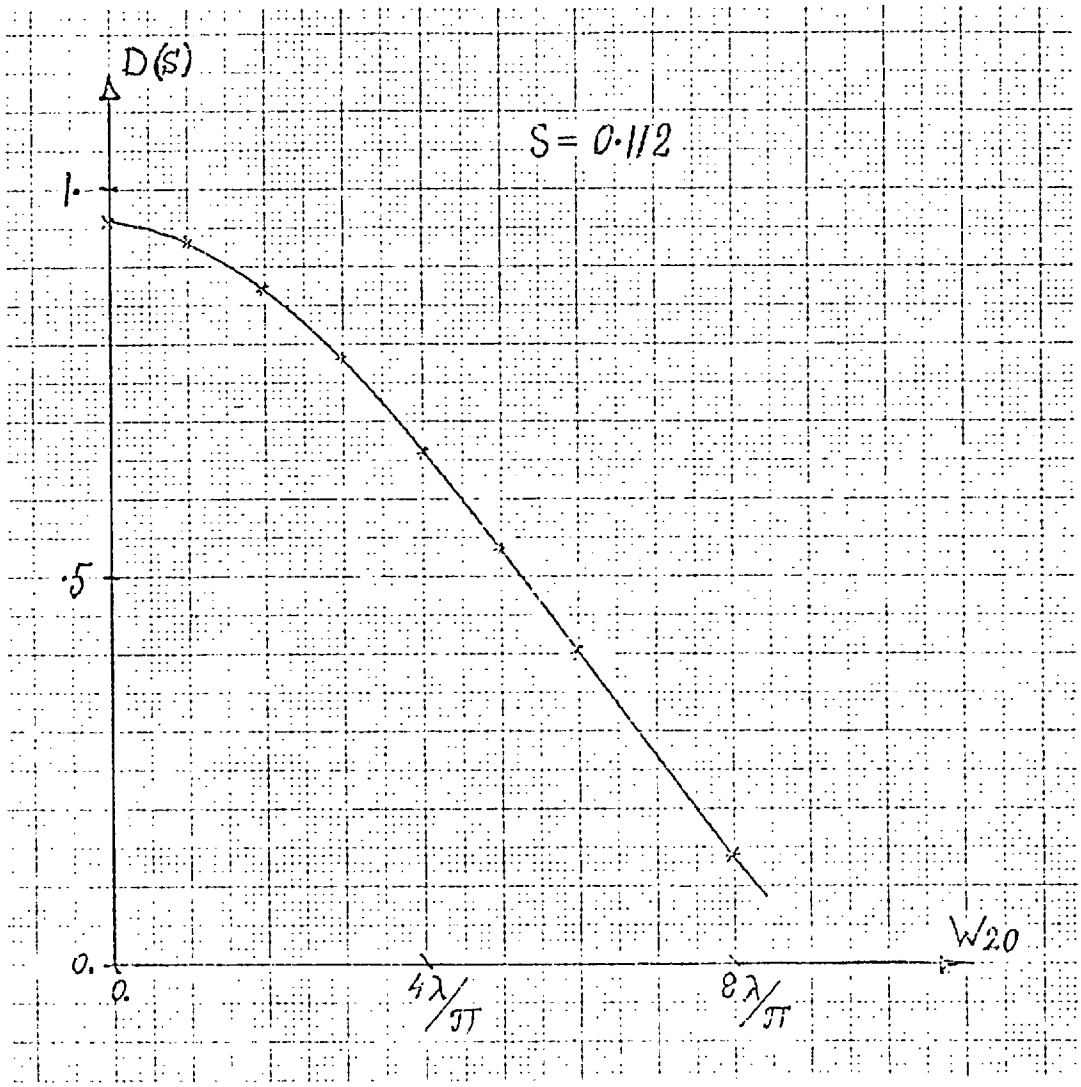

3.a - The effect of defocusing on the MTF.

In this aberration free system, the MTF reaches 40% at $W_{20} = \frac{6\lambda}{\pi}$ for which the longitudinal defocusing is given by equation 2-15, yielding $\delta z' = N \times 0.1597$ mm; The DOF in this symmetrical case, is given by DOF=12x0.1597=1.92 mm. At the edge of the DOF range the geometrical MTF value is about 10% below the diffraction theory value.

From the results described by Goodbody (1958) the effect of primary and secondary spherical aberrations on the DOF can be seen, as illustrated in Figure 3.b:

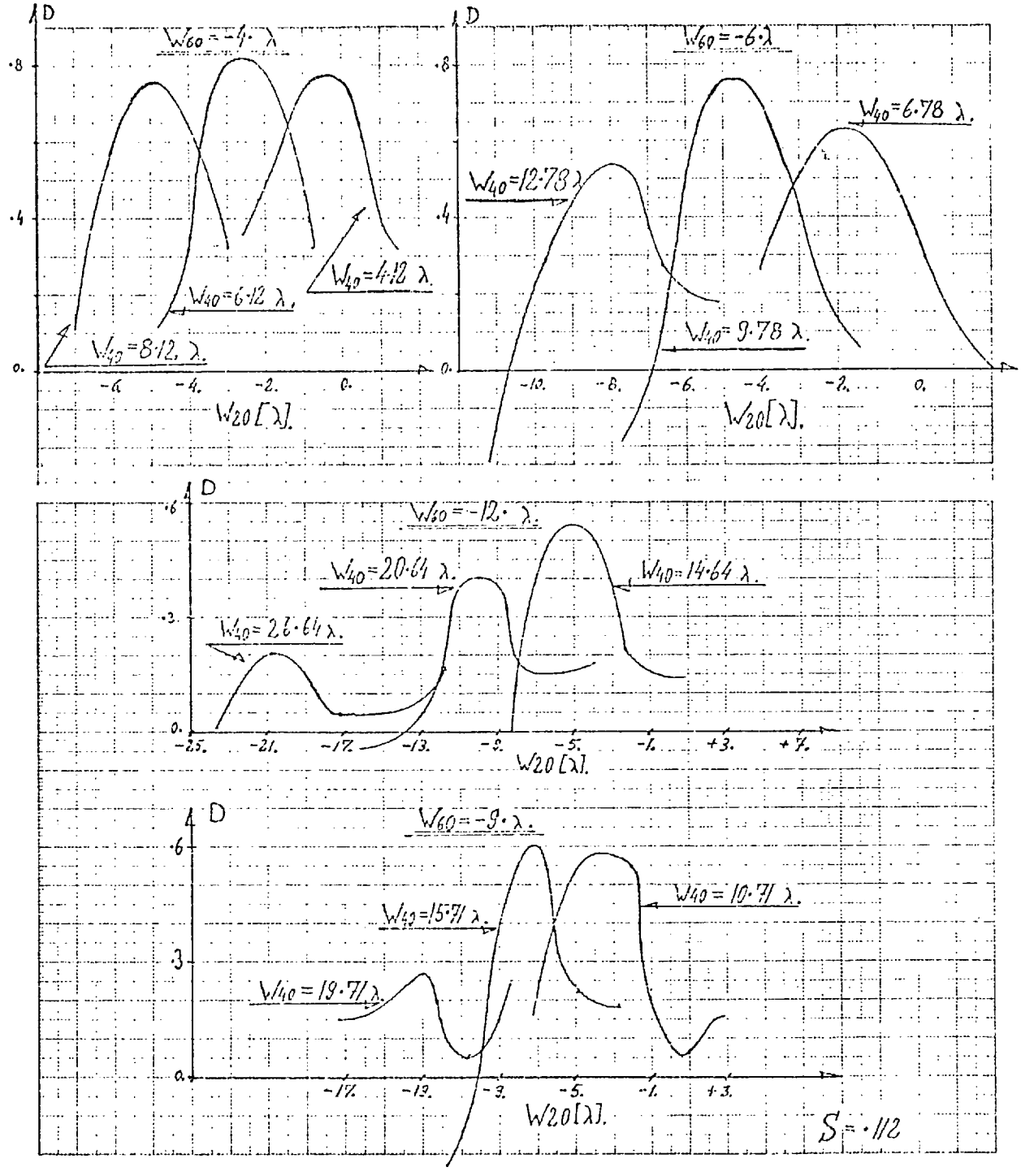

3.b - depth of focus in the presence of spherical aberrations.

It can be seen that when W_{60}=-4λ and W_{20} takes values between 4 and 8 wavelengths, the DOF remains approximately the same (about 3.5λ), the main difference is found to be a drop in the maximum response. In the presence of W_{60}=-6λ, a similar DOF can be achieved by a correct aberration balance as illustrated by the cases where W_{40}= 6.78 and 9.78 wavelengths, but if the primary spherical aberration is increased to W_{40}= 12.78λ, the DOF is reduced to approximately 2λ. Even in the presence of secondary spherical aberrations of W_{60}= -9λ the DOF is kept well above 1.5λ by values of W_{40} between 10 and 20λ. No DOF can be measured when W_{60}=-12λ since the response curve did not rise above 40%.

The effect of non-symmetrical aberrations on the DOF of the above system can be seen from Goodbody's (1959) work which studied the case of coma. This case might be regarded as of minor interest when considering copying lenses, since coma does not occur in symmetrical lenses. However, it is of interest once reducing systems and copying systems capable of conversions to reducing systems are included. The results are now discussed in the sagittal and tangential planes.

In the case of primary coma, the following results were illustrated in Figure 3.c;

From Figure 3.c it can be seen that even though W_{31} was increased by a factor of 3, from .0.63 to 1.89λ, the DOF remained in the region of 3.5λ. The limiting direction, in all cases, was the sagittal azimuth where ψ=0. In this case one should consider the lateral phase shift. For example, where W_{31}=0.63λ, the lateral phase shift for all W_{20} values used in the calculations was found to be θ=.22.

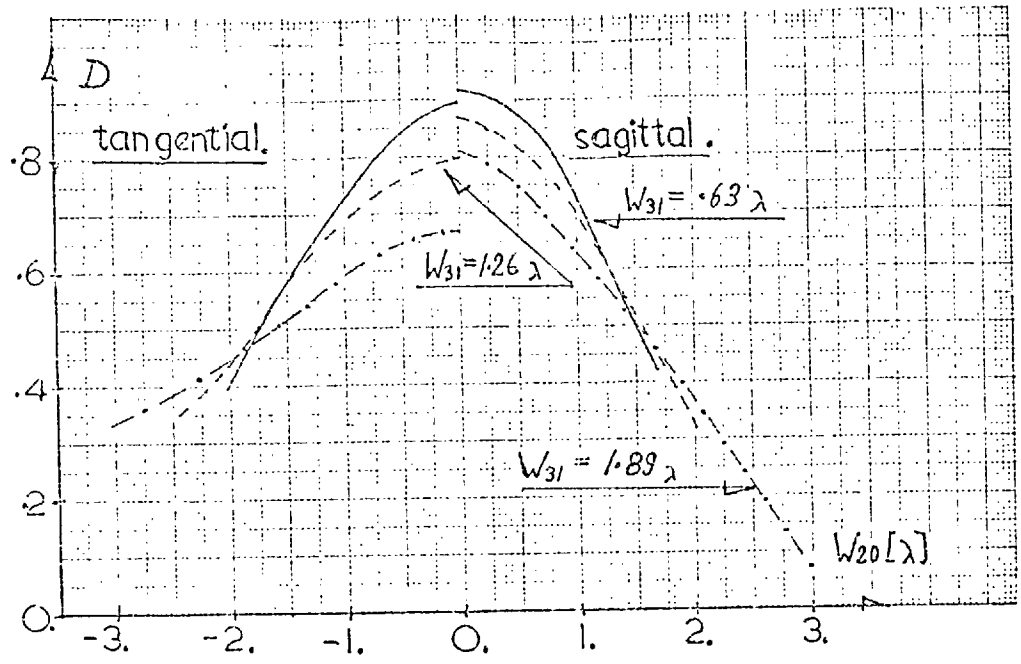

3.c - depth of focus in the presence of primary coma.

This may cause contrast reduction, especially at the edges of the DOF range and may reduce the range of the DOF.

When secondary coma was also included, the results were illustrated in Figure 3.d below; The additon of secondary coma made it possible to improve the DOF, by correct balancing of aberrations. For values of W_{51} between -2.6 and -7.8λ it was possible to maintain a DOF of 3.6λ. The values of W_{31} required for this balance, were in the range of 4 to 7 wavelengths. In this case, the tangential azimuth was the limiting direction. For higher aberrations the effect of the lateral phase shift should be considered, especially in view of the fact that it varies with defocus. The following table gives some values for the lateral phase shift in the case of W_{51} = -2.6λ.

W_{31}	W_{20}		
	0	$\pm\lambda$	$\pm 2\lambda$
4.6λ	.90	.82	.50
3.3λ	.40	.40	.35
2.0λ	-.05	.00	.12

Lateral Phase Shift for Defocused Image $W_{51} = -2.6\lambda$.

As one would expect, the lowest phase shift results in higher response and hence higher DOF. Figure 3.d confirms this argument, the DOF increased by 10% when W_{31} was decreased from 4.6 to 2.0λ for the case where $W_{51} = -2.6\lambda$.

The data described above, which was obtained from the work mentioned in chapter 2, gives some idea about the characteristics of DOF with respect to aberrations. The results are limited in their practical use, related to the increase in DOF, since the aberrations were balanced so as to produce the highest response in a given image plane.

3.3. Effect of Aberrations on the 'Depth of Focus'.

A previous study (Finkler, 1975) was concerned with the effect of aberrations on the DOF, as defined in this context, and may give a better idea of the characteristics of the DOF. This work has been concerned with the design of a system capable of sending 5 cycles per mm, with limiting response values of 40%, and normalised spatial frequency of 0.05, all aberrations values were given in wavelength units.

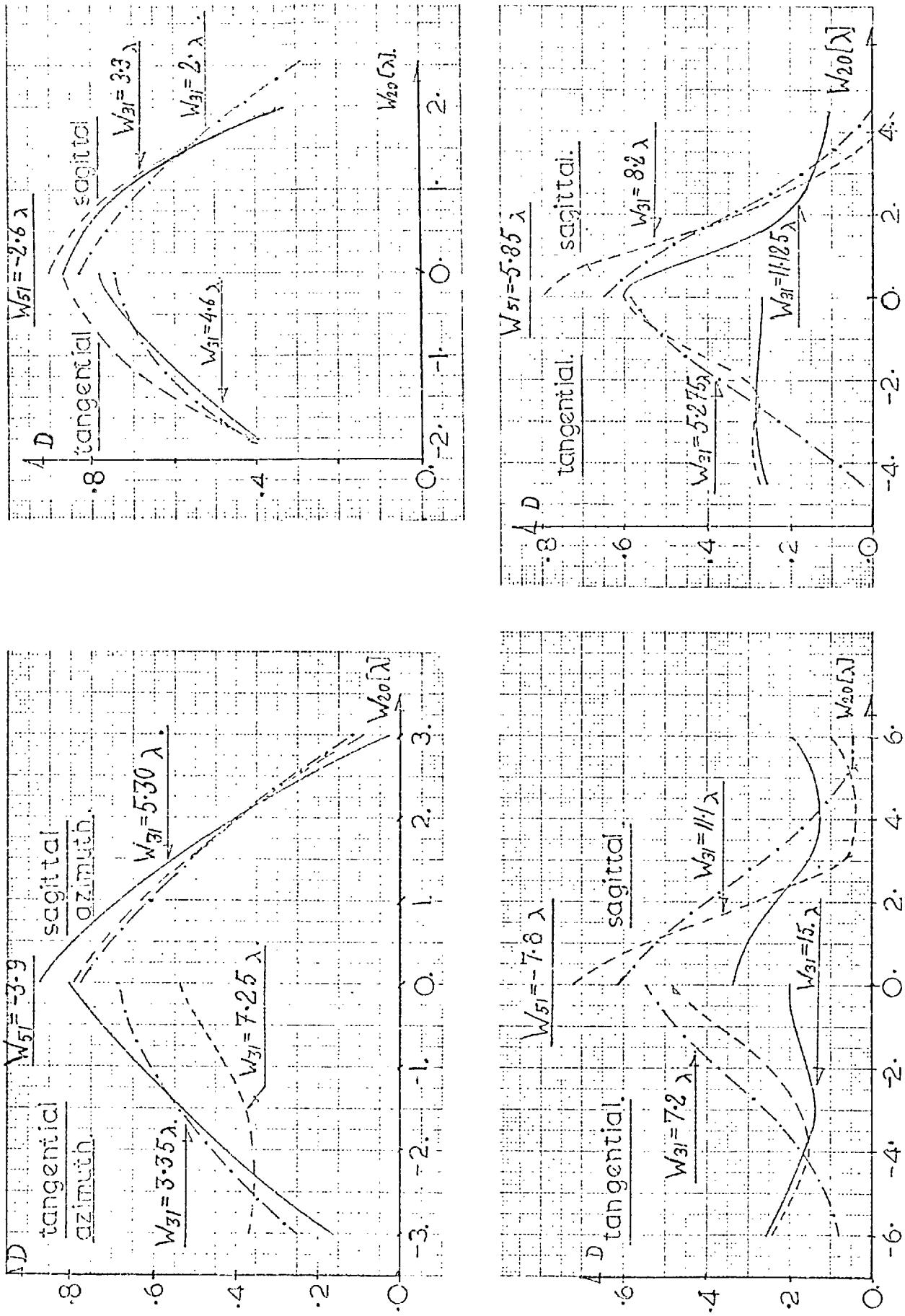

Figure 3.d - depth of focus in the presence of primary and secondary coma.

Considering cases with single aberrations gives the following results ; In the presence of W_{22}, which was not included in the previous section, the DOF range remained the same when the aberrations were increased. The main effect was that of shifting the DOF range which is the same as finding the best focal plane for changed aberrations. The DOF range was 7λ of W_{20} and remained unchanged when W_{22} was increased up to 12λ, which was the largest aberration value studied, as illustrated in Figure 3.e below;

In the case of primary spherical aberration, the DOF range did not change for values of W_{40} up to 8λ, and was approximately 8λ of W_{20}. On increasing the value of W_{40} to 10λ the maximum response dropped by 50%, and the DOF range was reduced to 5λ of W_{20}.

In the case of coma, the DOF remained nearly the same for W_{31} values of up to 6λ (DOF range approximately 7λ of W_{20}). For higher aberration values the tangential response dropped in the middle of the DOF range, where the sagittal MTF was above 40%, thus no DOF range was found. In the presence of secondary coma on its own, similar results were observed, and the limit of W_{51}=7λ was found for any DOF range above 40%.

The cases concerning a single primary aberration show that the DOF can be maintained over a large range of aberration values, the main effect is a drop of the maximum response. More careful study of the results show that in some cases addition of other aberrations results in increased DOF.

Systems of practical interest are likely to suffer from combinations

3.e - depth of focus, in the tangential azimuth in the presence of W_{22}.

of primary and secondary aberrations, therefore, the above results are mainly of theoretical value and these studies were followed by some more realistic cases of two aberrations combined together. The cases of interest include the combination of primary and secondary coma and the combination of primary and secondary spherical aberrations. The primary and secondary aberrations were of opposite signs which is the case in most practical systems suitable for copying lenses.

The results are in agreement with Hopkins' prediction that for a constant ratio of primary and secondary aberrations the DOF can be maintained. For example, if the relation W_{51}=-0.4566 W_{31} is kept, the DOF is of the same order, even when W_{31}=10λ. Similarly, in the case of spherical aberrations, for a ratio of W_{40}=-1.49 W_{60}, the DOF remains the same even when W_{40}= 12λ. Figure 3.f illustrates this property clearly;

Comparison of the results for systems with a single aberration with those combining two aberrations leads to the conclusion that the addition of suitable aberrations in a balanced way, may appreciably increase the DOF of the optical system.

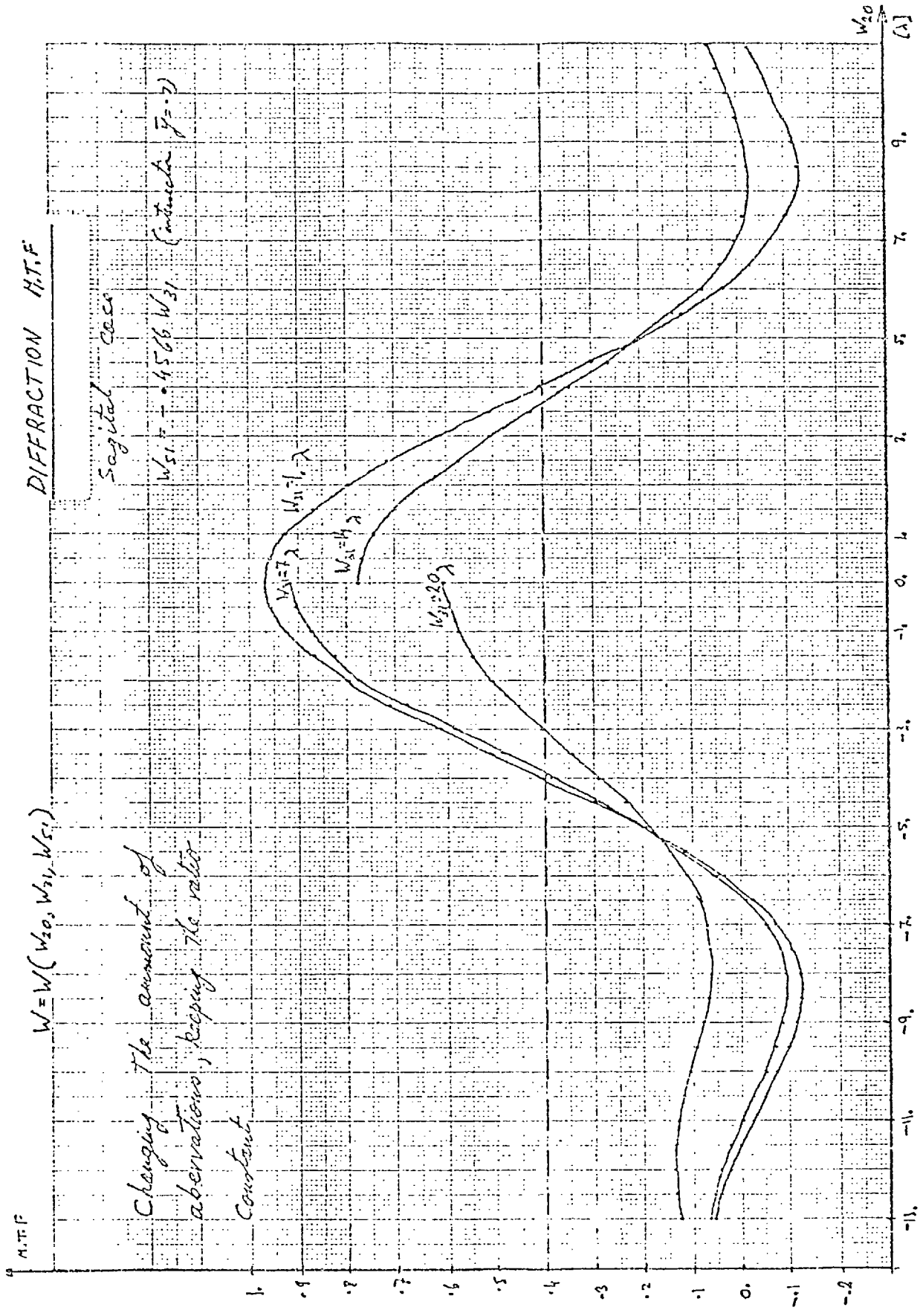

3.f - (i) depth of focus in the presence of coma, in the sagittal azimuth (FINKLER 1975)

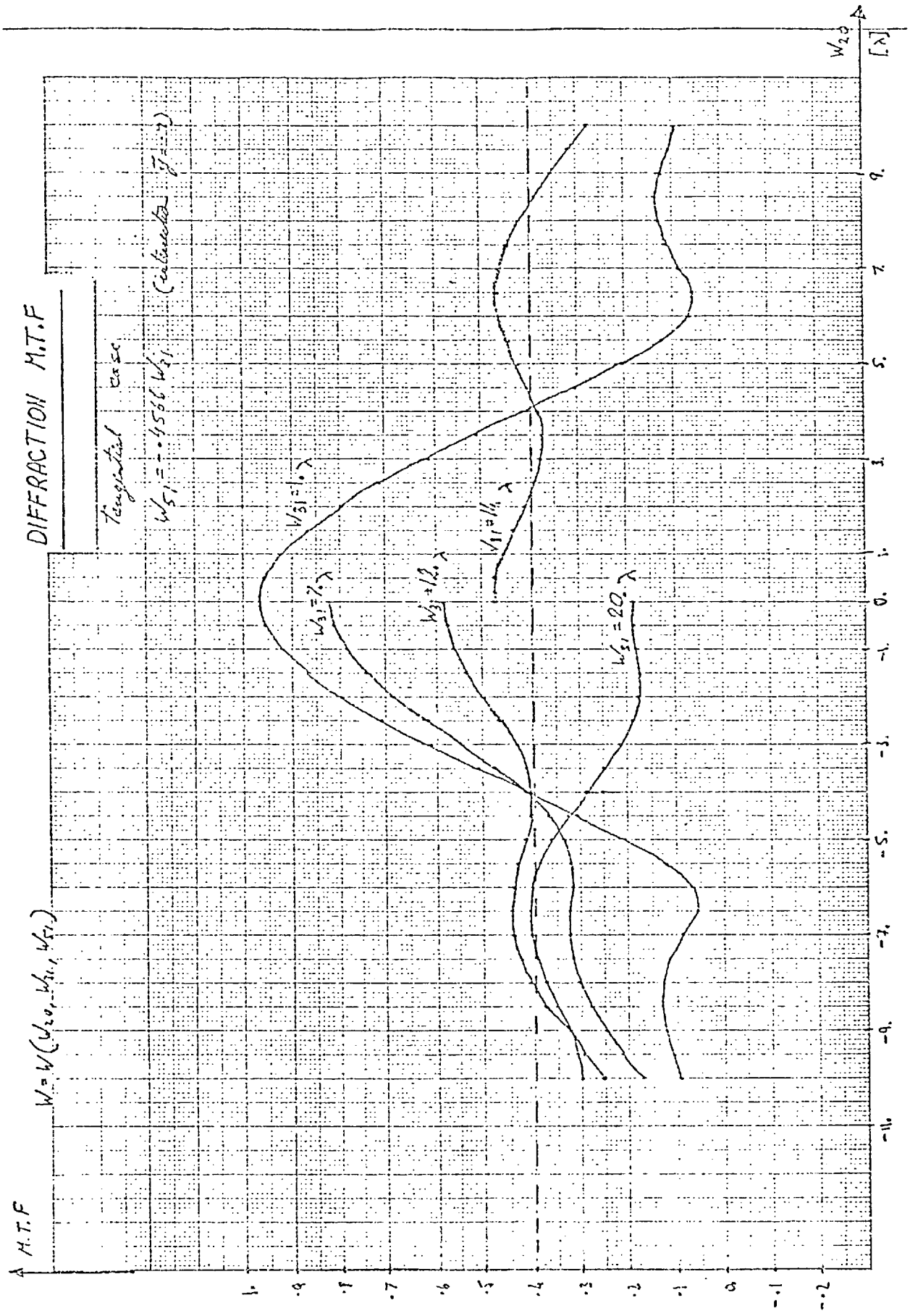

3.f - (ii) depth of focus in the presence of coma, in the tangential azimuth (Finkler 1975)

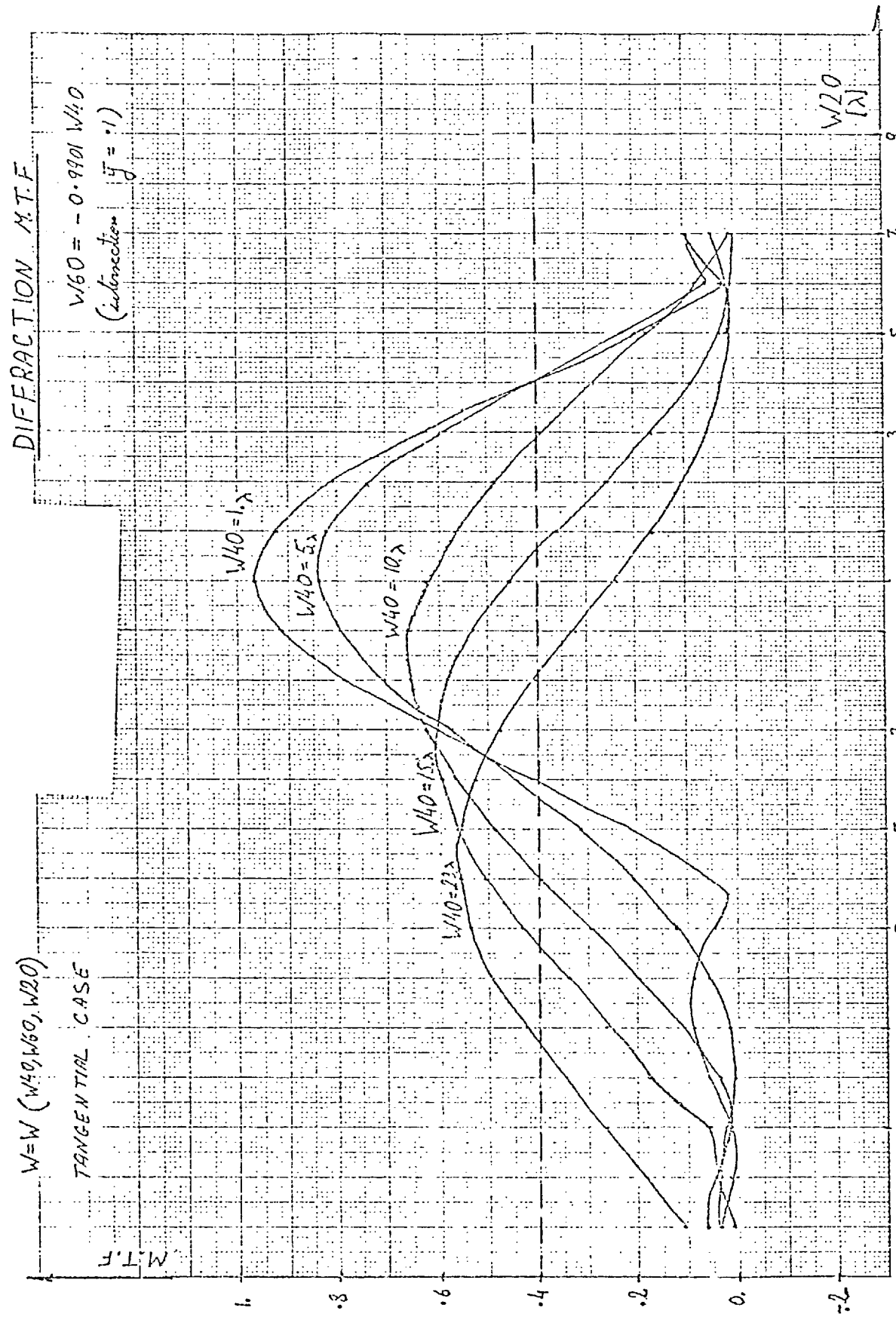

3.f - (iii) depth of focus in the presence of spherical aberration (Finkler 1975)

CHAPTER 4

OPTICAL OPTIMISATION IN TWO IMAGE PLANES AND THE DEPTH OF FOCUS.

4.1. Optimisation for Larger DOF.

This work concentrates on the design of lenses for low frequencies with limited resolution, and with large DOF maintaining a target MTF values. As mentioned above, lenses of this type might be used in copying systems, in the production of printing plates for monochrome and for colour work and in various detection systems. This work considers mainly lenses for office photocopying machines with unit magnification and reduction capabilities. The DOF is an important characteristic in systems with moving components such as flickering mirrors, and with a moving image surface such as a rotating drum, especially when the image surface is non planar and the width of the field is determined by a finite slit. In systems of this type the DOF may be a key criterion setting the mechanical tolerances of the system and hence the properties of the machine. Since such systems are not diffraction limited and as suggested by Chapters 2 and 3, reduction of aberrations will not necessarily improve the DOF, conventional optimisation methods may not be the best for the design of these lenses.

On the basis of Chapter 2 it is possible to calculate aberration ratio for practical cases which will maintain or increase the DOF of the system without necessairly reducing the aberrations, the use of these ratios as optimisation criteria will require a new optimisation program with a new type of merit function, which is not a simple task.

Alternatively one may calculate aberration targets by algorithms similar to those in Chapter 2 which may in turn be used as target values in a "conventional" optimisation program, such as V14 with the option of wavefront aberration incorporated in the merit function. This is a possible solution but it involves a complicated algorithm, which does not use practical parameters, as a primary stage and does not involve the use of the required criterion of MTF values directly in the program.

Another approach might be the use of a "conventional" optimisation program such as V14 or VGOTF where after each stage the MTF as a function of defocus is studied, at the frequency of interest, and a set of wieghting factors chosen to improve the design. This method requires an experienced optical designer and involves, in certain cases, a tedious process of trial and error.

A simple modification of the existing program may be possible in such a way that the DOF criterion is included in the merit function. The simplest way of doing this is probably optimisation in two different image planes. The VGOTF program was chosen for this experiment since it involves the MTF in the merit function. The new version of the program resulting from this modification is referred to throughout this work as the VDOF program and is described below.

4.2 The Construction of the Merit Function of VDOF.

The merit function in the VDOF program may be considered as a sum of three different merit functions;

$$\Psi=\Psi_1+\Psi_2+\Psi_3 \qquad (4\text{-}1)$$

The first merit function Ψ_1 is a function of aberrations in the image plane, which is normally chosen by the program as the plane with the maximum MTF value, at the limiting frequency. The other two merit functions Ψ_2 and Ψ_3 are the differences between the geometrical MTF values and 1. at two defocused image planes situated symmetrically on both sides of the image plane in which Ψ_1 is calculated.

The merit function may be written as;

$$\Psi=\sum_j W_j^2 f_j^2 + \sum_k W_k^2 f_k'^2 + \sum_l W_l^2 f_l''^2 \qquad (4\text{-}2)$$

where f_j is an aberration in the focal plane weighted by W_j and similarly f_k' and f_l'' are the aberrations in the defocused planes. The f_j terms consist mainly of aberrations such as chromatic aberrations where the Conrady formula is used, distortion at each field angle used in the optimisation, primary Seidel coefficients if required, offence against the "Sine Condition" and any special aberration included by the designer. The f_k' terms consist of differences of the following type;

$$f_k' = \text{Sin}\ (\ \pi F \delta \hat{\eta}) - t_k \qquad (4\text{-}3)$$

where $\delta\hat{\eta}$ is the transverse ray aberration in the defocused image plane, F is the optimisation frequency and t_k is a target value for the geometrical MTF component at the point in which the aberration is calculated and normally t_k is zero. The calculation of $\delta\hat{\eta}$ (aberration in the defocused image plane) requires a simple algorithm which uses values already available to the program. Let us consider a defocus distance D which results in defocused planes distance D on either side of the image plane, as illustrated below in Figure 4.a.

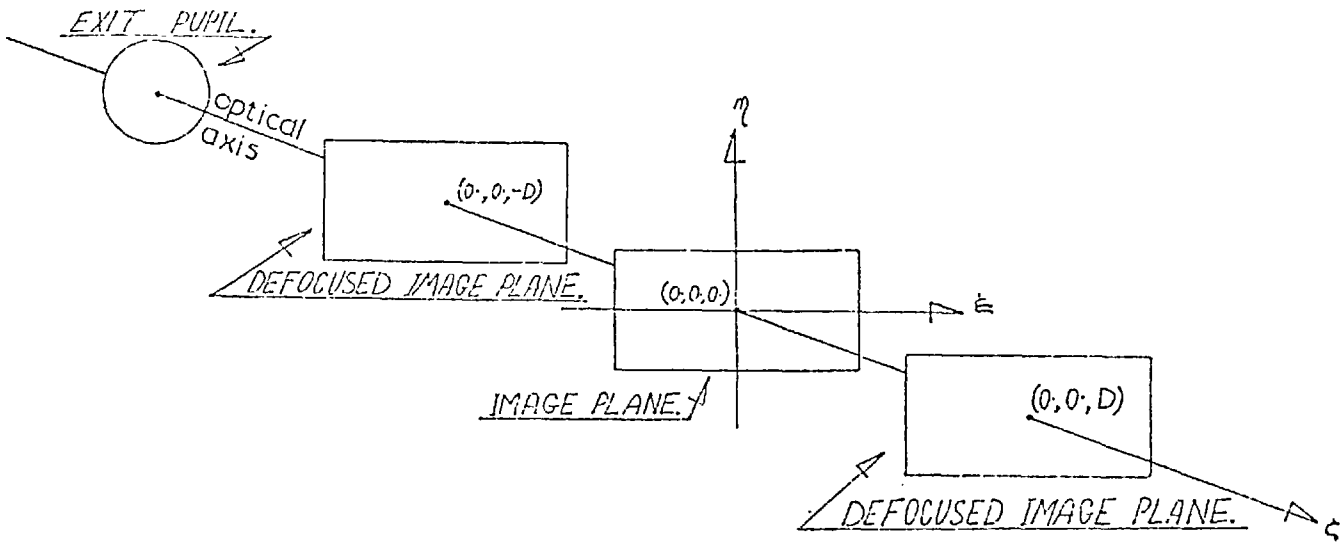

Figure 4.a - The coordinates of the image plane.

If we add a skew ray and a principal ray to this diagram the transverse ray aberration will be as shown in Figure 4.b.

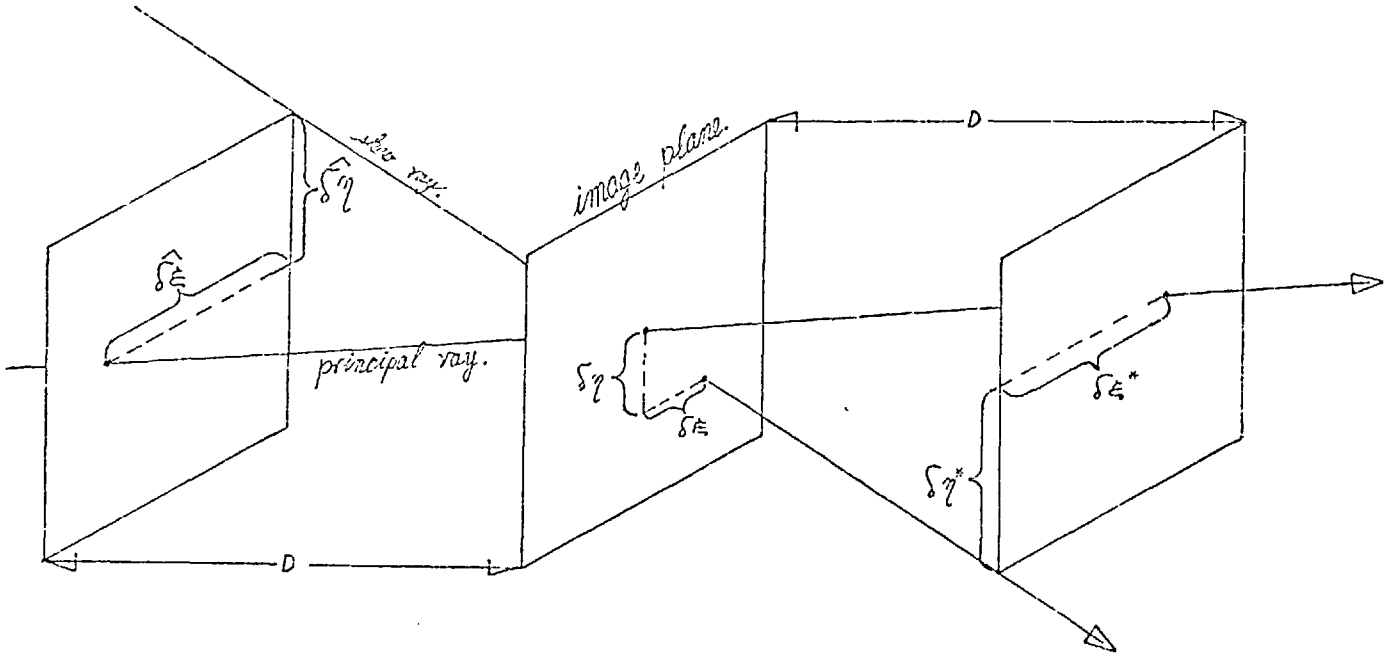

Figure 4.b - the aberrations in the defocused planes.

The angle between the principal ray and the optical axis is given by $\bar{u}$, the angle between the skew ray and the optical axis is given by u. The skew ray direction cosines are known from the ray tracing routine and are denoted by L, M and N, which defines tan(u).

The calculation of $\delta\hat{\eta}$ and $\delta\eta^*$ can be illustrated by the following two dimensional projection shown in Figure 4.c;

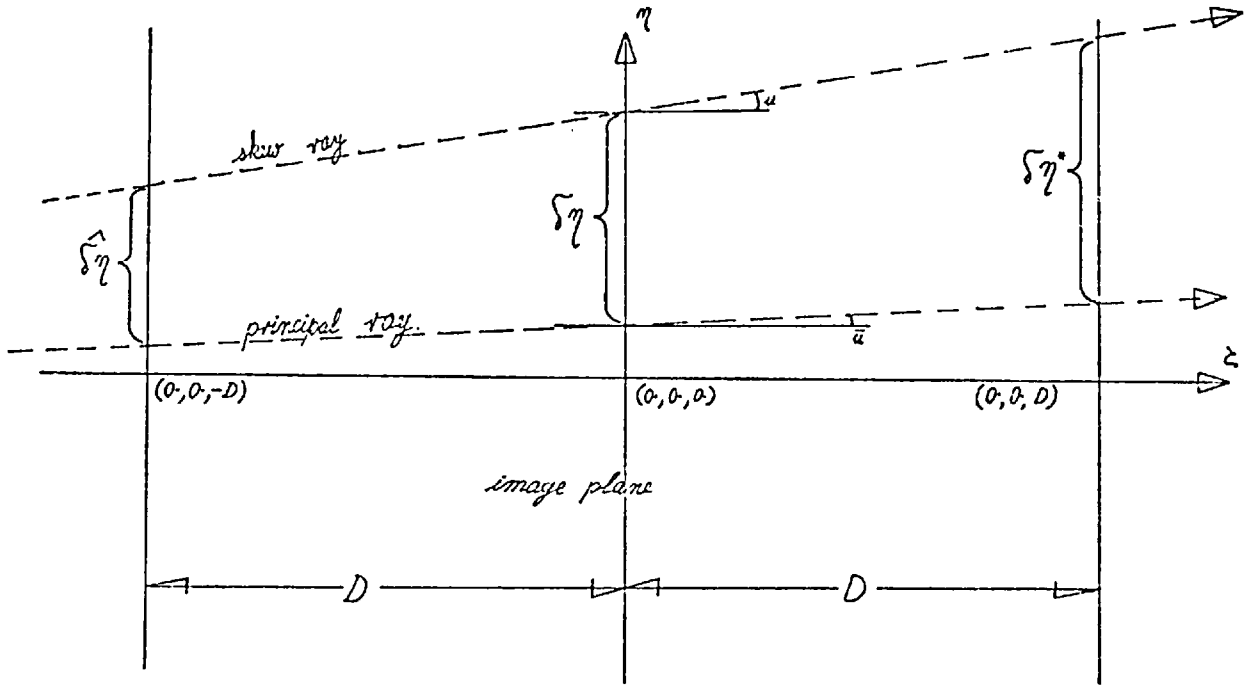

Figure 4.c - The effect of defocus on $\delta\eta$.

which leads to the following solution;

$$\delta\hat{\eta} = \delta\eta - D\tan(u) + D\tan(\bar{u}) = \delta\eta - D\left[\frac{M}{N} - \tan(\bar{u})\right] \qquad (4\text{-}4)$$

and similarly;

$$\delta\eta^* = \delta\eta + D\left[\frac{M}{N} - \tan(\bar{u})\right] \qquad (4\text{-}5)$$

where $\delta\eta^*$ is the other defocused aberration.

In the other azimuth the transverse ray aberrations are:

$$\hat{\delta\xi} = \delta\xi - D\frac{L}{M} \qquad \text{and} \qquad \delta\xi^* = \delta\xi + D\frac{L}{M} \tag{4-6}$$

the principle ray component disappears since L=0 for the principle ray.

Thus the merit function can be written as:

$$V = \sum_{j=1}^{n_1} W_j^2 f_j^2 + \sum_{1}^{n_2} W_k^2 \{\mathrm{Sin}[\pi F(\delta\xi + D\frac{L}{N})] - t_k\}^2 + \sum_{1}^{n_2} W_k^2 \{\mathrm{Sin}[\pi F(\delta\eta + D[\frac{M}{N} - \tan(\bar{u})])] - t_k'\}^2 +$$
$$+ \sum_{1}^{n_2} W_k^2 \{\mathrm{Sin}[\pi f(\delta\xi - D\frac{L}{N})] - t_k\}^2 + \sum_{1}^{n_2} W_k^2 \{\mathrm{Sin}[\pi F(\delta\eta - D[\frac{M}{N} - \tan(\bar{u})])] - t_k'\}^2 \tag{4-7}$$

The modification to the program is minute and consists of the following transform:

$$AB(i) \rightarrow \begin{cases} AB(i) = \mathrm{Sin}[F\pi(\delta\eta - D\frac{M}{N} + D\tan\bar{u})] \\ AB(i+1) = \mathrm{Sin}[F\pi(\delta\eta + D\frac{M}{N} - D\tan\bar{u})] \end{cases} \tag{4-8}$$

where AB(i) is the i^{th} transverse ray aberration, the same transform is repeated for the $\delta\xi$ aberration, where $\tan(\bar{u})=0$. This operation results in an increased number of aberrations which requires a similar increase in the number of target values and the weighting factors. For simplicity we may specify two conversion factors, FW and Ft, and the following transform follows:

$$W(i) \rightarrow \begin{cases} W(i) = FW.W(i) \\ W(i+1) = FW.W(i) \end{cases} \tag{4-9}$$

and similarly,

$$t(i) \rightarrow \begin{cases} t(i) = FT.t(i) \\ t(i+1) = FW.t(i) \end{cases} \qquad (4\text{-}10)$$

normally the choice of the factors will be FT=1 and FW=$2^{-\frac{1}{2}}$, as explained later. For reasons similar to those relating to the VGOTF program (as explained above) it follows that the minimisation of a merit function in which the aberrations, weighting factors and target values are transformed by the above transform, will result in the maximisation of the geometrical MTF values in the two defocused image planes, as long as the frequency-aberration product is kept below 0.5.

4.3. Validity of the Mathematical Procedure for the New Merit Function.

It is obvious from Chapter 1 that the optimisation procedure is dependent on the structure of the merit function. Hence it is necessary to show that the mathematical treatment of the damped least squares method used by the SLAMS program is still applicable to the new merit functions.

The optical designer controls the optimisation frequency as well as the defocus distance, this might lead to the conclusion that the designer has a large choice of optimisation parameters, which is misleading. The magnitude of the aberrations will obviously increase with the defocusing distance which limits the choice of D, since the rule of maintaining an aberration product which is applied in the VGOTF program is still valid in this case and one should be careful to satisfy the following relations;

$$\left|\delta\eta \pm D\left(\frac{M}{N} - \tan\bar{u}\right)\right| < \frac{1}{2F}$$

and $\qquad (4\text{-}11)$

$$\left|\delta\xi \pm D\,\frac{L}{M}\right| < \frac{1}{2F}$$

A simple test can be included in the program to list the violations of this condition in each iteration which will enable the designer to reduce the defocus distance or the frequency if required.

If one restricts the aberration product to 0.5, as given by equation 4-11, the values of the aberrations in the merit function vary slightly from those in the image plane, therefore the concept of linear behaviour for small parameter changes is conserved. Since the new aberration values are calculated by a simple linear transform, and assuming that the VGOTF program operates with a continous merit function, the suggested new merit function must be continous too. Thus the differentiation procedure is valid and correct from the mathematical point of view.

The merit function above will not be ill-conditioned, in the case where the initial system has been previously optimised by VGOTF. The merit function consists of the geometrical MTF values, calculated with the same number of rays; both defocused image planes are equally represented none of which is favoured by the program. The combination of two sine terms in the merit function may increase the non linearity of the function but this should be compensated by the choice of the appropriate damping factor.

The designer will start his design by V14 steering the system into the right region of parameter space, further improvement by the MTF criterion may be achieved by using VGOTF as a second stage. The VGOTF procedure may require a few steps during which the optimisation frequency is gradually increased, whilst maintaining the correct aberration product, until the correct frequency is reached. To

increase the DOF of the final design a third stage is used, applying the VDOF program, during which the defocus distance and sometimes the frequency value will be changed gradually by the designer to produce the required system.

4.4 The VDOF Program.

The modifications required so as to convert VGOTF into VDOF are minimal. Subroutine MIXAB is modified slightly to read in four new imput values, as listed below;

a. a switch which indicates that the VDOF option is to be used.

b. a defocus value D which indicates the defocus distance of the image planes considered.

c. a factor FW which will factorise all weighting factors as given by 4-9.

d. a factor Ft for the target values, as given by 4-10.

A short subroutine SPLIT has been added to the program, which is called by subroutine MIXAB, and splits each transverse ray aberration into the two defocused aberrations and creates the appropriate weighting factors and target values as described by (4-8), (4-9) and (4-10). This subroutine also tests the aberration product and in the case of a violation will print a comment which suggests the maximum frequency allowed by this aberration at the present defocus distance.

A general flow diagram of V14 is given in the appendix, but so as to illustrate the modifications required a flow diagrams of the raytracing routine is repeated in Figure 4.d below, where the dotted lines indicate parts added to produce the VGOTF program, and double lines indicate additions to produce the VDOF.

As follows from the above diagram, one extra subroutine is needed to convert the V14 to VGOTF, which increases the number of subroutines from 48 to 49. To convert VGOTF to VDOF a few more statements are added to the RAYTRS subroutines to store the values required by the transform formula, and an additional common block with dimensional arrays is required to transfer these values to other subroutines. The rest of the changes take place in subroutine MIXAB which is illustrated in Figure 4.e below. This subroutine can be replaced by a dummy subroutine in V14, and the parts marked by double lines are required only for the VDOF program.

This diagram shows that the VDOF program requires an extra subroutine SPLIT, and hence consists of 50 subprograms. Subrotuine SPLIT is very short and is described in Figure 4.f below in a flow diagram;

A modification to the dimensions of the arrays used might be found necessary, due to the increase in the number of aberrations, weighting factors and target values. In this case the matrix of the differentials whose dimensions are "the number of controlled parameters times the number of controlled aberrations", must be increased together with the array containing the upper triangle of the product matrix and a few other and smaller related arrays.

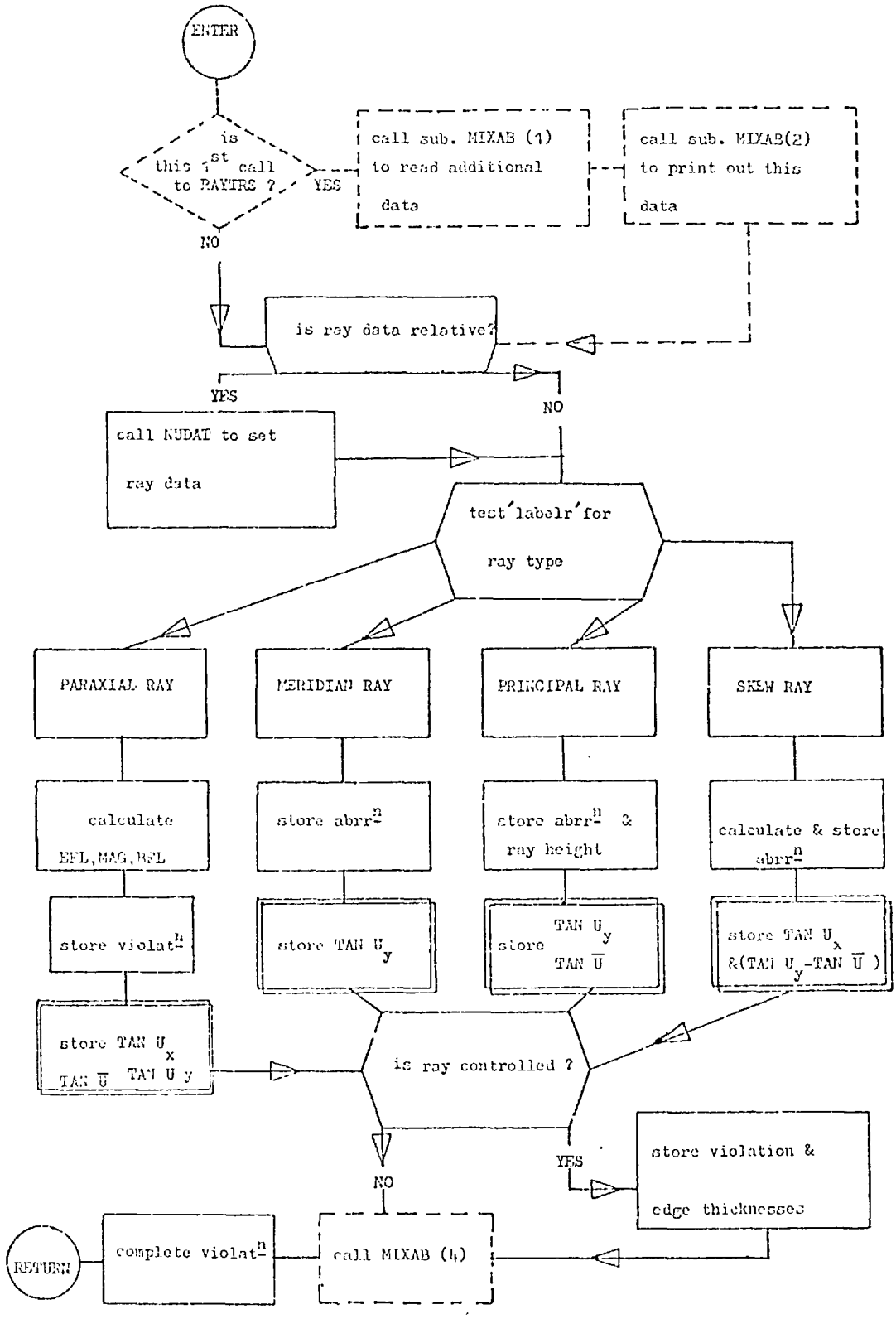

4.d - Flow diagram of the ray tracing routine, dashed line indicates additions in VCOTF, double lines indicate additions in VDOF.

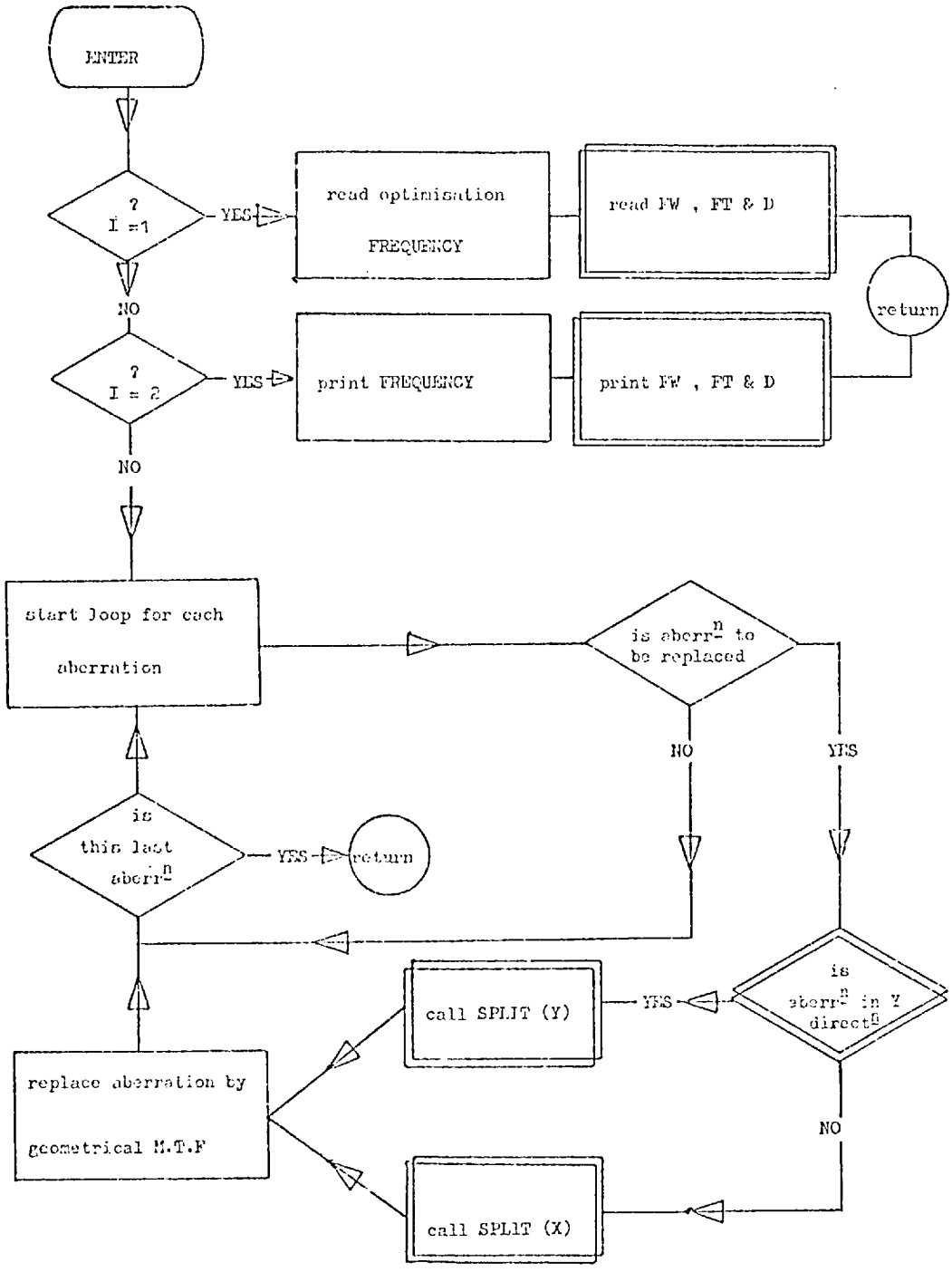

4.e - Flow diagram of subroutine MIXAB, double line indicates addition in VDOF.

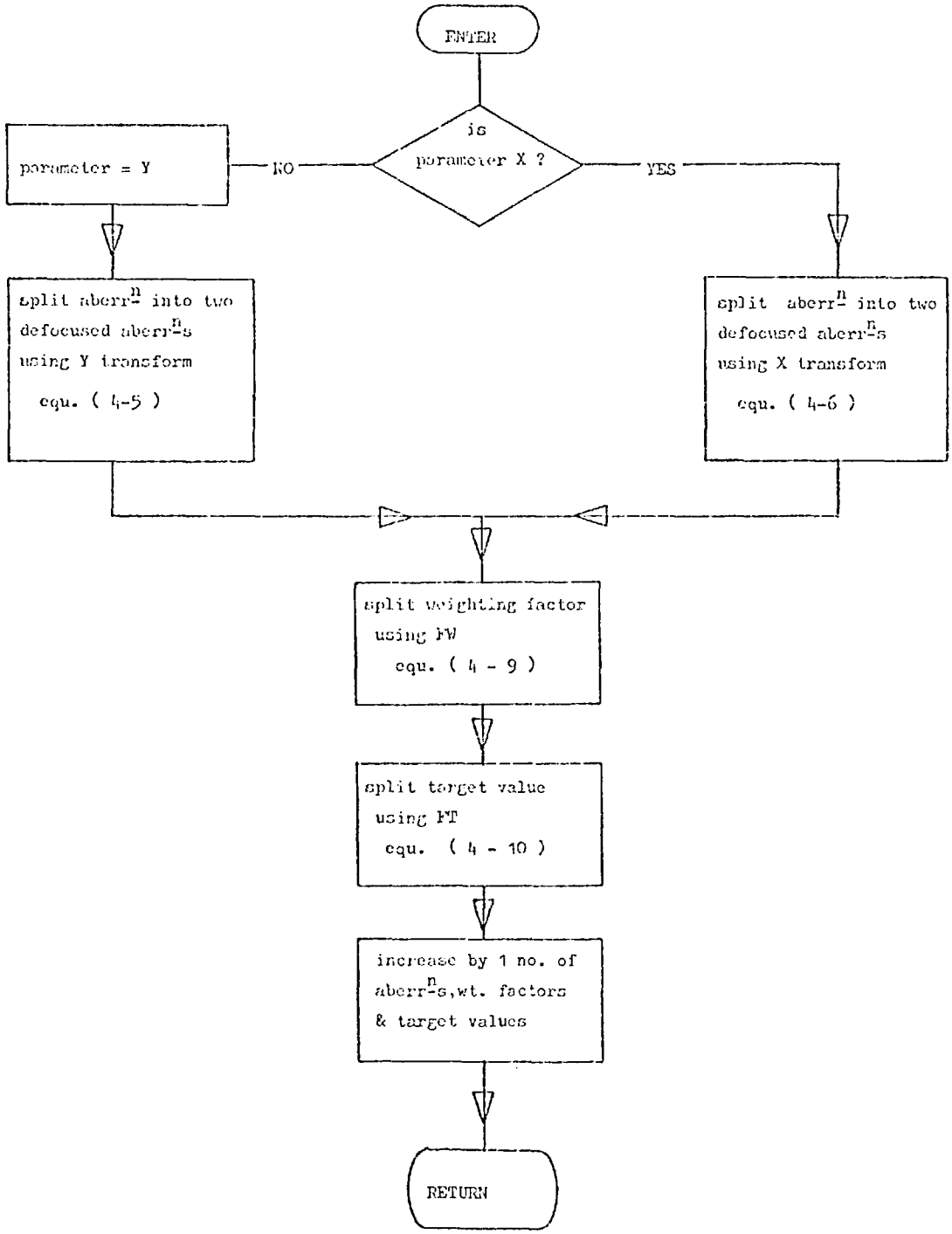

4.f - Flow diagram of subroutine SPLIT.

If one uses the maximum of 50 rays allowed by the program, which is necessary in order to approximate the MTF calculation by summation, the program can cope with a monochromatic case, here VOOF contains 250 aberrations and leaves the other 50 aberrations for special requirements such as Seidel coefficients. In this case on a COC 6000 series computer, the file length required for loading the program is 127,700 (octal) or 44,992 (decimal), running the program requires about 73,600 (octal) or 30,592 (decimal). If polychromatic cases are to be considered the storage capacity of some computers might be found insufficient, as for example on the COC 6400 at Imperial College, the maximum file length is 51,200 (decimal), and the program will overflow the system. In this case one may reduce the number of variable parameters which is 50 at the moment. Further core might be saved by reducing the maximum number of surfaces of the optical system, which is 50 at the moment and is rarely fully used. For example, if 35 variable parameters are used, instead of the 50 available in the VGOTF, the maximum number of aberrations can be increased to 575 which allows an extra 275 aberrations to be used for optimisation in three wavelengths (Two λ values and mean λ). Where more parameters need to be varied the initial optimisation can be done at a "mean wavelength" then after freezing some parameters a polychromatic optimisation can be carried out, alternatively a larger computer (e.g. COC 6600, 7600, etc) with larger core can be used.

VOOF, which is the most general optimisation program described here, can be used as the only SLAMS program. In the case of zero defocus distance (O=0.), with FT=1 and FW=$2^{-\frac{1}{2}}$, the result will be the same as for VGOTF since each of the split aberrations will be one half of the original aberration. By choosing a low frequency

such that F→0. the sine term will be reduced such that Sinα=α and the program reduces into V14. This is not very practical under normal usage conditions since this equivalent to V14 will consume more core and time on execution than the conventional V14 program.

CHAPTER 5

SIX ELEMENTS MONOCHROMATIC COPYING LENS

5.1 The Design of The Six Elements Copying Lens

This chapter describes the design of a six element copying lens, corrected monochromatically. Lenses of this type are useful in colour reproduction processes, in colour copying machines which use separate optics for each of the primary colours, in systems with narrow spectral sensitivity curves which often are due to the spectral characteristics of the light source and in various other situations.

The design is symmetrical, with a stop at the central plane, which is the plane of symmetry. The specifications were for a numerical aperature of 0.04464 working at a wavelength of 500. nm, which yields in the case of unit magnification a f/5.6 lens. Initially, the focal length was set to 25. cm which resulted in a lens - to - image distance of 45.33 cm, in this case the object - to - lens distance was the same. The Object- to - image distance, the throw, was controlled at 100.cms, the axial glass thickness was limited by a maximum of .125 cm, and the minimum axial air separation was .01 cm. The total axial glass thickness was restriced to 6. cm and the total system length was limited to 10.cm on the axis. Only two types of glass were used in the design which was found to be sufficient in this monochromatic case.

During the early stages of the optimisation, the V14 program was used with an initial damping factor of .05. The merit function was calculated from the aberrations of 24 rays from four field positions which were defined by the corresponding object heights.

This method of defining the field position is usual when finite objects are considered, in this particular design the object heights were 0., 6.06, 12.12 and 18.18 cms, the largest height being half the length of the diagonal of an A4 size page.

The V14 optimisation was terminated when the maximum value of the transverse ray aberrations was small enough for the geometrical MTF optimisation to be valid at a frequency of 50. cycles/cm, as determined by the aberration product. The glasses which had been allowed to change in a theoretically continuous refractive index-dispersion plane by the program, were frozen at the LaK N9 and LF 2 values from the Schott range of glasses.

The VGOTF program is limited to 50 rays in three field angles, which results in 300 transverse ray aberrations, so for this case the field positions were re-defined as object heights of 0., 12.73 and 18.18 cms. The optimisation was carried out in several steps during which the optimisation frequency was increased gradually up to 100. cycles/cm, which was the frequency of interest for this design and at which the DOF had to be improved. The MTF of the final VGOTF design at this frequency was .713 on axis, at the full field angle of 19.51 degrees the MTF was .678 in sagittal azimuth and .813 in the tangential azimuth. Both the designs, produced by the V14 and by the VGOTF optimisation, are shown in figure 5.a, in which all the parameters are given in cms.

As expected, on the basis of chapter 1, the second system produced by the VGOTF program resulted in higher MTF values at the design frequency of 100. cycles/cm. This is illustrated in figure 5.b which compares the MTF of these designs.

FINAL VGOTF DESIGN - 6 ELEMENTS COPYING LENS
1 FOCAL LENGTH

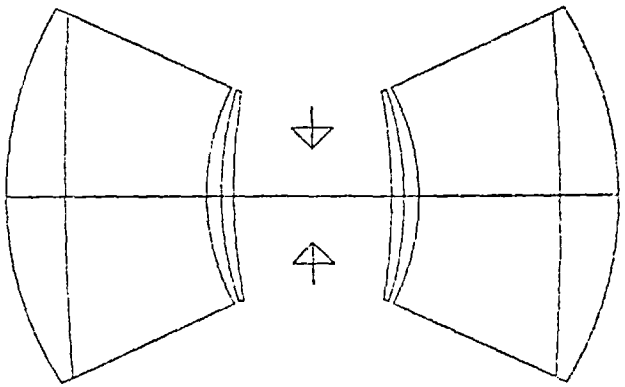

CURVE	SEPN	INDX/DIS
0.120430	0.000000	1.000000
0.014680	1.383510	1.694010
0.163570	3.324200	1.592630
0.123090	0.345510	1.000000
0.070040	0.292510	1.694010
0.000010	1.856060	1.000000
-0.070040	1.856060	1.000000
-0.123090	0.292510	1.694010
-0.163570	0.345510	1.000000
-0.014680	3.324200	1.592630
-0.120430	1.383510	1.694010
0.000010	-0.193920	1.000000

FINAL V14 DESIGN - 6 ELEMENTS COPYING LENS
.05 FOCAL LENGT

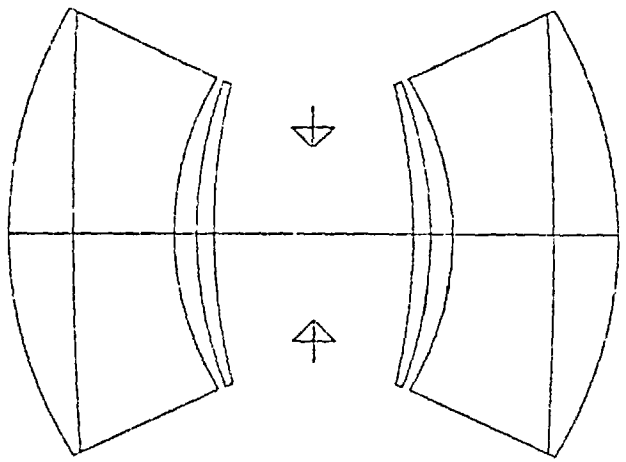

CURVE	SEPN	INDX/DIS
0.144300	0.000000	1.000000
0.014130	1.057660	1.694010
0.205230	1.657290	1.592630
0.143270	0.367160	1.000000
0.096250	0.285050	1.694010
0.000010	1.633280	1.000000
-0.096625	1.633280	1.000000
-0.143270	0.285050	1.694010
-0.205230	0.367160	1.000000
-0.014130	1.657290	1.592630
-0.144300	1.057660	1.694010
0.000010	0.000000	1.000000

5.a The systems produced by the V14 and VGOTF programs

FINAL V14 DESIGN - 6 ELEMENTS COPYING LENS
M.T.F VS. FREQUENCY AND DEFOCUS
ON AXIS

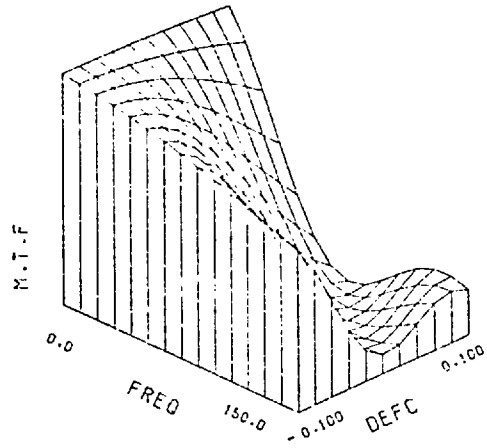

FINAL VGOTF DESIGN - 6 ELEMENTS COPYING LENS
M.T.F VS. FREQUENCY AND DEFOCUS
ON AXIS

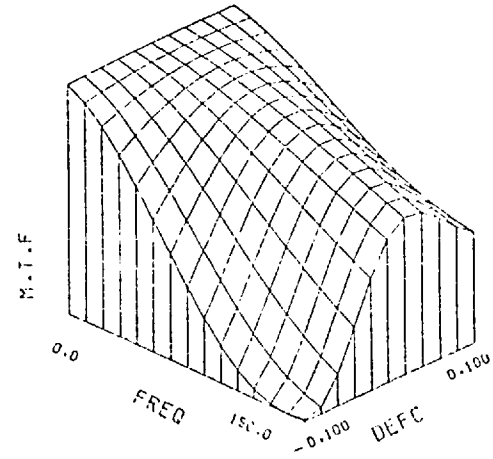

5.b (i) MTF as a function of frequency and defocus for the final V14 and VGOTF systems, on axis.

FINAL V14 DESIGN - 6 ELEMENTS COPYING LENS

M.T.F VS. FREQUENCY AND DEFOCUS

FIELD ANGLE =14.22 DEGREES

SAGITTAL M.T.F TANGENTIAL M.T.F

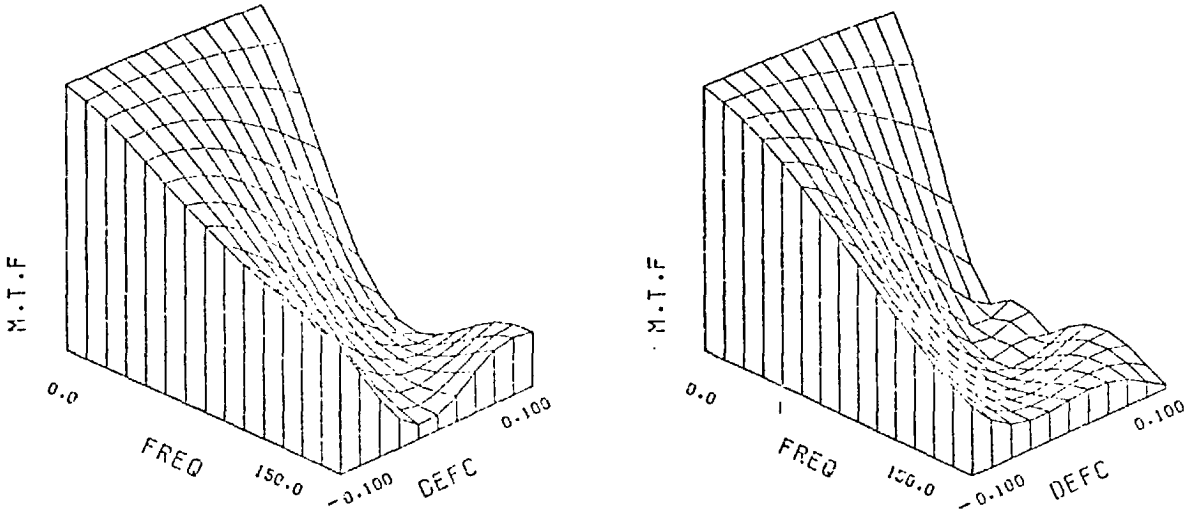

FINAL VGOTF DESIGN - 6 ELEMENTS COPYING LENS

M.T.F VS. FREQUENCY AND DEFOCUS

FIELD ANGLE =13.97 DEGREES

SAGITTAL M.T.F TANGENTIAL M.T.F

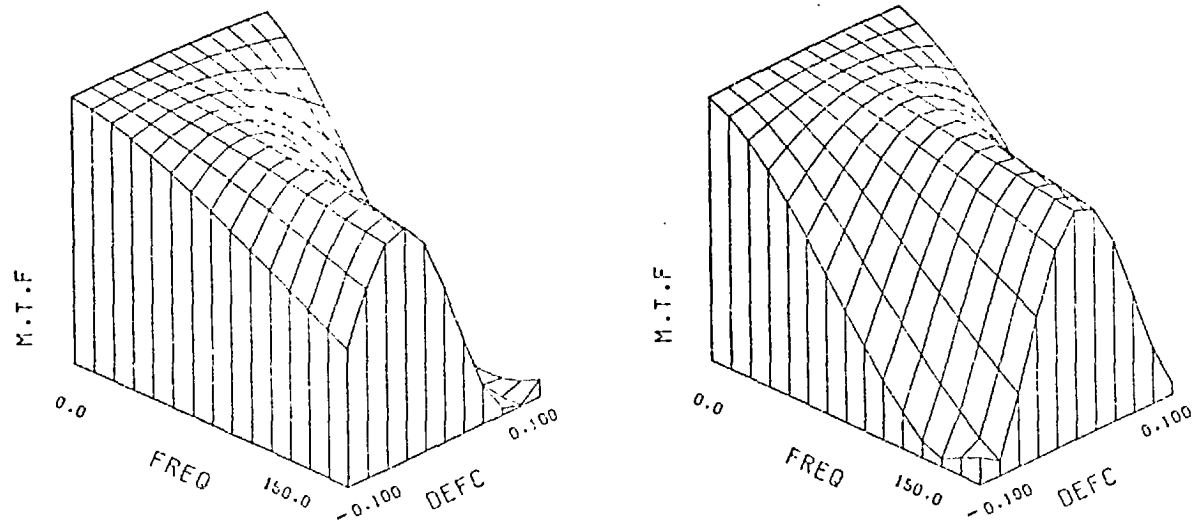

5.b (ii)

MTF as a function of frequency and defocus, at .7 of the full field angle.

FINAL V14 DESIGN - 6 ELEMENTS COPYING LENS

M.T.F VS. FREQUENCY AND DEFOCUS

FIELD ANGLE =19.87 DEGREES

SAGITTAL M.T.F TANGENTIAL M.T.F

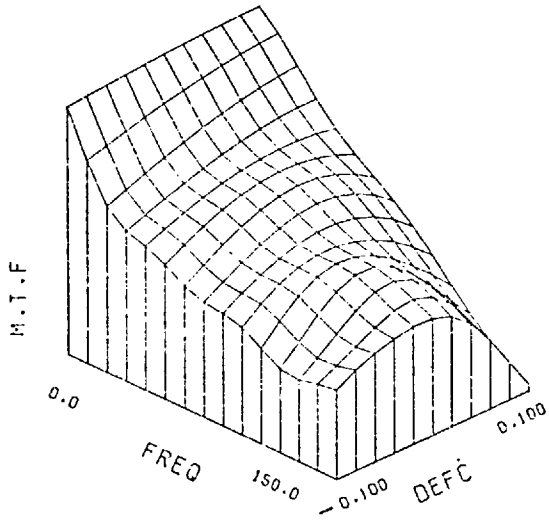

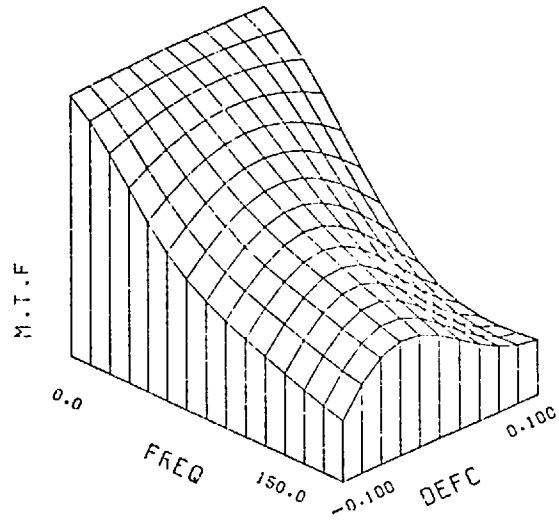

FINAL VGOTF DESIGN - 6 ELEMENTS COPYING LENS

M.T.F VS. FREQUENCY AND DEFOCUS

FIELD ANGLE =19.51 DEGREES

SAGITTAL M.T.F TANGENTIAL M.T.F

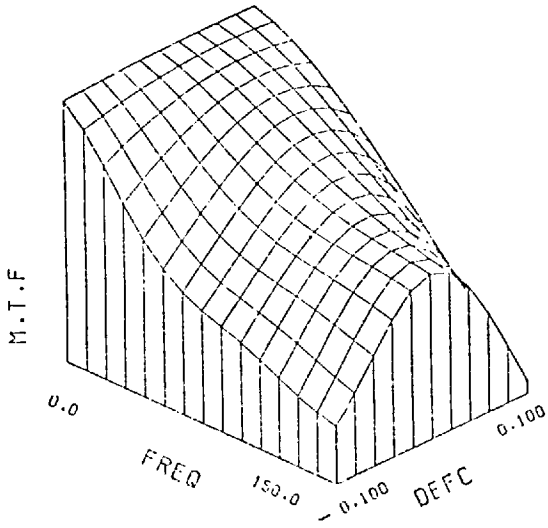

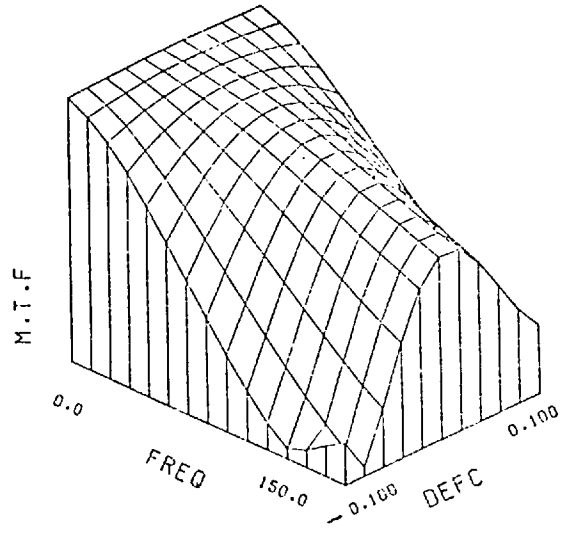

5.b (iii)

MTF as a function of frequency and defocus, at the full field

The improved MTF values, produced by the VGOTF optimisation, also increase the DOF at 40% which is the target value in this work.

The VGOTF design was produced by re-optimising the V14 system, which obviously resulted in reduced wavefront aberrations. Figure 5.c compares the wavefront aberrations of both designs in the form of cross-sections through the wavefront aberration function. Due to the nature of the program used to produce figure 5.c (details of program PARTC are given in appendix A), the aberrations are scaled differently in each case. In the case of the VGOTF system, the axis is scaled to $^2/_3$ of its size with the V14 design, this is approximately the ratio between the maximum wavefront aberrations of the two systems.

The final VGOTF system was tested with regard to the tolerances of the copying machine for which it was to be used. Distortion and field curvatures will normally be the limiting aberrations in the case of symmetrical lenses. On the assumption that the aberrations are acceptable and lie within the tolerance range (otherwise further VGOTF optimisation will be necessary) the depth of focus maintaining an MTF of 40% is studied. Figure 5.d shows the DOF determination for the two systems described above, calculated at the three field angles used through the optimisation procedure.

As predicted earlier, the lens produced by VGOTF had a larger DOF, which was .084 cm, as shown by figures 5.b and 5.d. Since this work is concerned with the improvement of this DOF, the rest of this chapter describes in some detail possible optimisation techniques for increasing the DOF.

5.2 DOF Optimisation Based on the VDOF Program

The system produced by the VGOTF program , as described above, was used in turn as an input to a VDOF optimisation, the weighting factors for

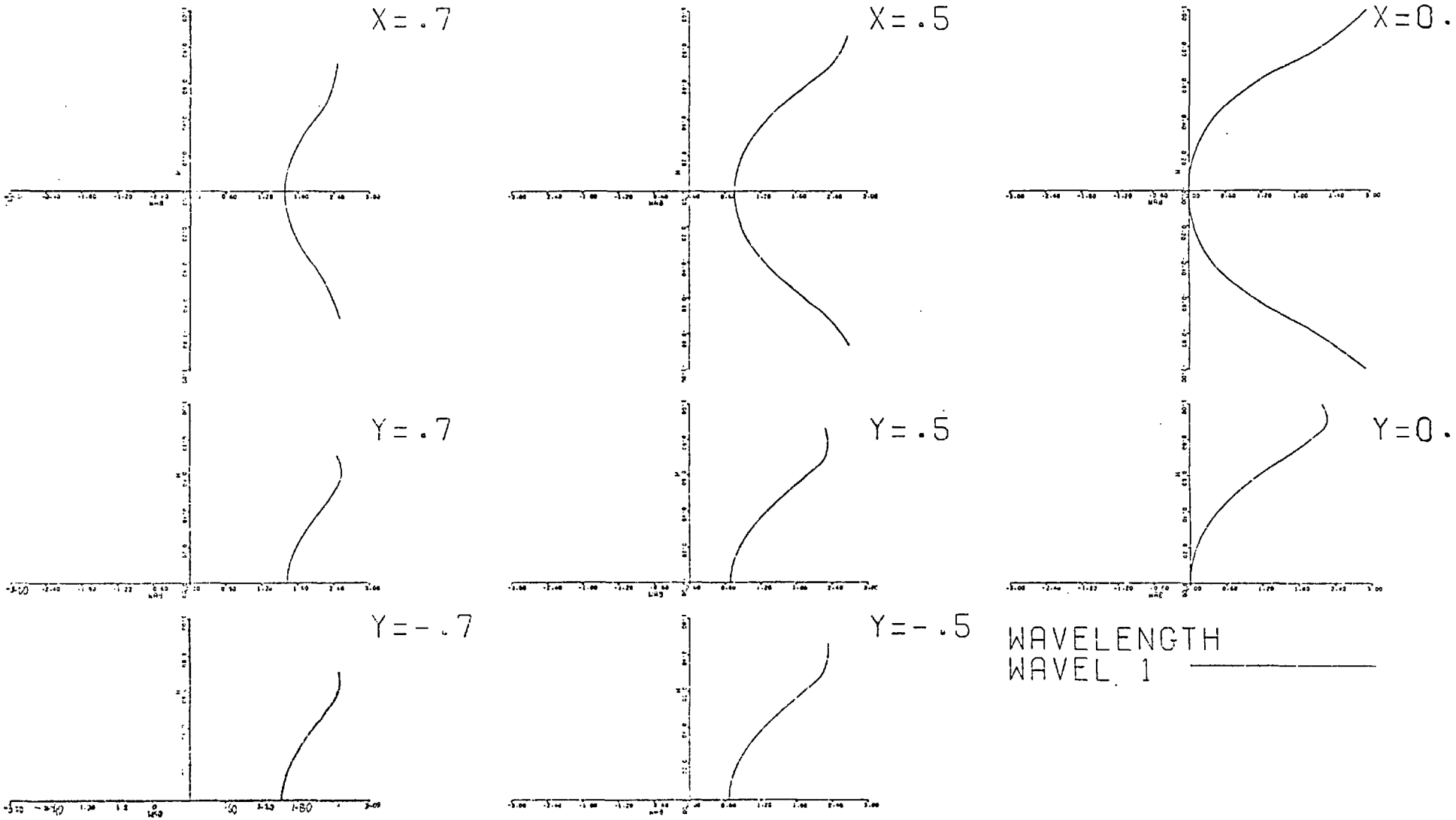

5.c (i) The wavefront aberrations of the V14 system, at .7 of the full field

FINAL VGOTF DESIGN - 6 ELEMENTS COPYING LENS
CROSS SECTIONS THROUGH THE WAVEFRONT ABERRATIONS OBJECT HEIGHT=12.7300

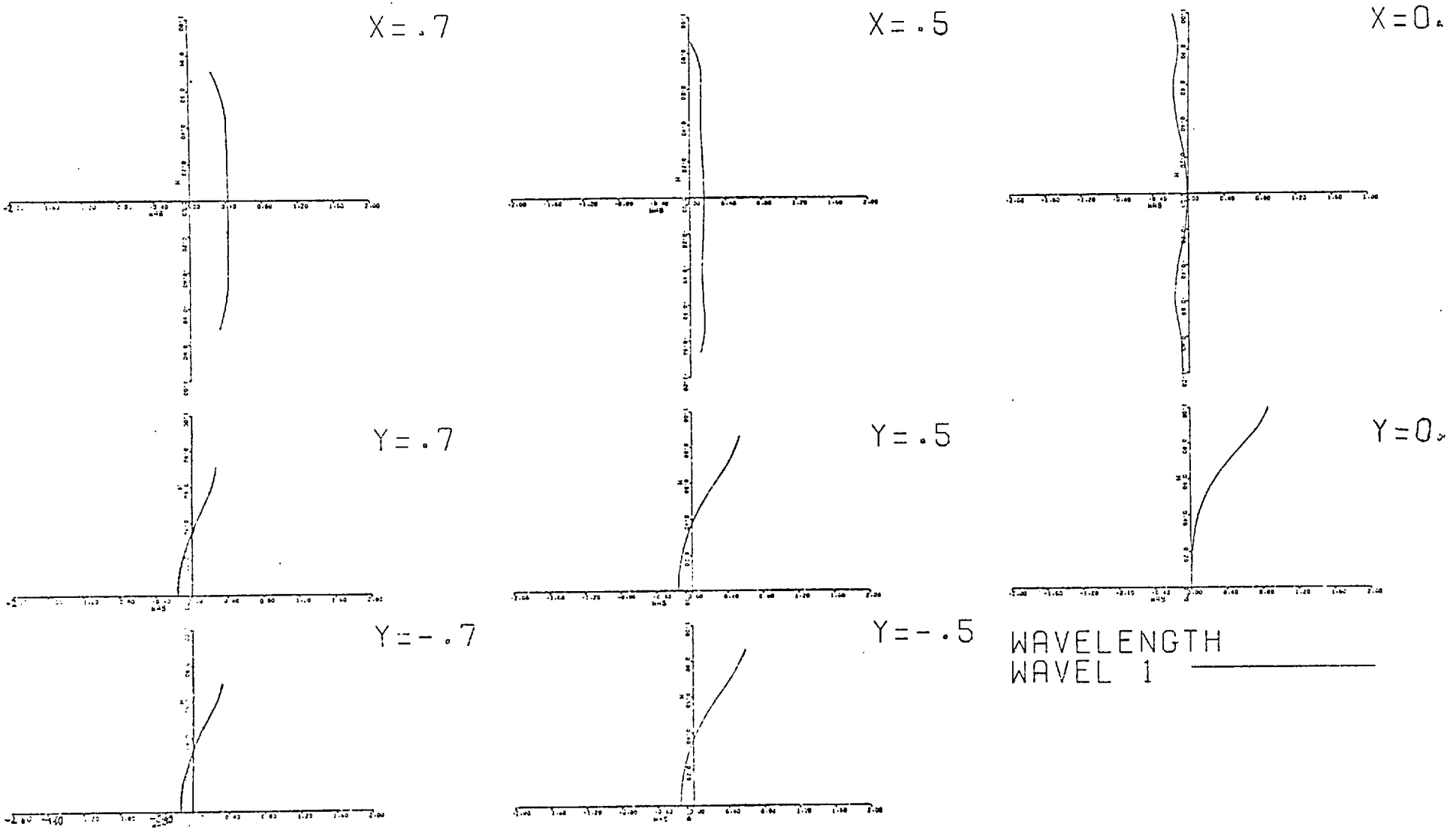

5.c (ii)
The wavefront aberrations of the VGOTF system, at .7 of the full field.

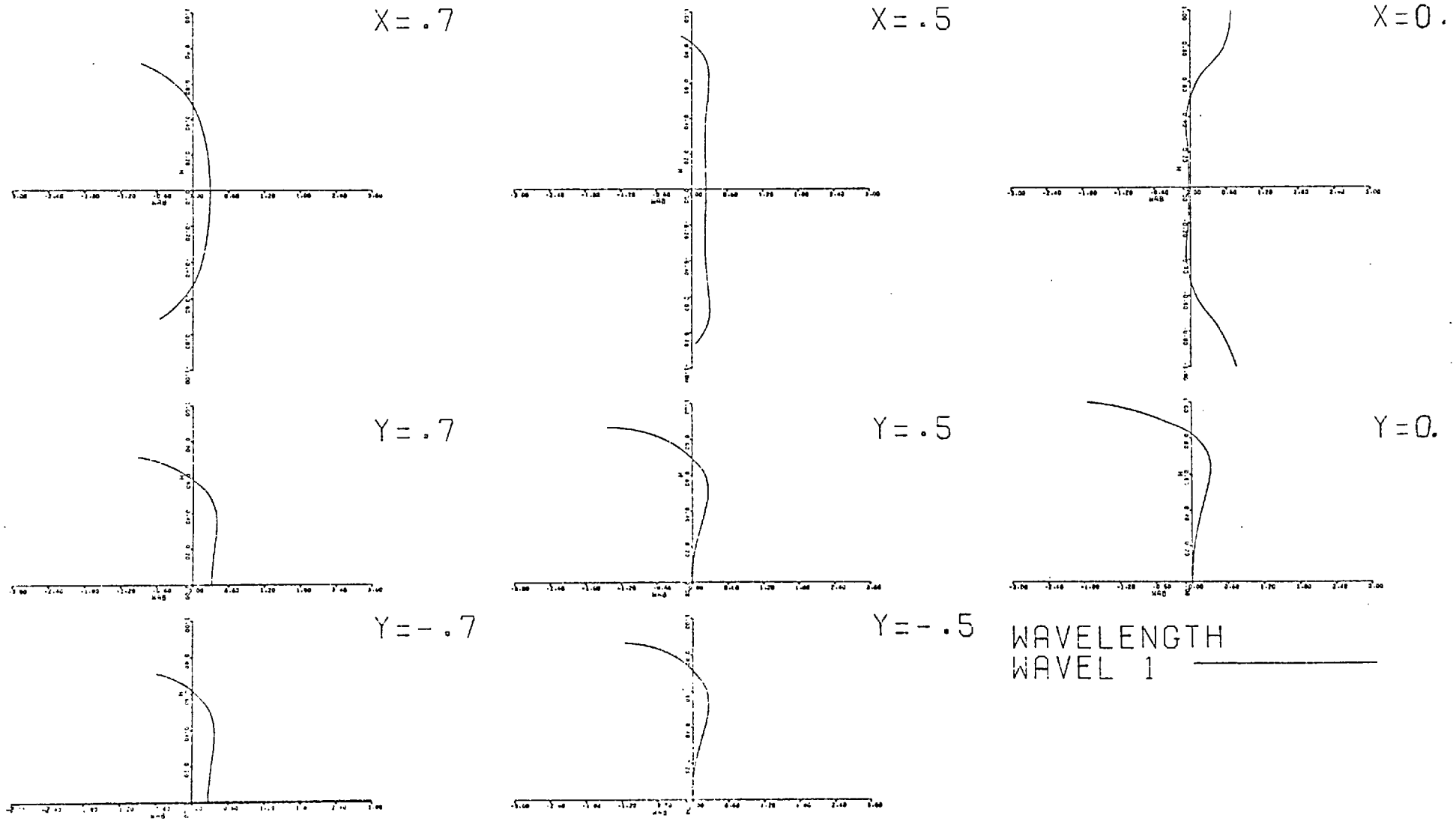

5.c (iii)
The wavefront aberrations of the V14 system, at the full field.

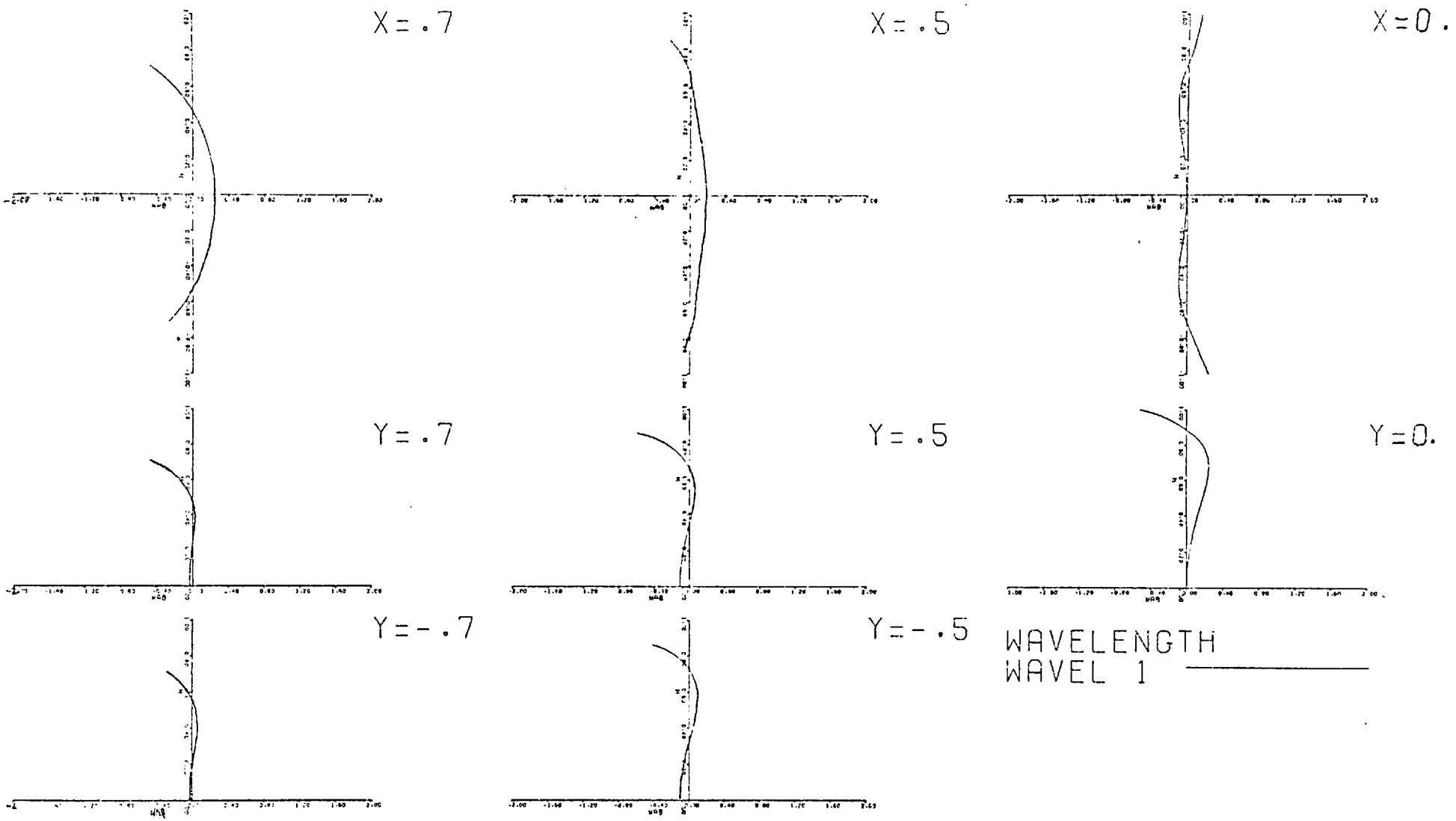

5.c (iv)

The wavefront aberrations of the VGOTF system, at the full field

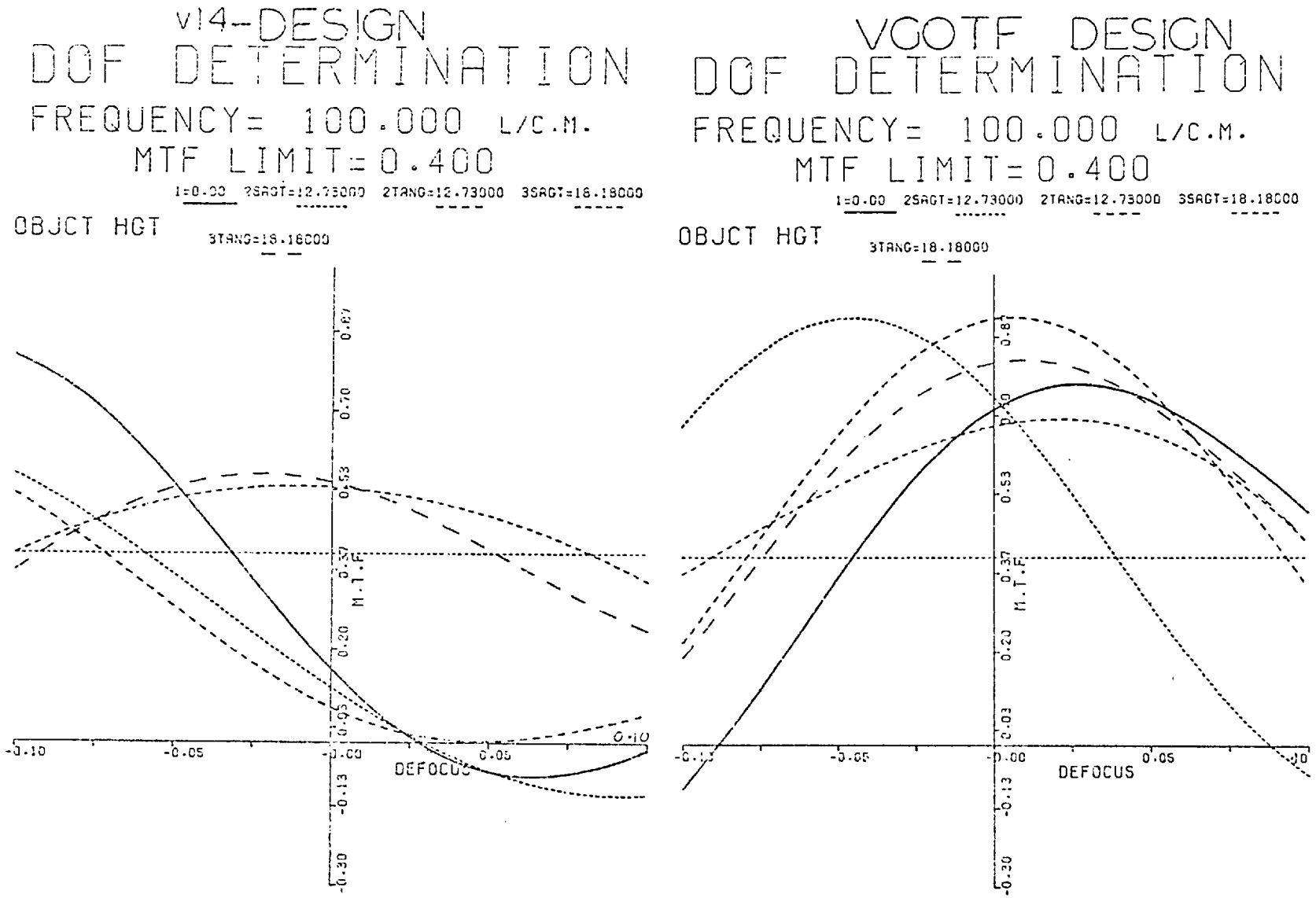

5.d DOF determination for the V14 and VGOTF systems

the aberrations at the various field angles and azimuths were kept the same. Hence,the only variable left was the defocusing distance, which is equal to half the separation between the two image planes at which the merit function is to be calculated. This separation had been limited by the range which satisfied the aberration product as described in equation 4-11. If we consider the initial design as a special VDOF case with zero defocus, the DOF was increased from .084 to .100 cm by defocusing the optimisation image planes from o. to .062 cm. Further increase of this defocusing distance resulted in a steep drop of the DOF, for example a defocus of .07 cm resulted in a DOF below the initial value of .084. The DOF behaved linearly with defocus in certain regions which is not surprising if the structure of the merit function is considered. The characteristics of the DOF as a function of the defocus distance through this optimisation sequence are illustrated in figure 5.e.

The Seidel aberration coefficient and the defocus of the best image plane from the Gaussian position, which were selected by the program, could be studied through the range covered by this optimisation sequence, and is represented graphically in figure 5.f.

The design produced by this sequence is different from the initial system (illustrated in figure 5.a) and is illustrated in figure 5.g. The wavefront aberrations of this design, at the full field angle, are given in figure 5.h below. This design was put through another VDOF optimisation sequence, with the defocus distance as the only variable. The DOF at 40% MTF did not improve. The weighting factors, for the different field angles and azimuths, were kept constant throughout the sequences described above.

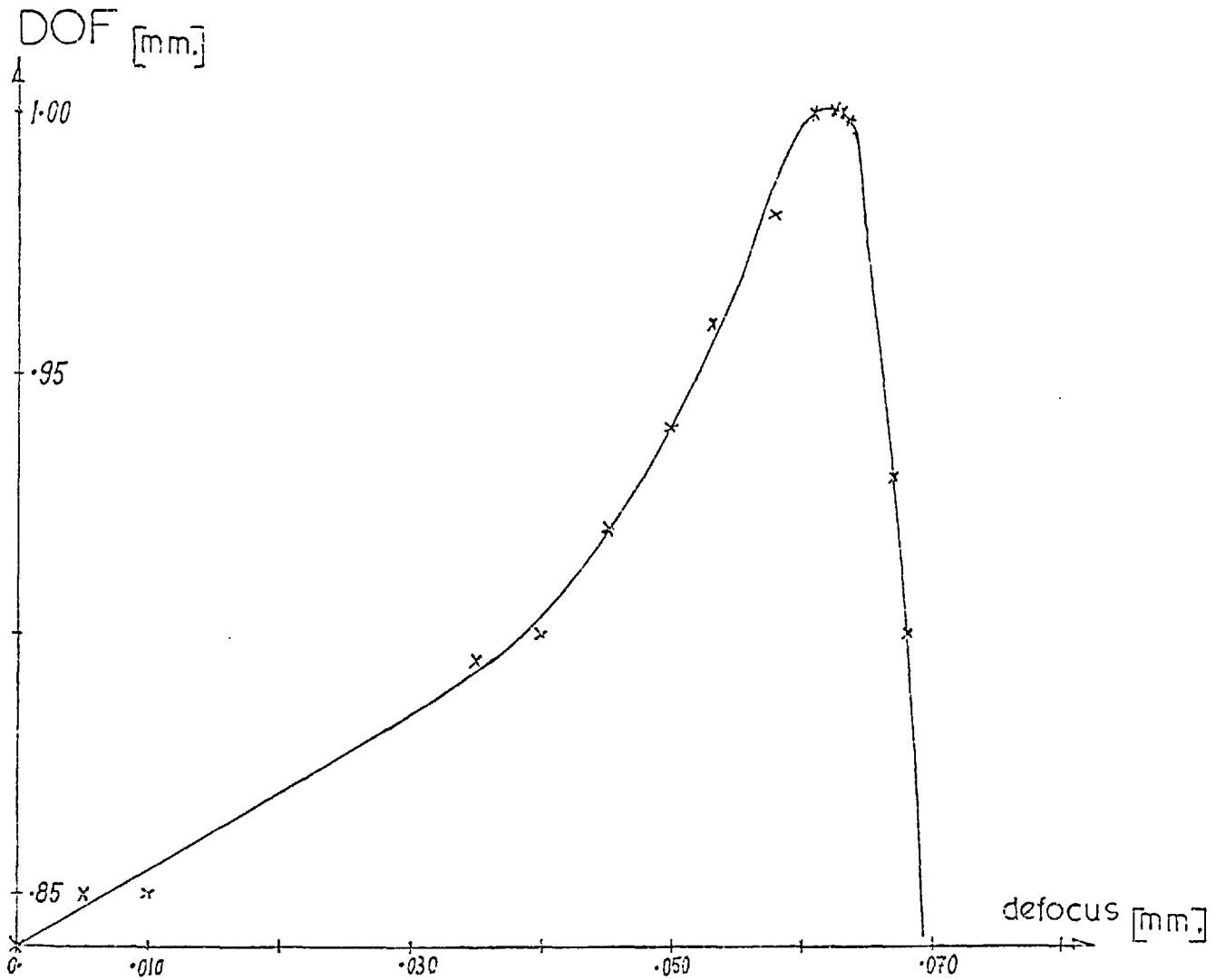

5.e DOF vs. the defocusing of the optimisation image planes (half the separation between the two image plane)

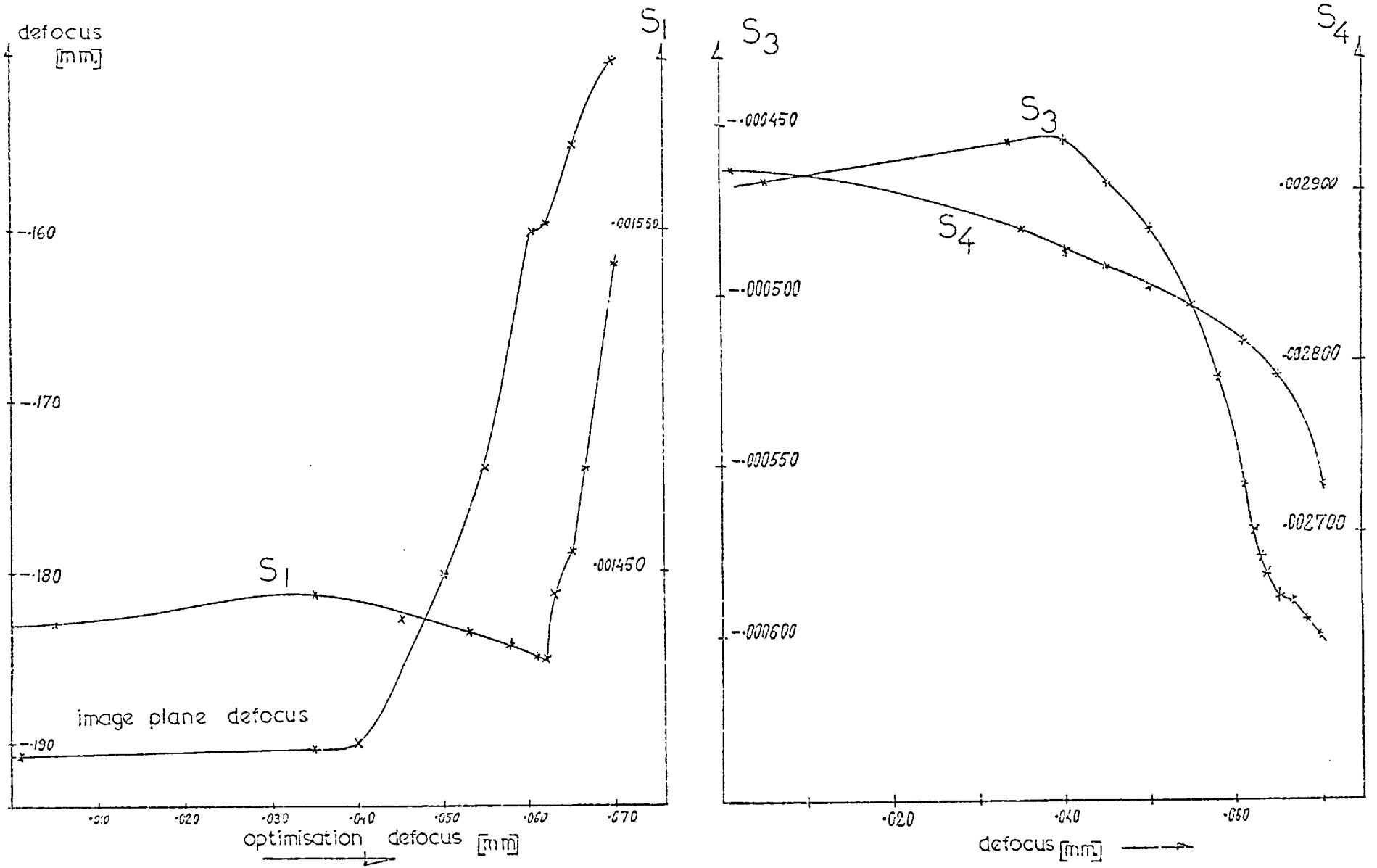

5.f Seidel aberration coefficient and the best image plane defocus from Gaussian position as a function of the defocusing distance of the optimisation image planes.

6 ELEMENTS COPYING LENS
⟵1 FOCAL LENGTH

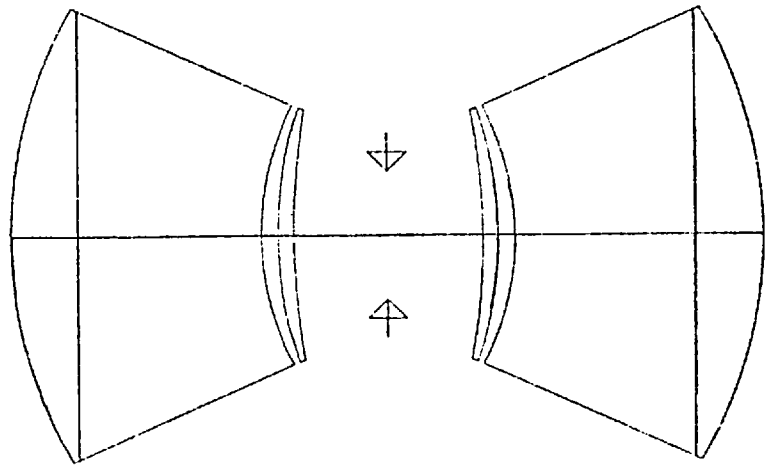

CURVE	SEPN	INDX/DIS
0.117560	0.000000	1.000000
0.002102	1.279360	1.694010
0.184137	3.428480	1.592630
0.130877	0.314320	1.000000
0.075793	0.292400	1.694010
0.000010	1.790370	1.000000
-0.075793	1.790370	1.000000
-0.130877	0.292400	1.694010
-0.184137	0.314320	1.000000
-0.002102	3.428480	1.592630
-0.117560	1.279360	1.694010
0.000010	-0.158290	1.000000

5.g
The optical system produced by the VDOF optimisation program.

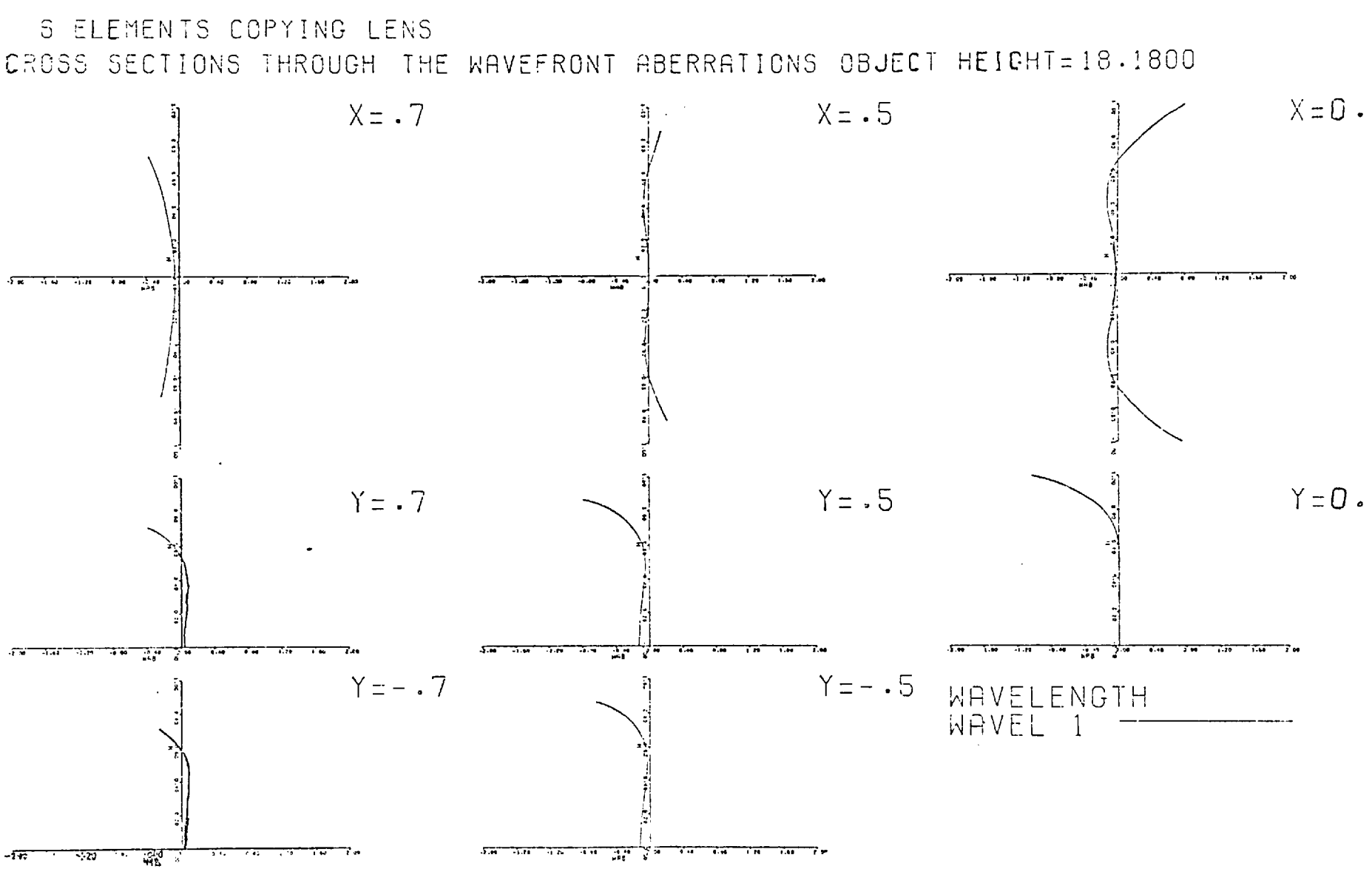

5.h The wavefront aberration, at the full field, for the system produced by the VDOF program.

The design produced by the VDOF technique was used as an input to a VGOTF optimisation, which is known to be sensitive to weighting factors and aberration balancing between the various field angles and azimuths, but little improvement was found. A tedious and time consuming process resulted in 1% increase in the DOF which was negligible compared with the 20% improvement in DOF produced by the earliest part of this sequence, as described above. The DOF measurement for this final design is illustrated in figure 5.i.

5.3 Optimisation Based on the VGOTF Program

The system produced by the VGOTF optimisation (shown in fig 5.a) was used as an input to another VGOTF optimisation sequence. It is clear from figure 5.d that the DOF is limited by the MTF values on axis and in the sagittal azimuth at object heights of both 12.73 and 18.18cm. The negative defocusing range is determined by the 0. and 18.18 cm values since the corresponding MTF curves intersect in the 40% MTF point. Therefore, it was assumed that it would be easier to control the positive defocusing limit of the DOF which was defined by a single MTF value, at 12.73 cm object height. At this field angle in the sagittal azimuth the peak of the MTF curve is about 90%, while the 18.18 cm sagittal azimuth peak at about 70%, thus the first MTF should be easier to control.

The weighting factors for the second field angle sagittal azimuth were therefore altered gradually from 10 to 35, but the weighting factors for the other field angles were kept constant at 10 throughout this optimisation sequence. As expected this resulted in a larger DOF; for very large weighting factors the MTF values of the first and third field angles started to deteriorate and this resulted in a slightly narrower DOF.

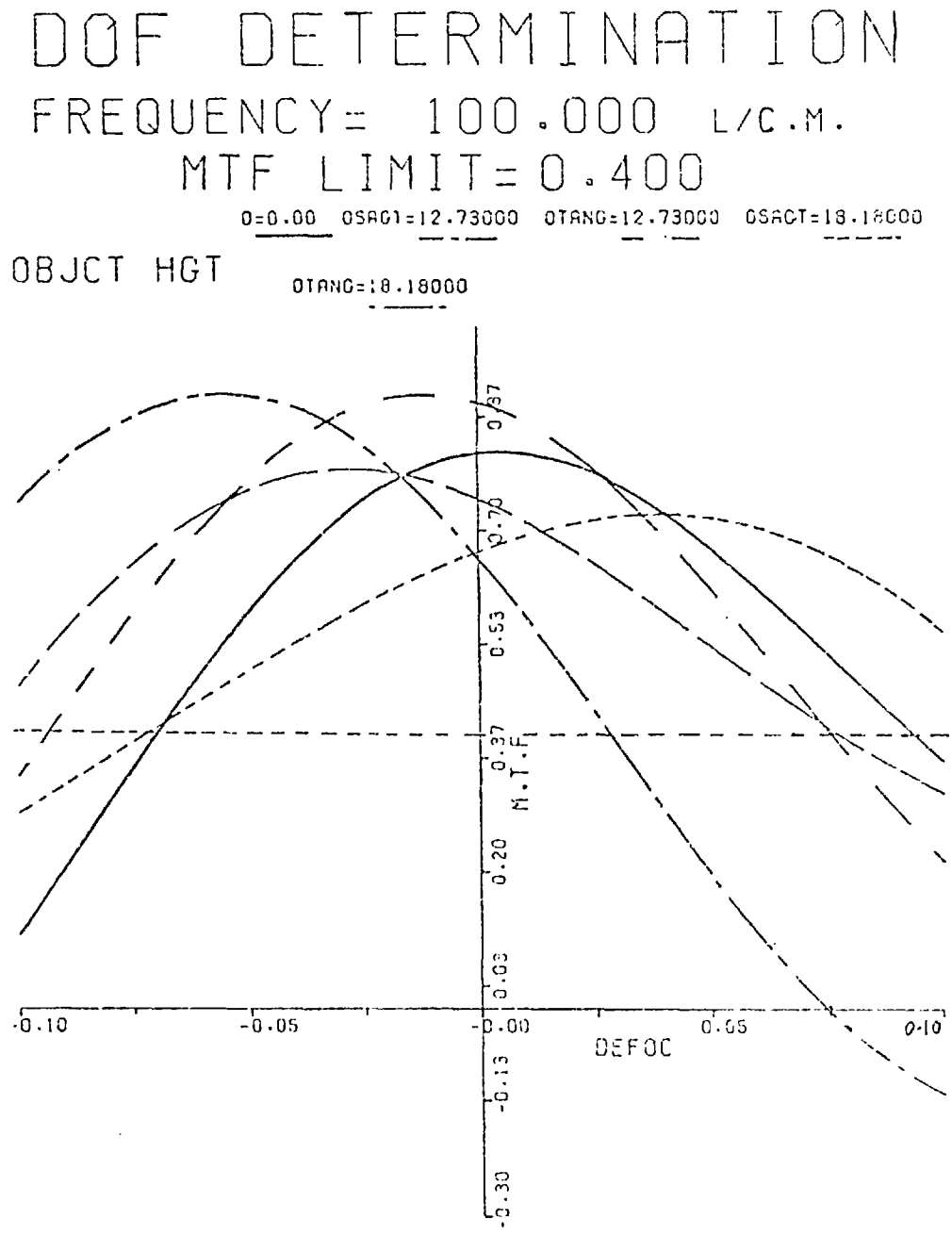

5.i

The DOF determination for the VDOF design.

The best design was produced with weighting factors of 25. this had a DOF of .111 cms. This single optimisation step improved the focal depth by nearly 32%, which is 10% better than that produced by the VDOF technique. The characteristics of the DOF as a function of the weighting factors of the second field angle sagittal azimuth are illustrated in figure 5.j.

The choice of the weighting factors is not critical, a slightly higher weight produced a system with .110 cm DOF which was only 1% below the optimum results but was easier to find and used less computer time. The Seidel aberration coefficients and the defocus of the best image plane of the final design from the Gaussian position, are sketched as a function of the weighting factor, in figure 5.k.

Three methods had been tried to improve the DOF further. the first of which consisted of a VDOF optimisation using the design produced by the above VGOTF sequence as an input. This resulted in a reduced DOF (.101 cms) which was the same as achieved by the VDOF optimisation described in the previous section.

A VGOTF sequence in which the weighting factors on the first field angle and the full field sagittal azimuth were increased with the intention of improving the DOF limit, in the negative defocusing range, whilst maintaining 40% MTF, did not prove effective.

An additional VGOTF sequence was tried with reduced weighting factors in the full field tangential case. This improved the DOF slightly up to .112 cm, which was less than 1% improvement on the initial system. Further reduction of the weighting factor of the second field angle, tangential azimuth, was not useful and did not improve the DOF.

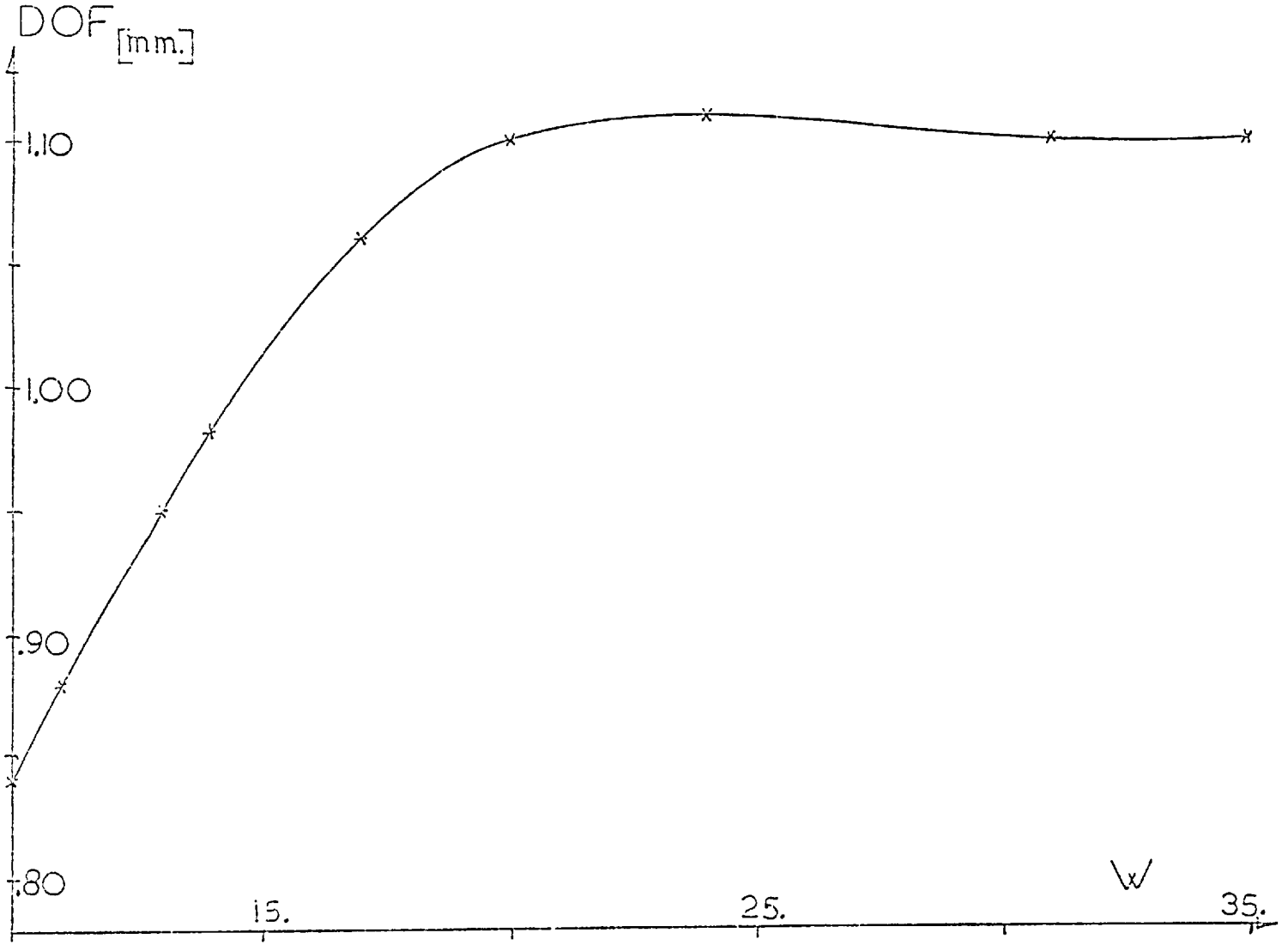

5.j DOF vs. the weighting factor, w, of the second field angle sagittal azimuth.

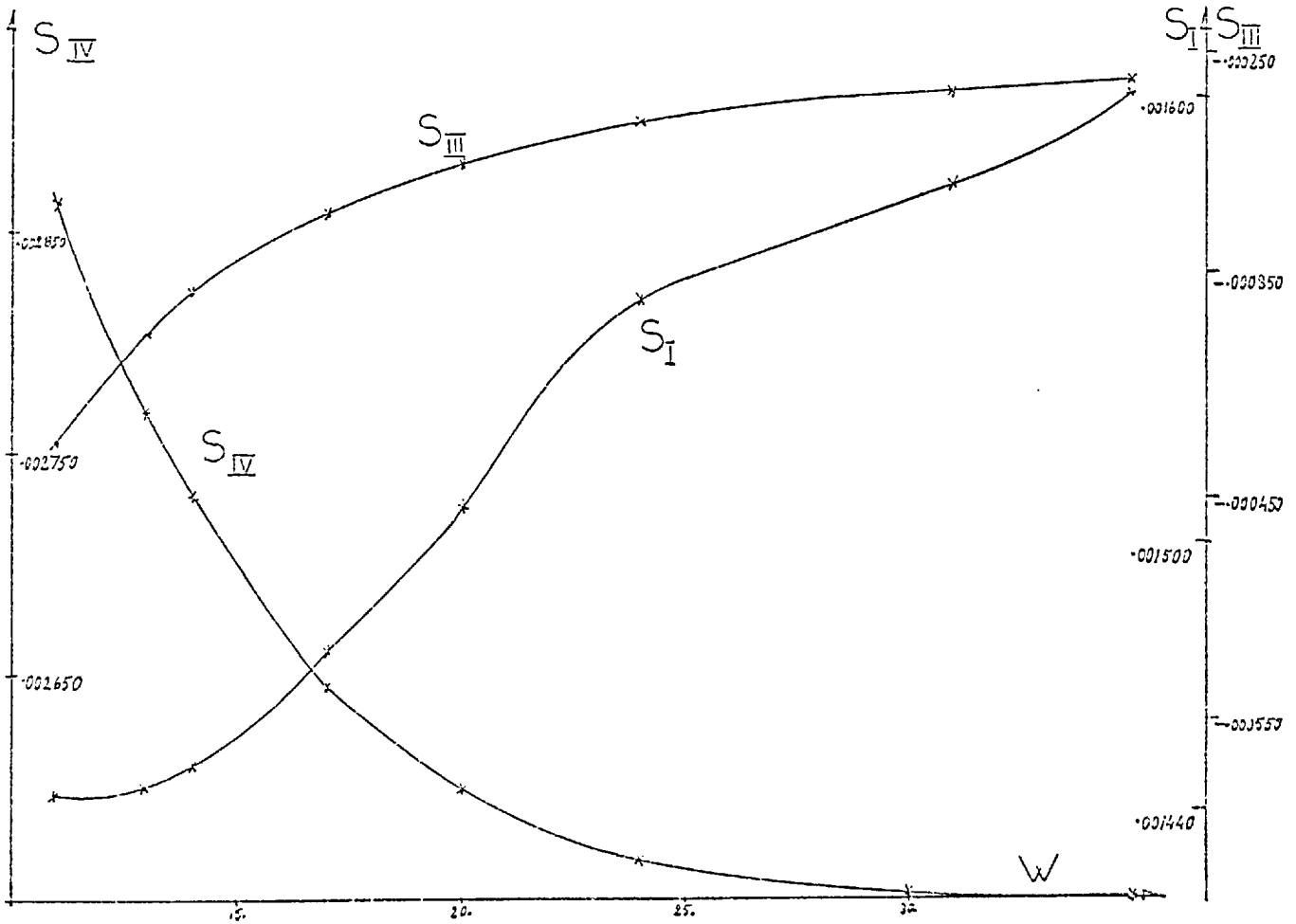

5.k Seidel aberration coefficients vs. w, the weighting factor of the second field angle sagittal azimuth

The balance between the various field angles and azimuths is complex and hence the optimum weighting factors may be chosen in various ways each yielding a solution but giving the same DOF. To illustrate this effect a system was chosen from the last sequence, with a weighting factor of 9. on the third field angle in the tangential azimuth, this resulted in a DOF of .103 cm (the initial value was .111 cm). The weighting factor in the second field angle sagittal case was then increased from its original value of 10. to a value of 14.8 producing a design with .112 cm DOF. This result is equivalent to the best result in previous optimisation sequence, a further improvement was not possible but a different balance of aberration was found which maintained the same DOF. The optical system and the DOF determination curves are shown in figure 5.1 for the first design to produce .112 cm in focal depth.

5.4 Verification of the Results

The above results show that in the case of the six element copying lens for monochromatic work the VGOTF optimisation is suitable and more sophisticated and expensive methods are not advantageous. If the way in which this optimisation is carried out, is examined, two points are found which require investigation. The first is the use of the geometrical MTF values as defined in this case, and the second is the determination of the DOF which is carried out by considering only three field angles; the full field, the zero field angle and another intermediate field angle chosen arbitrarly. Therefore, a confirmation of the results was carried out by means of the diffraction OTF program (see appendix A for details); the optical system produced by the first leg of the VGOTF technique, with DOF .111cm, was tested by the

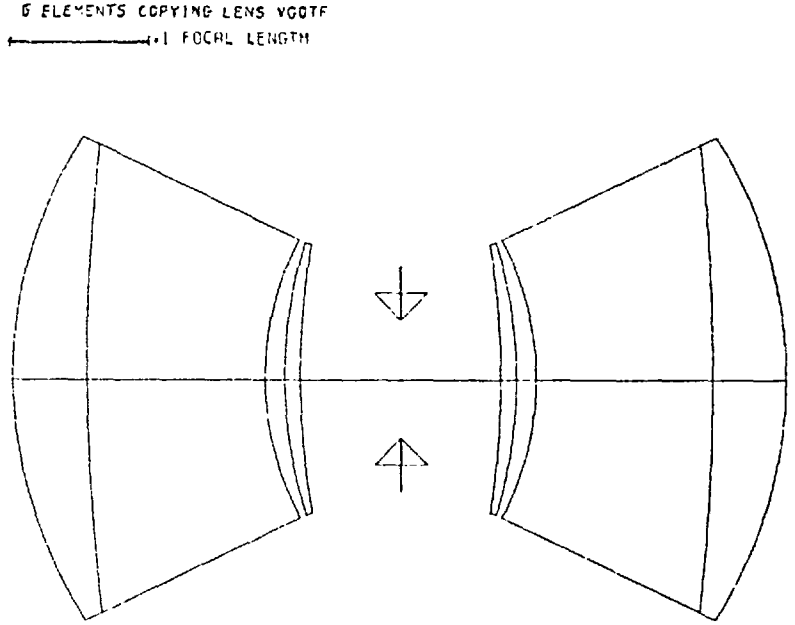

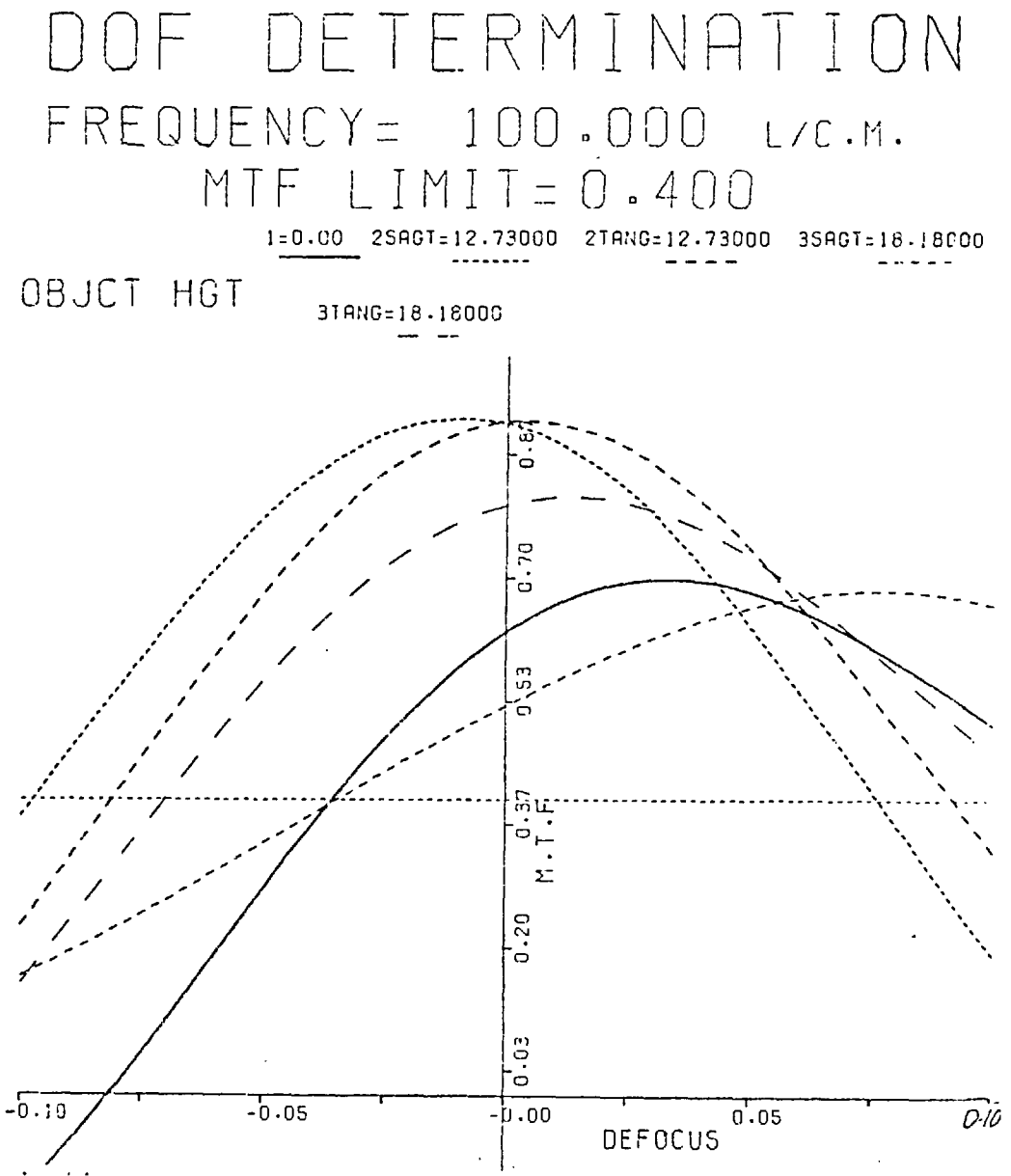

CURVE	SEPN	INDX/DIS
0.124089	0.000000	1.000000
0.026760	1.380120	1.694010
0.186930	3.328360	1.592630
0.121029	0.369620	1.000000
0.068121	0.291960	1.694010
0.000010	1.881800	1.000000
-0.06812	1.881800	1.000000
-0.12103	0.291960	1.694010
-0.18693	0.369620	1.000000
-0.02676	3.328360	1.592630
-0.12409	1.380120	1.694010
0.000010	-0.223490	1.000000

5.1 The system with largest DOF and its DOF determination

diffraction OTF program. The comparison between the geometrical and diffraction results at the "best image plane" are given in figure 5.m. The maximum deviation between the two MTF curves in the three field angles used throughout the optimisation is 10% at a frequency of 150 cycles/cm, at 100 cycles/cm which is the optimisation frequency, the deviation between the geometrical and diffraction MTF values is minimal.

Figure 5.n compares the DOF determination in the cases of geometrical and diffraction MTF, and it is clearly shown that both calculations lead to the same results. Similar studies carried out on other optical systems confirmed those results.

In figure 5.p the DOF range for 12 objects' heights was plotted. The three field positions used throughout the optimisation procedure are clearly dominating the DOF range for the system. In this case the DOF derived from these three object positions is about 1.5% larger than the real range established by considering 12 field angles. This is largely due to the realistic choice of the optimisation field angles (the two extreme field angles and .7 of the full field), and to the fact that the same three object heights were used at all stages of the design. Similar results were obtained for six designs chosen from various stages of the above optimisation procedure.

A simple diagram, figure 5.q, can be used to summarise the various optimisation sequences described in this chapter.

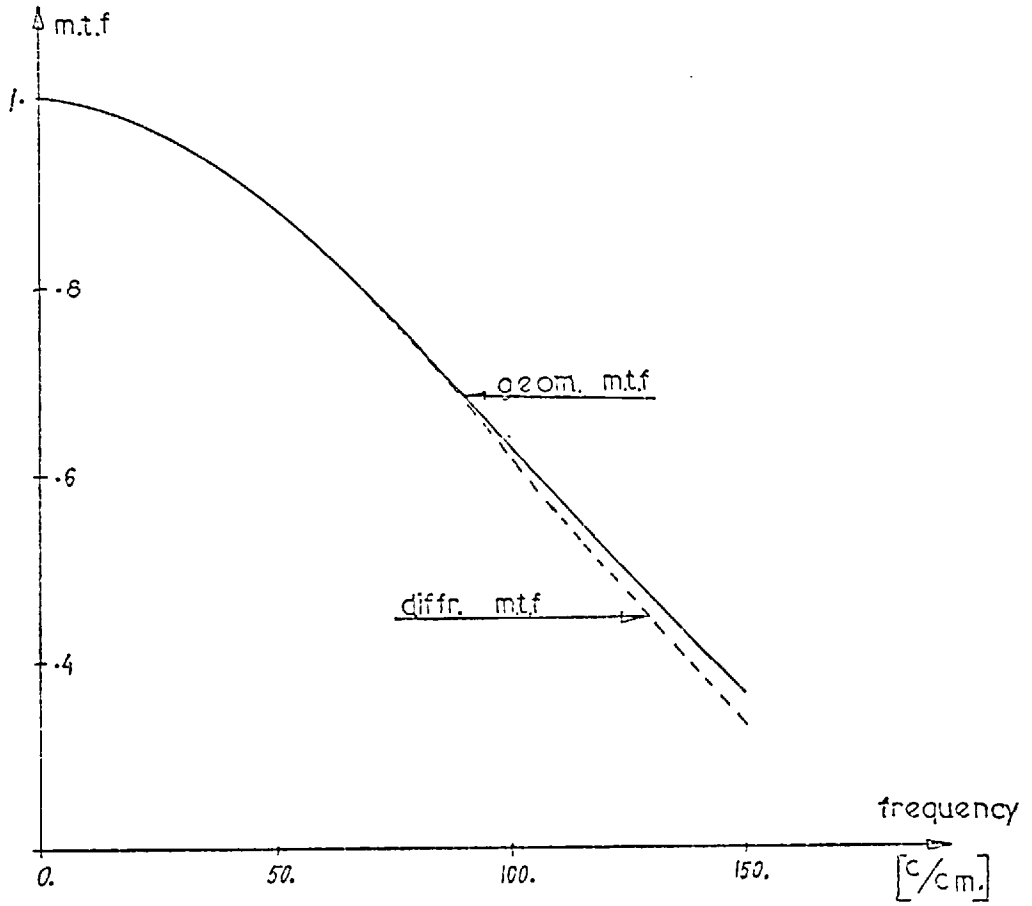

5.m Comparison between the geometrical and diffraction MTF, in the "best image plane" on axis. This system was produced by optimisation at 100 cycles/cm, where the deviation is near 2%.

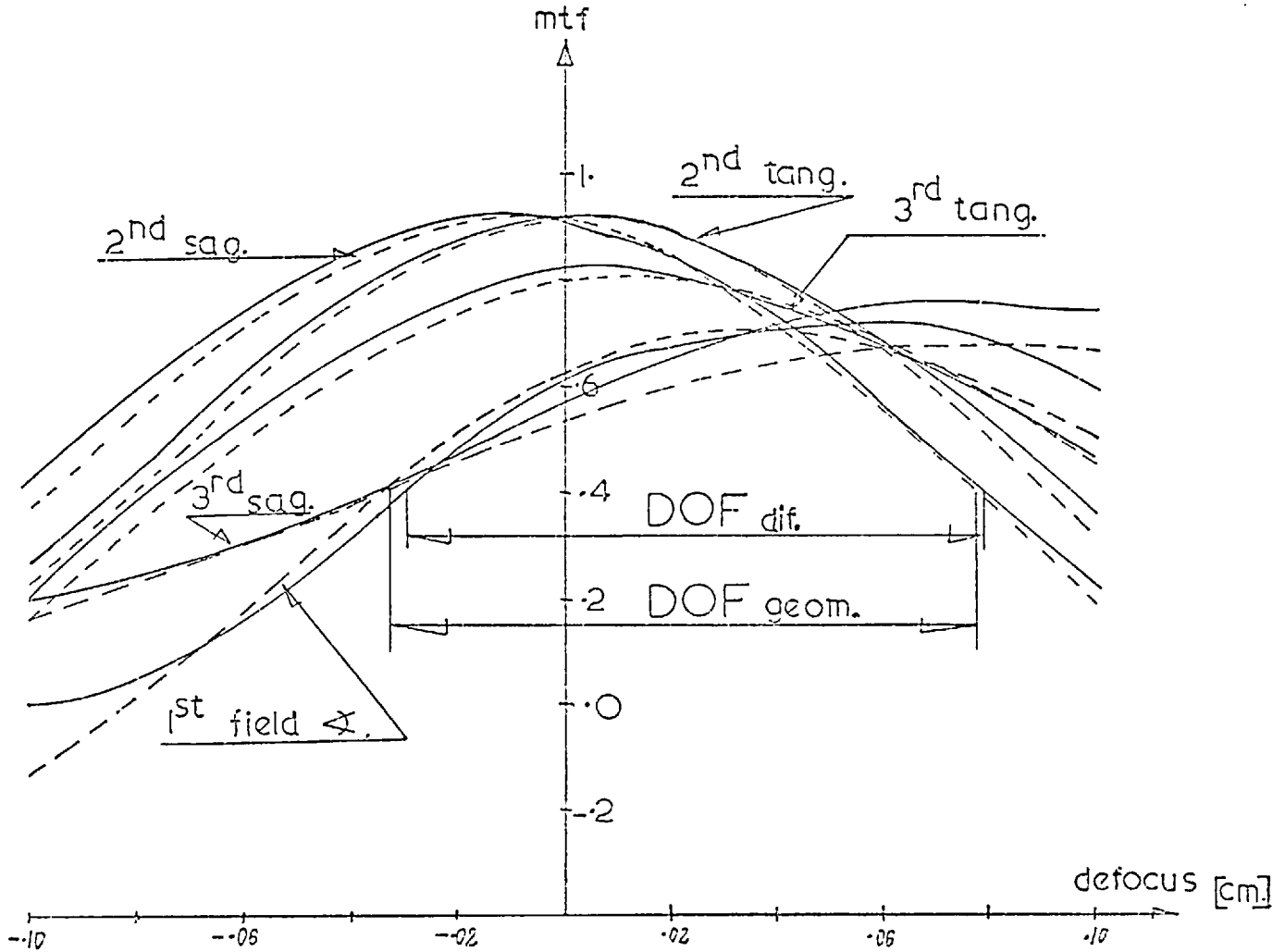

5.n DOF determination using diffraction and geometrical MTF values, the diffraction MTF is drawn in full lines and the geometrical values in dashed lines. The deviation in the DOF values is 1.5%.

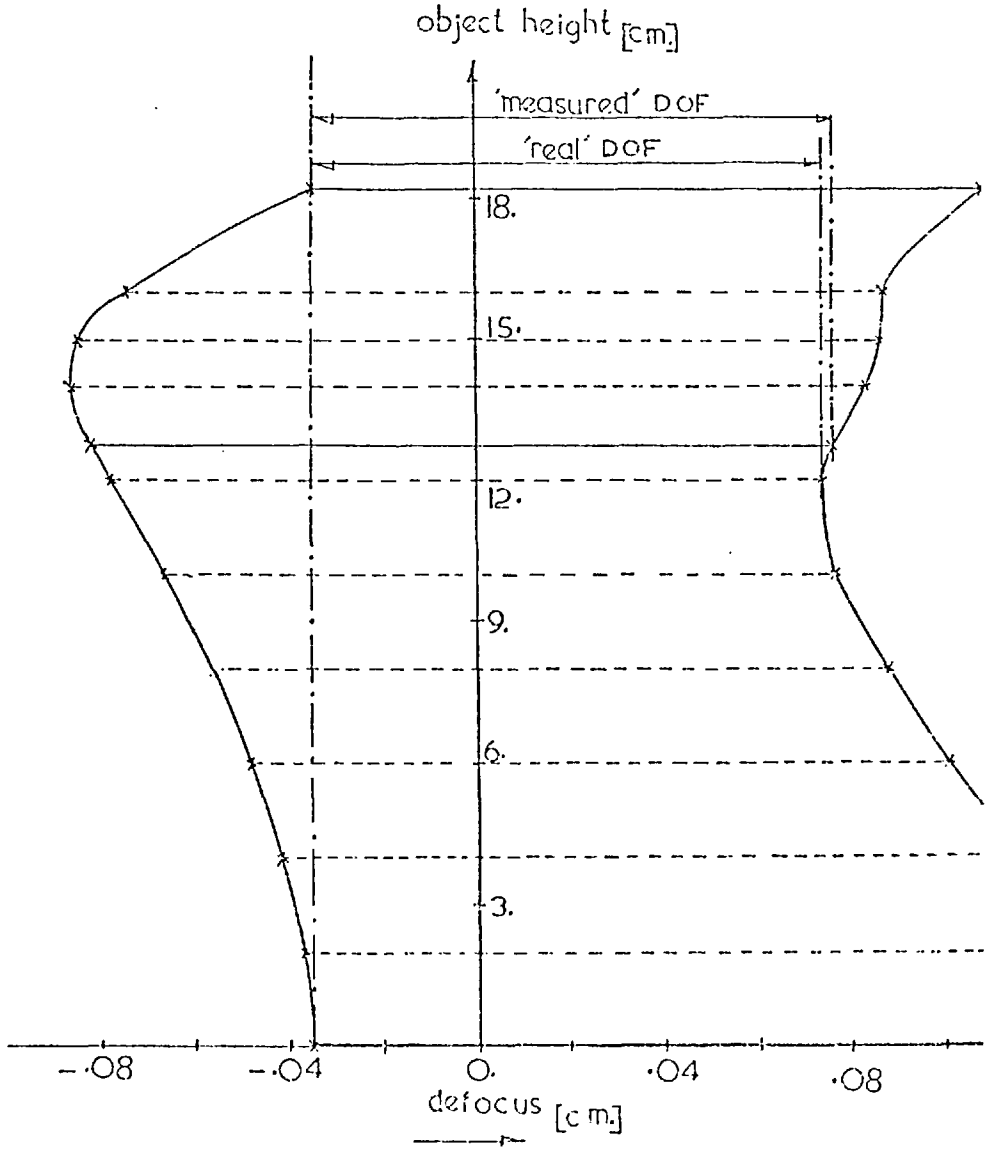

5.p

Comparison between the "measured DOF" based on the three field positions used through the optimisation and the "real DOF" measured at 12 object positions. The difference in this case is 2%.

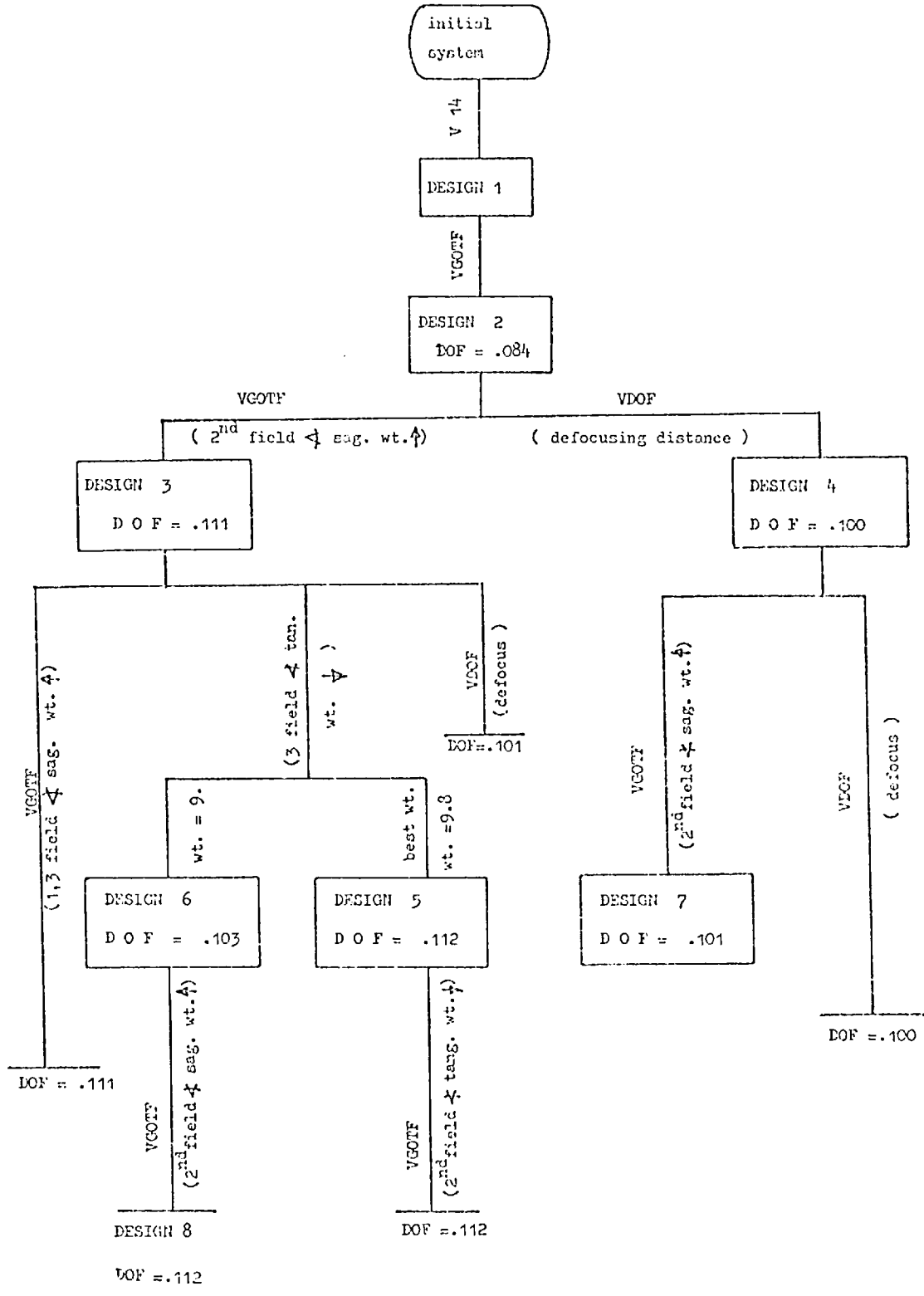

5.q A schematic diagram showing the various optimisation techniques used in Chapter 5.

CHAPTER 6

SIX ELEMENTS MONOCHROMATIC REDUCING LENS

6.1 The Design of a Six Elements Monochromatic Reducing Lens

In this chapter, the designs of a monochromatic reducing lens is described. The basic design was a derivative of the monochromatic copying lens, described in chapter 5, but it has been designed to reduce an A4 size original by two, hence the maximum height of the image is 9.09 cm, and the magnification $-\frac{1}{2}$. This design has a stop in the central air space and the specification was for a numerical aperture of .0670 working at a wavelength of 500 nm, yielding in this case a f/4.975 lens which was considered practically (e.g.exposure determination) as a f/5 lens. The object-to-image distance, or throw, was controlled at 112.5 cm and the focus was initially set to 25 cm which resulted in an object-to-lens distance of 69.05cm and lens-to-image distance of 30.28cm, the total glass thickness was 10. cm. As with the copying lens, described earlier, two types of glass were found to be sufficient and the same glasses as before were used. The minimum limits for axial separation and edge thickness were set to .125 and .01 cm respectively.

The design procedure was divided into two main stages; a V14 optimisation with 24 rays at four field positions (the same field positions and rays as for the copying lens were used) followed by a VGOTF optimisation with 50 rays at three field positions. The optimisation frequency was gradually increased up to 100. cycles/cm, which was the frequency of interest, and a system was produced with maximum wavefront aberration of 0.5.

The final VGOTF design is shown in figure 6.a, the characteristics of the MTF are shown in figure 6.b. The DOF determination,

for the above design, is illustrated in figure 6.c, and is 1.016 mm: The MTF characteristics in this case are different from those of the basic copying lens, described in chapter 5 (fig.5d). All the curves peak near the image plane and their maximum value is above 83%, mainly around the 90%. Therefore it is not possible to improve the already satisfactory OOF value as dramatically as in the previous case.

6.2 OOF Optimisation Based on the VOOF Program

The VGOTF design, with OOF of 1.016 mm, had been used as an input in a VOOF optimisation series. The defocus, which is half the separation between the two optimisation image planes, was the only variable throughout this sequence. The value of the optimisation defocus is limited by the aberration product formula, equ. 4-11, which ensures that the sine term stays within the interval $(-\pi/2 \; ; \; \pi/2)$.

An optimum OOF value, of 1.120 mm, was found by a defocus of .0600 cm. As predicted earlier, the improvement in focal depth was of the order of 10%, and further optimisation techniques failed to extend this OOF value.

The OOF values of the systems produced in this design sequence are illustrated as a function of the optimisation defocus, in figure 6.d. The structure of the merit function used in this sequence, is responsible for the sharp drop in OOF with increased defocus values. For example, a defocus of .0605 cm resulted in OOF of .056 cm which is half the optimum value and about 40% below the focal depth of the initial system.

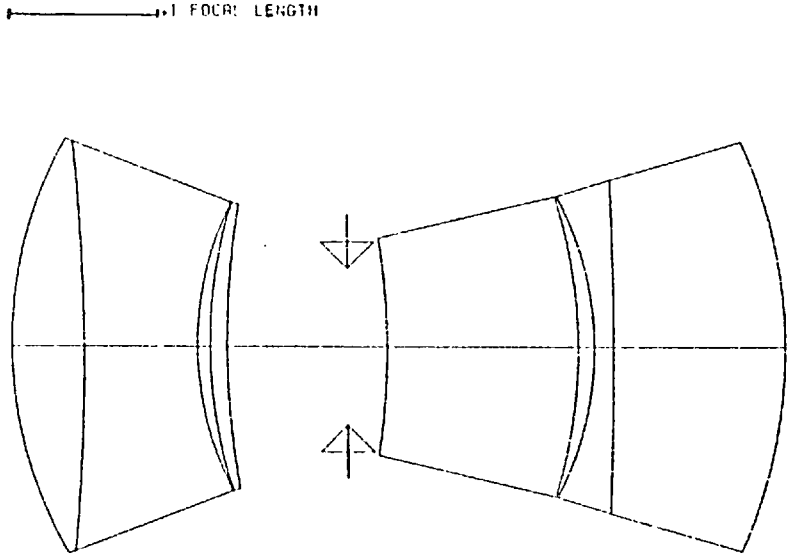

CURVE	SEPN	INDX/DIS
0.139657	0.000000	1.000000
-0.02835	1.226840	1.694010
0.186823	1.930440	1.592630
0.122435	0.218890	1.000000
0.069628	0.292240	1.694010
0.000010	2.052300	1.000000
-0.08582	0.678900	1.000000
-0.11677	3.274100	1.694010
-0.18214	0.277720	1.000000
-0.01539	0.333420	1.592630
-0.11874	2.947010	1.694010
0.000010	-0.065270	1.000000

6.a Final VGOTF reducing lens

ON AXIS

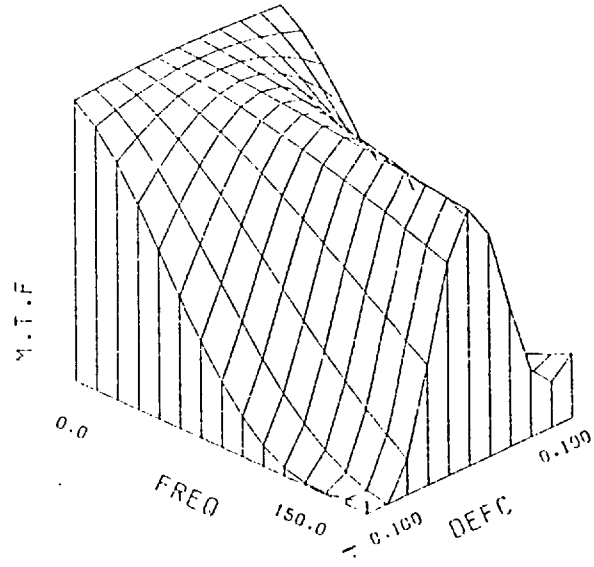

FIELD ANGLE =9.54 DEGREES

SAGITTAL M.T.F TANGENTIAL M.T.F

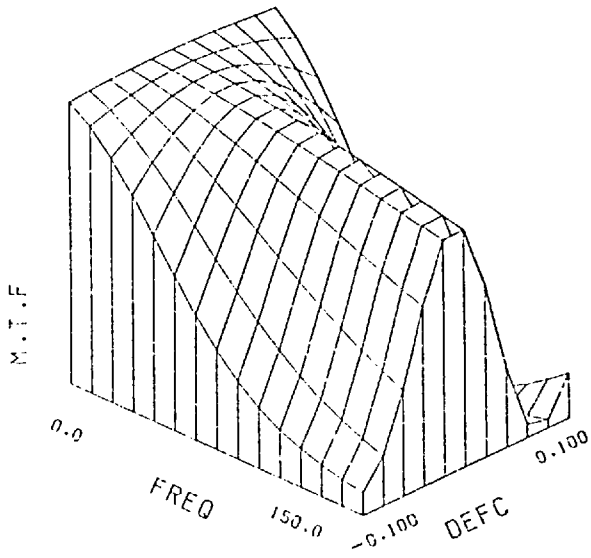

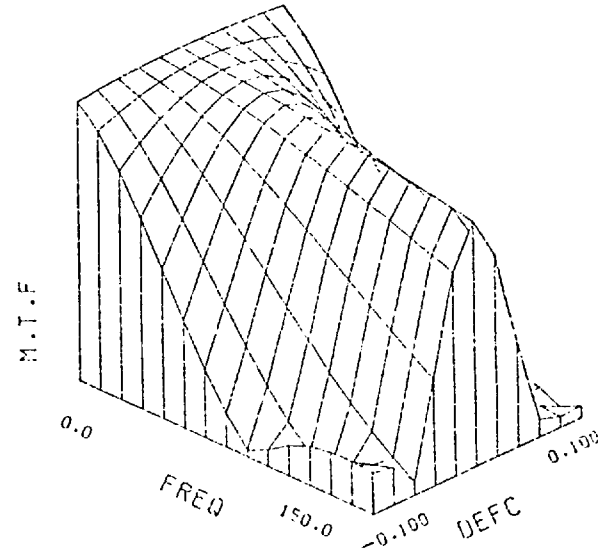

FIELD ANGLE = 13.53 DEGREES

SAGITTAL M.T.F TANGENTIAL M.T.F

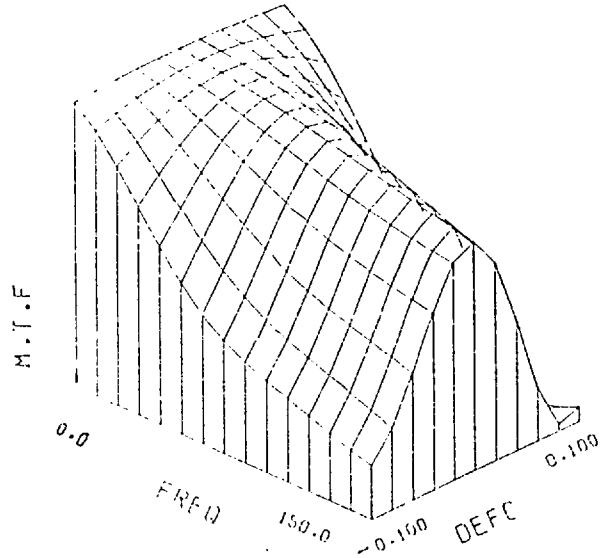

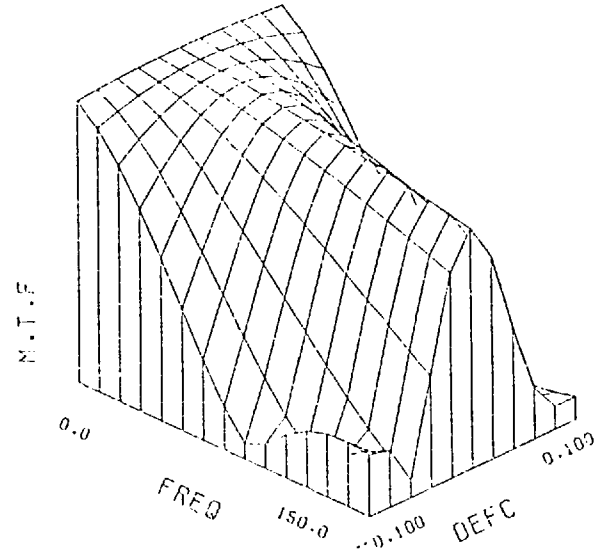

5.b MTF characteristics, for final VOCTF lens, at the optimisation field positions.

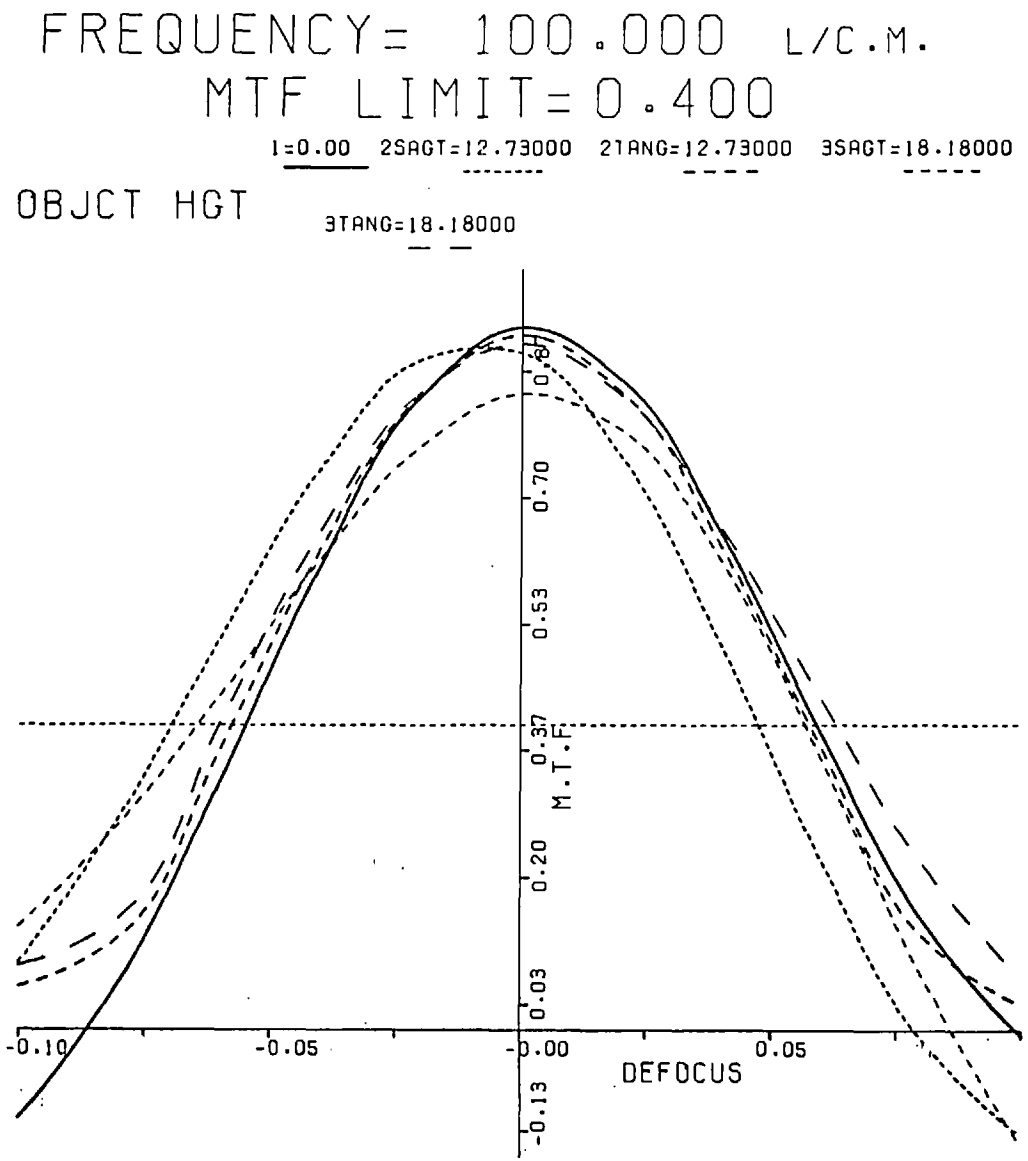

6.c DOF determination for the final VGOTF lens

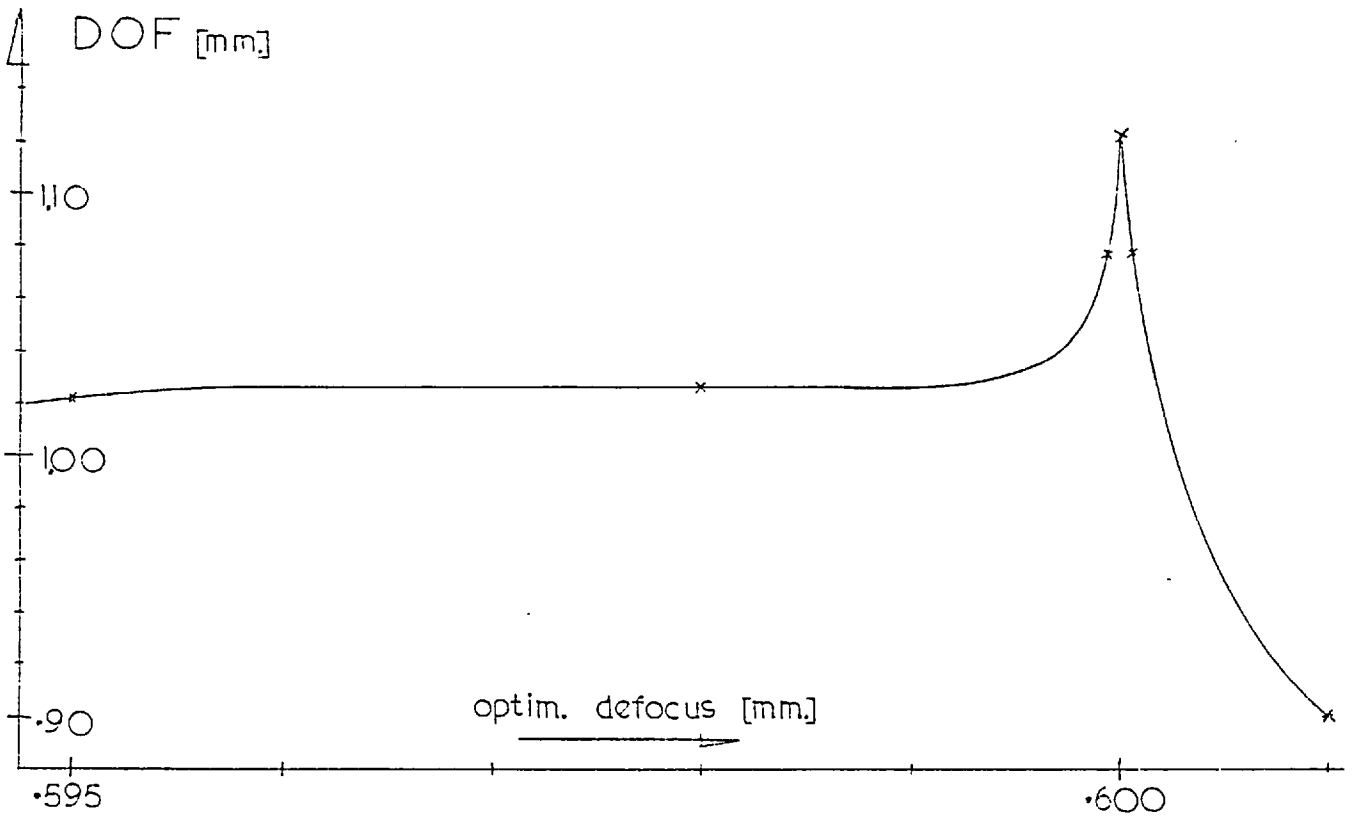

6.d DOF vs. optimisation defocus for the VDOF sequence

The optimum system obtained in this series is shown in figure 6.e, the characteristics of its MTF are illustrated in figure 6.f and the OOF determination is respresented in figure 6.g below;

The Seidel aberration coefficients for the above sequence were studied, and are plotted as a function of the optimisation defocus in figure 6.h.

6.3 OOF Optimisation Based On The VGOTF Program

As with the copying lens described in chapter 5, the second field position defined by an object height of 12.73 cm in the sagittal azimuth, was the positive defocus range limit in the OOF determination (see fig.6.c). A VGOTF optimisation sequence was tried, throughout which the weighting factor at the second field angle sagittal case, was varied. This weighting factor was increased from 10 to 40, and the corresponding OOF values are shown in figure 6.i.

The optimum factor of 27. resulted in a system with OOF just above .104 cm, which was a 2% improvement on the initial focal depth. Further increase of the weighting factor resulted in deterioration of the negative defocus range of the MTF curves at the frequency of 100. cycles/cm, which reduced the OOF value. The optimum system for the sequence and its OOF determination are shown in figure 6.j.

FINAL VDOF DESIGN (OFF=0.0500 CM.)
) FOCAL LENGTH

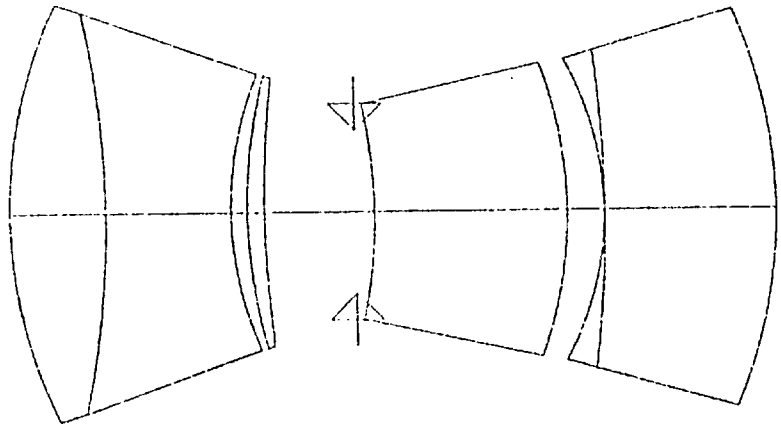

CURVE	SEPN	INDX/DIS
0.125754	0.000000	1.000000
-0.063224	1.581950	1.694910
0.171369	2.062190	1.592630
0.117284	0.260000	1.000000
0.057898	0.280020	1.694910
0.000010	1.522740	1.000000
-0.113755	0.305610	1.000000
-0.143215	0.200000	1.694910
-0.191533	0.614900	1.000000
-0.048322	0.010000	1.592630
-0.119491	2.858270	1.694910
0.000010	-0.029380	1.000000

6.e The final VDOF design.

FIELD ANGLE = 9.54°

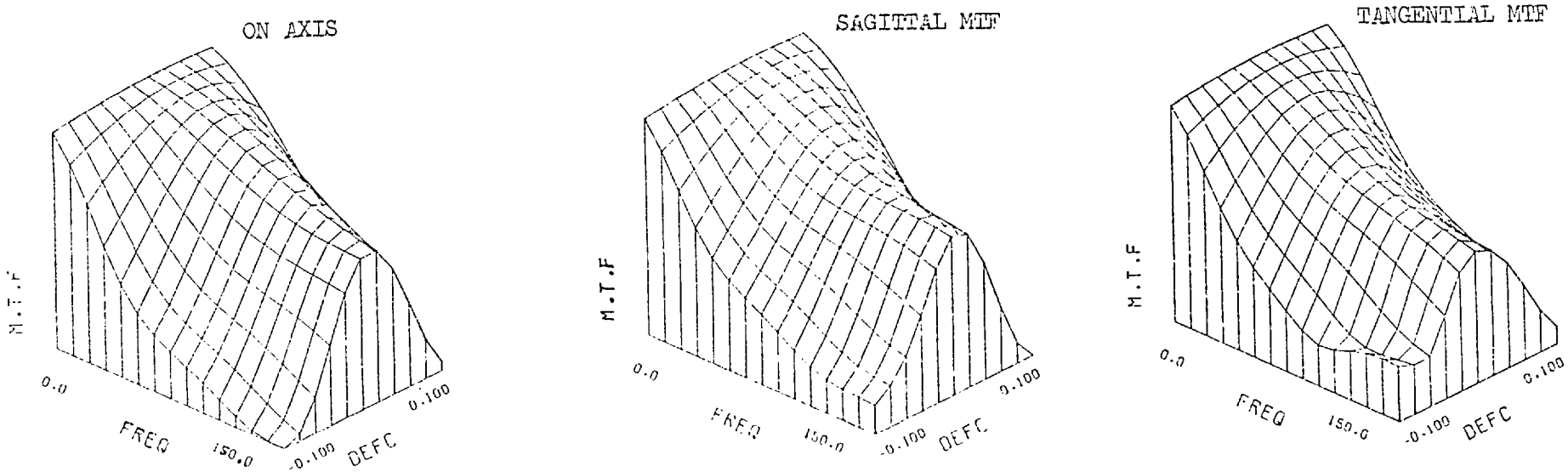

FIELD ANGLE = 13.51°

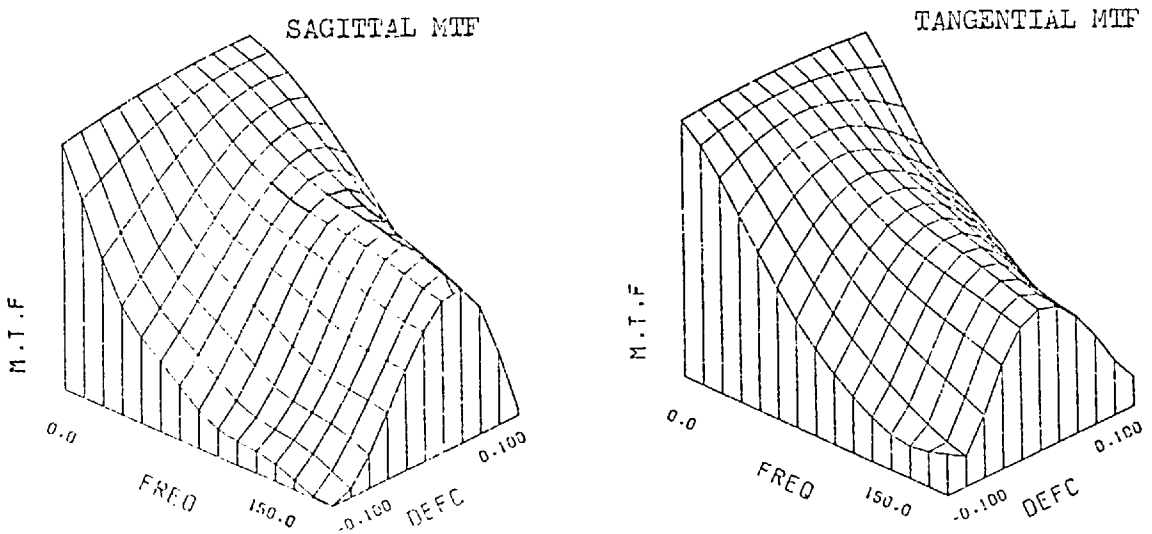

6.f MTF characteristics for the final VDOF system

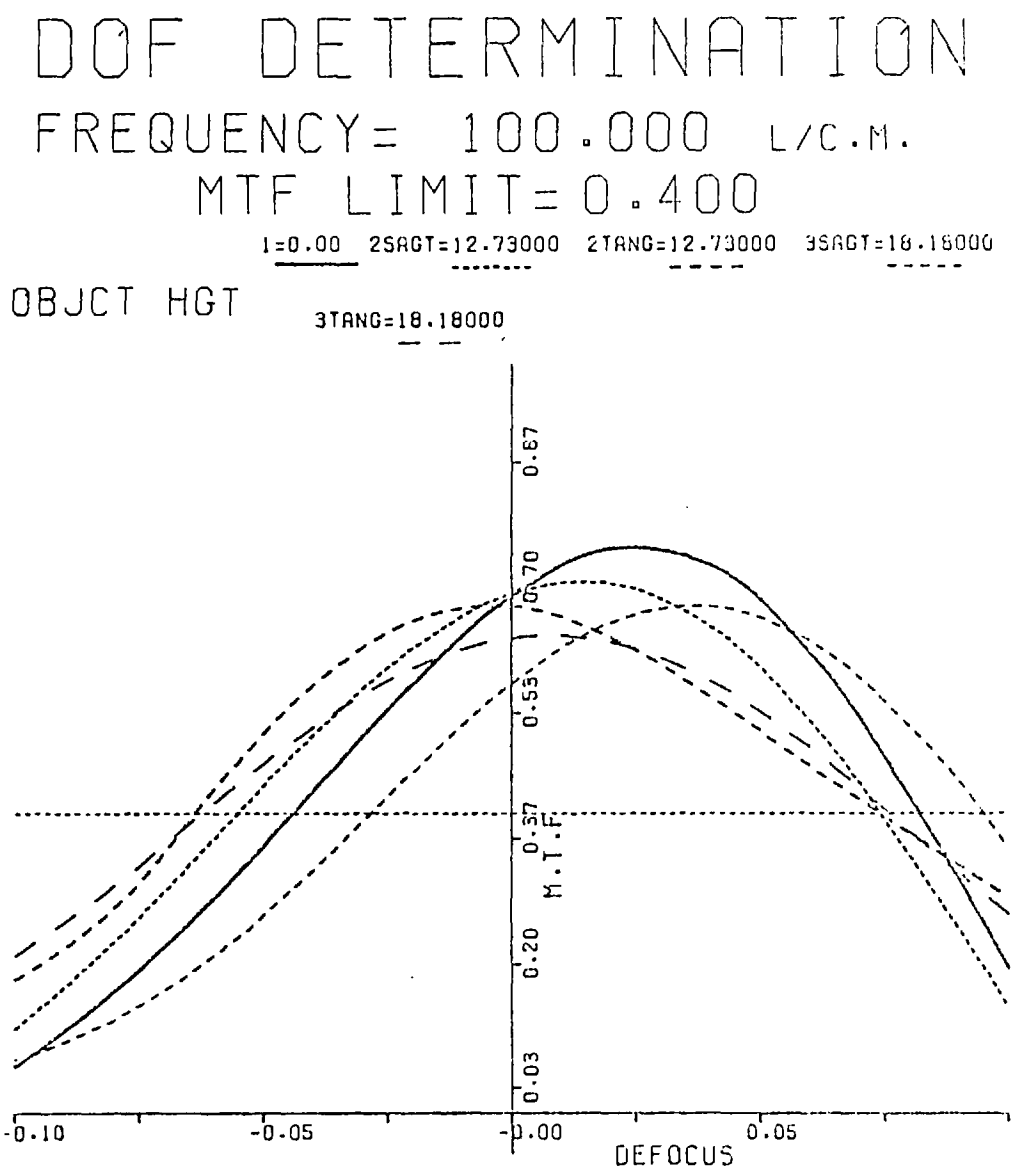

6.g DOF determination for the final VDOF lens

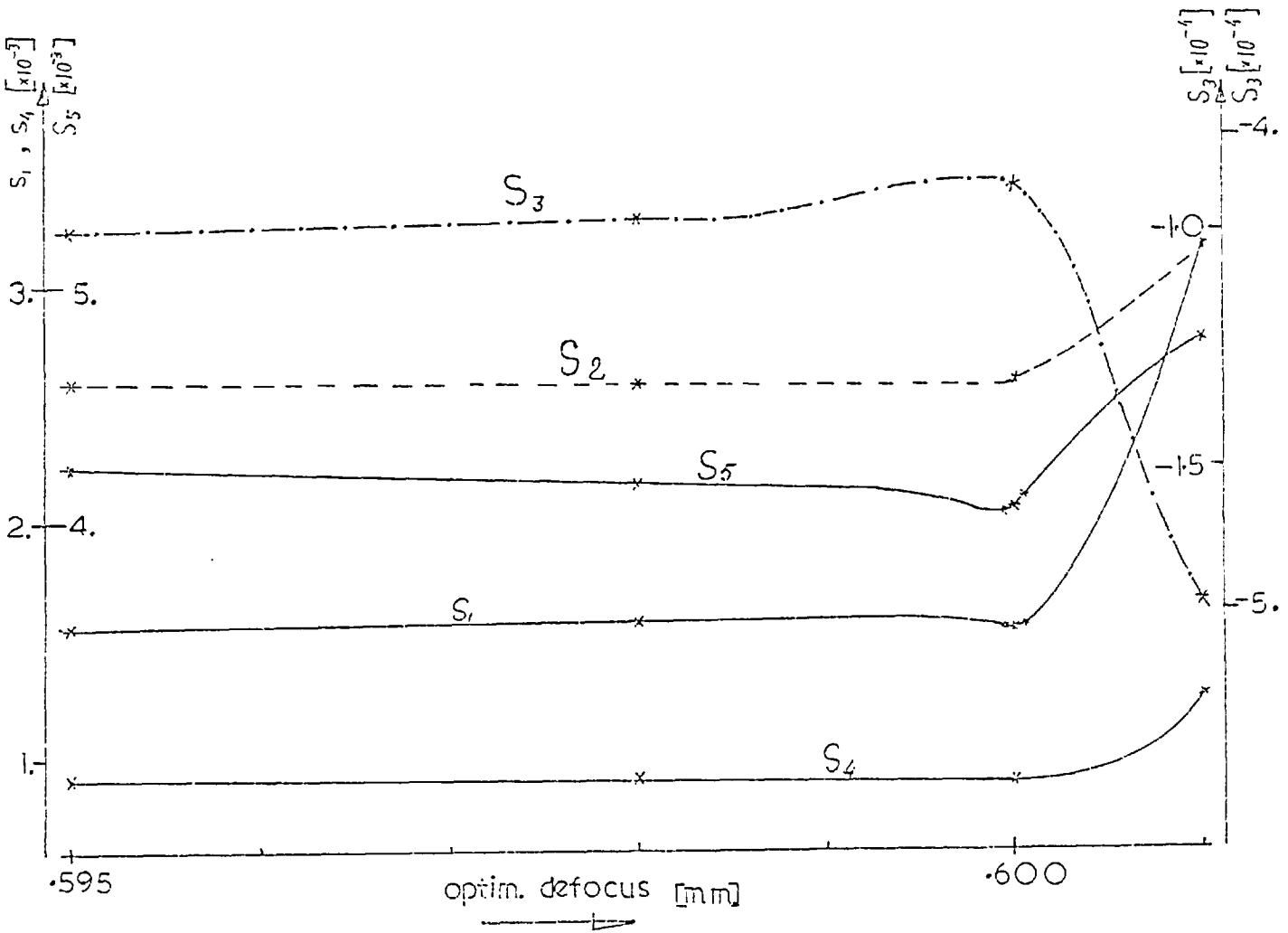

6.h Seidel aberration coefficients vs . optimisation defocus for the VDOF optimisation sequence.

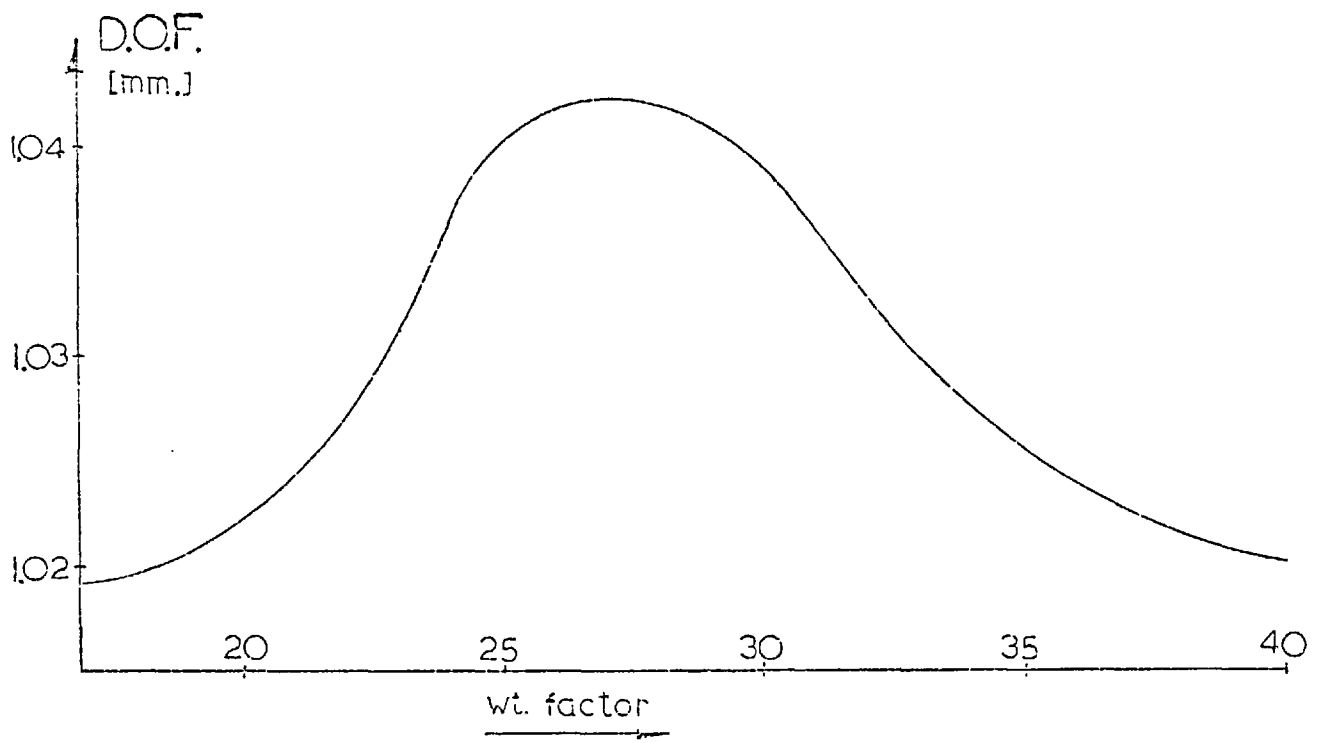

6.i DOF vs. weighting factor at the second field position sagittal azimuth for the VGOTF sequence.

FINAL VGOTF DESIGN (WT.=27.)

.1 FOCAL LENGTH

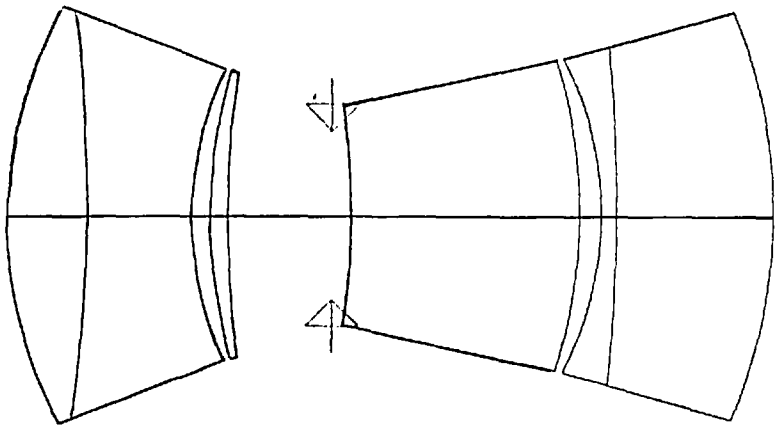

DOF DETERMINATION

FREQUENCY= 100.000 L/C.M.

MTF LIMIT= 0.400

1=0.00 2SAGT=12.73000 2TANG=12.73000 3SAGT=18.18000

OBJCT HGT 3TANG=18.18000

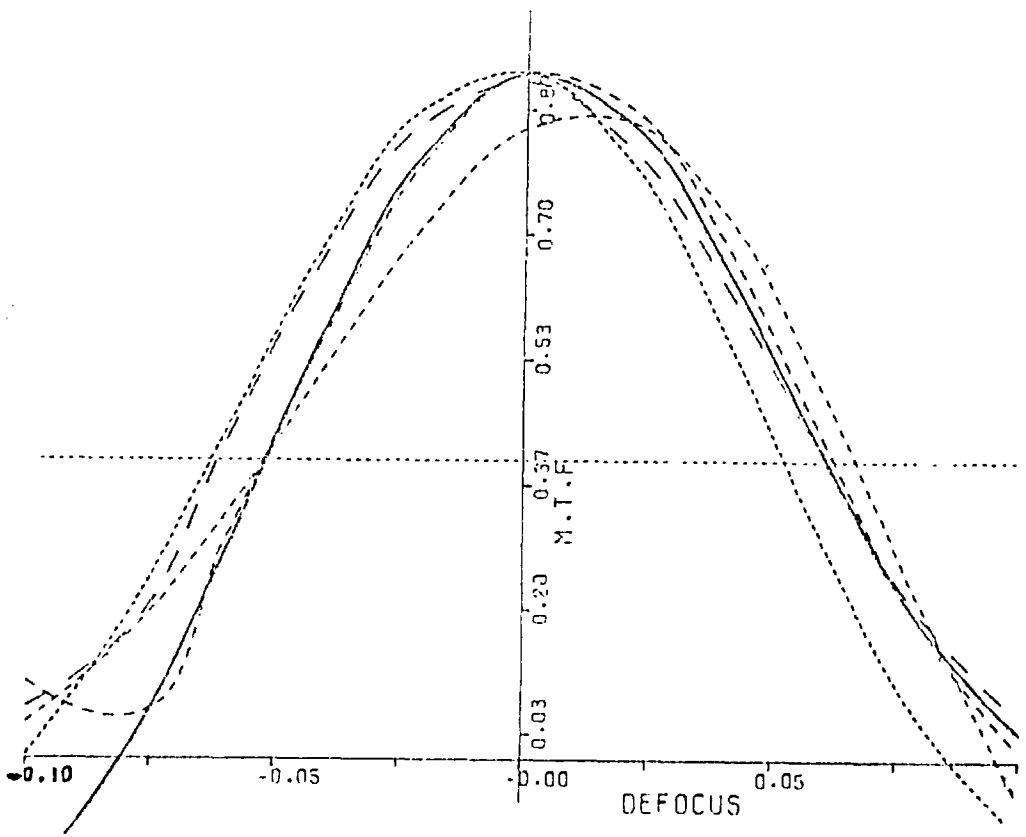

CURVE	SEPN	INDX/DIS
0.143271	0.000000	1.000000
-0.04473	1.343860	1.694010
0.187197	1.704410	1.592630
0.119247	0.314970	1.000000
0.062879	0.283610	1.694010
0.000010	1.709520	1.000000
-0.09220	0.313750	1.000000
-0.11764	3.791560	1.694010
-0.17991	0.361170	1.000000
-0.03375	0.254880	1.592630
-0.11556	2.630070	1.694010
0.000010	-0.078050	1.000000

6.j The optimum system and its DOF determination for the VGOTF sequence.

CHAPTER 7

THE DESIGN OF A SIX ELEMENTS COPYING LENS FOR POLYCHROMATIC WORK

7.1 The Design of a Six Elements Copying Lens

This Chapter describes the design of a copying lens for polychromatic work. Typical photocopying machines use gas discharge lamps as illuminating sources, which results in a spectral response curve with a finite number of lines. The main disadvantages of such a system might be low spectral sensitivity to objects of certain colour and a poor match between the emission spectrum of the light source and the spectral sensitivity of the reprographic process. A common means of correcting such systems might be by an appropriate mixture of gases at the right pressure, improved by incorporating fluorescing phosphors. The phosphor will broaden the spectral lines of the illuminating source and hence change the characteristics of the relative spectral response of the entire system.

As far as the optimisation of lenses for such systems is concerned, there are a few additional parameters to be considered. The number of the aberrations incorporated in the merit function must be increased, and even the simplest merit function such as the sum of the third order Seidel Coefficients, has to take C_1 and C_2 into consideration. The introduction of the secondary spectrum complicates the choice of the "best" image plane, the magnification variations within the spectral region at which this system is used will result in higher distortion values in non-symmetrical designs.

As far as the system parameters are concerned, the choice of the right glasses becomes more critical and requires more attention. The input data for the optimisation program takes into account the various wavelengths required and this results in additional weighting factors for the corresponding aberrations.

In this particular case a mercury source was considered with spectral emission at the e, g and h mercury lines with corresponding wavelengths of 546.07, 435.84 and 404.66 nm. The mercury green line was enhanced by means of phosphor, which resulted in the following spectral sensitivity for the entire system; 30% sensitivity at 404.66 nm, 75% at 435.84 nm and 100% at 546.07 nm. The ratio of the weighting factors for these colours was the square root of the ratio between the corresponding relative sensitivities, since the merit function is the sum of products of the squared aberrations by the squared weighting factors.

The initial system used for this design was equivalent to the monochromatic design, described in Chapter 5, but used La KN9 Kz FS 1 and Lg SK glasses (from the Schott range) which means that each of the triplets combined in this symmetrical lens incorporates three types of glass (whereas two glasses were used in the monochromatic case).

During the early stages of the design the V14 program was used, when the magnitude of the aberrations permitted, the VGOTF program was applied increasing the optimisation frequency gradually up to 100. cycles/cm which was the frequency of interest.

The final design had a numerical aperture of .04464 and an effective focal length of 25.18 cm, the throw length was 100.02 cm. The longitudinal range, containing the "best" image planes for the three wavelengths considered, was .086 cm.

The final VGOTF design is illustrated in figure 7.a, the MTF curves are shown in figure 7.b for objects with equal reflection coefficients in the optimisation wavelengths.

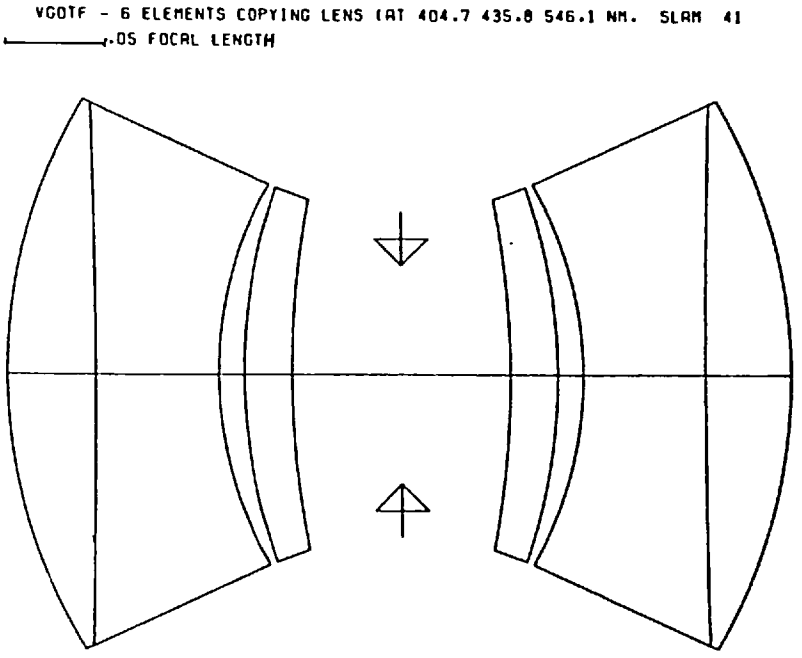

CURVE	SEPN	INDX/DIS
0.148036	0.000000	1.000000
-0.00739	1.108310	1.706670
0.206354	1.576190	1.630480
0.141971	0.325400	1.000000
0.086958	0.610190	1.598010
0.000010	1.386970	1.000000
-0.08696	1.386970	1.000000
-0.14197	0.610190	1.598010
-0.20635	0.325400	1.000000
0.007393	1.576190	1.630480
-0.14804	1.108310	1.706670
0.000010	-0.284620	1.000000

7.a Final VGOTF design

VGOTF - 6 ELEMENTS COPYING LENS AT 404.7 435.8 546.1 NM.

M.T.F VS. FREQUENCY AND DEFOCUS

ON AXIS

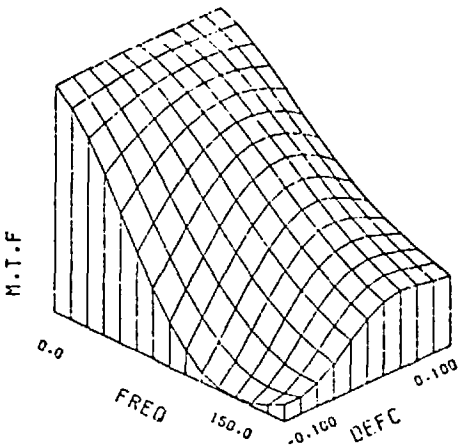

FIELD ANGLE =19.85 DEGREES

SAGITTAL M.T.F

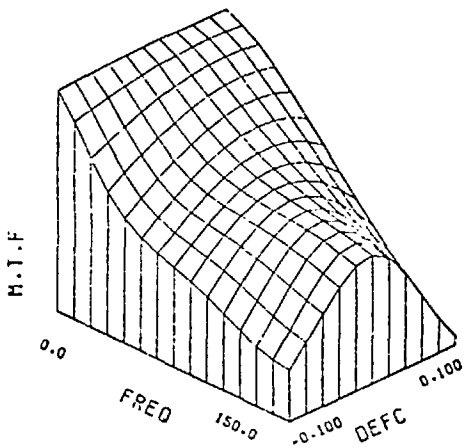

TANGENTIAL M.T.F

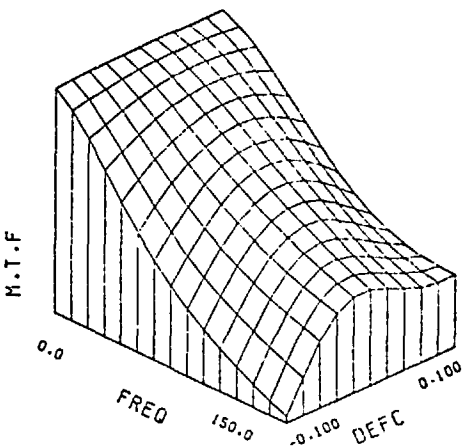

FIELD ANGLE =14.21 DEGREES

SAGITTAL M.T.F

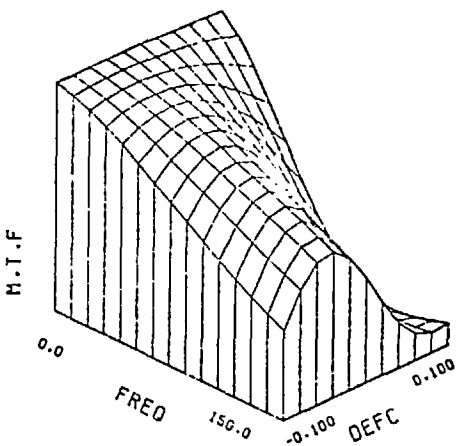

TANGENTIAL M.T.F

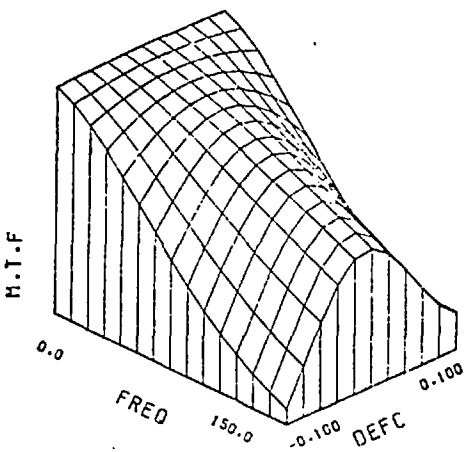

7.b MTF Characteristics

7.2 DOF Determination of Polychromatic Systems

Focal depth determination in the polychromatic case is complex compared with the monochromatic case, due to the definition of the polychromatic MTF. If an object with equal reflection throughout the spectral range of the system, i.e. a white object, is considered the MTF becomes the integral of the monochromatic MTF's over the wavelength range. In practice this integration is approximated by summation where each of the terms is multiplied by the relative sensitivity of the system in the wavelength at which the corresponding monochromatic MTF was calculated. In the case of a continuous spectrum, the relative sensitivity is proportional to the area under the relative sensitivity response curve for the corresponding waveband and the monochromatic MTF is calculated at the centre of this band, the integration over the spectrum being again replaced by a summation.

Alternatively, objects with varying reflection coefficients throughout the spectral range of the system, or "coloured objects", can be considered. In this case the spectral response curve changes its shape and is in fact the product of the relative sensitivity to a "white object" and the reflection characteristics of the "coloured object".

If a photocopying machine is designed for standard office work, it is assumed that the objects (originals to be copied) consist of black lettering against white paper, so the heterogenic MTF for "white object" is applied. In this case for each field angle and azimuth the MTF is the weighted sum of the three MTF values at the e, g and h

mercury spectral lines, the weighting factors being the relative spectral responses in the particular case. An example of DOF determination in such a case is illustrated in figure 7.c below.

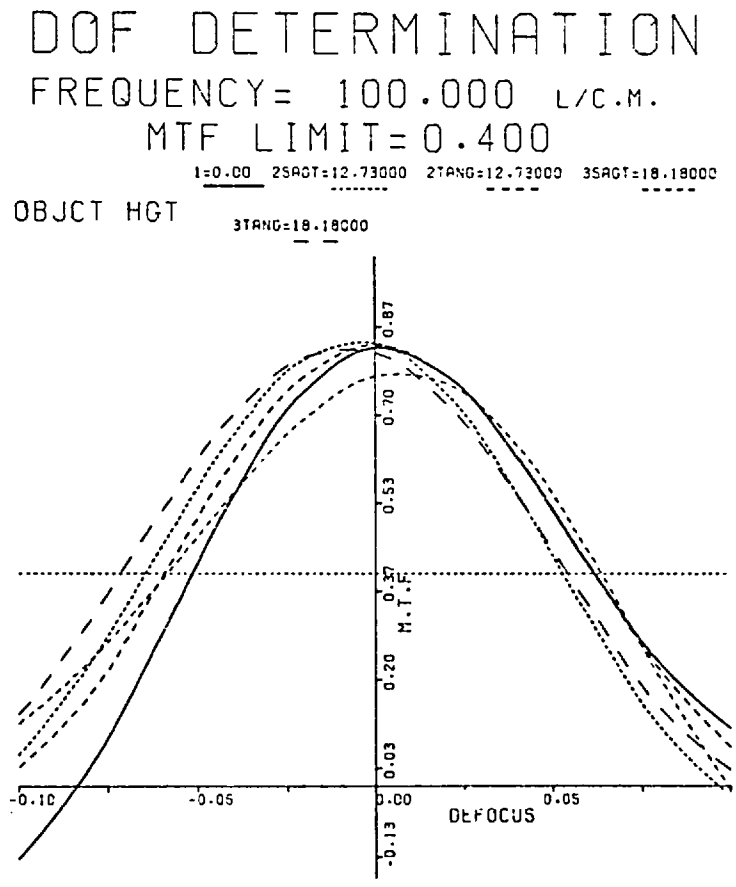

7.c DOF for "white object"

This is not the case if the system is to be used for various objects which include text printed on coloured backgrounds. For example, if the background is a blue paper with high reflection at 404.66 nm and no reflection at 546.07 nm the relative sensitivity of the blue will become 100% while that of the green will drop to zero. If objects

of any possible colour are considered, the MTF behaviour as a function of defocus in the three optimisation wavelengths must be studied as illustrated in figure 7.d. In this case an axial and two off axis object positions are considered for each wavelength, where each of the non-axial objects is studied in the two azimuths, resulting in five MTF curves. Considering three wavelengths results in fifteen MTF-against-defocus curves (the combination of the three graphs in figure 7.d), the DOF being the longitudinal defocus range for which all these fifteen MTF values are above the limiting MTF at the frequency of interest.

Obviously, consideration of "coloured objects" rather than "white" will result in complex DOF determination. There is no simple way of combining the three monochromatic MTF values into a single heterogenic MTF. The choice of weighting factors for the optimisation program is very complicated, and the resultant DOF is narrower than for most practical cases. Therefore, throughout this work, when polychromatic cases are discussed, only "white objects" are considered. All DOF determinations are done by examining curves of the type shown in figure 7.c, which is the weighted sum of three monochromatic DOF curves of the type shown in figure 7.d, the weighting factors throughout this work were 0.3, 0.75 and 1 for the e, g and h spectral lines, respectively.

7.3 DOF Optimisation Based on the VGOTF Program

The lens shown in figure 7.a was used as input in an optimisation sequence using the VGDTF program. The DOF of this

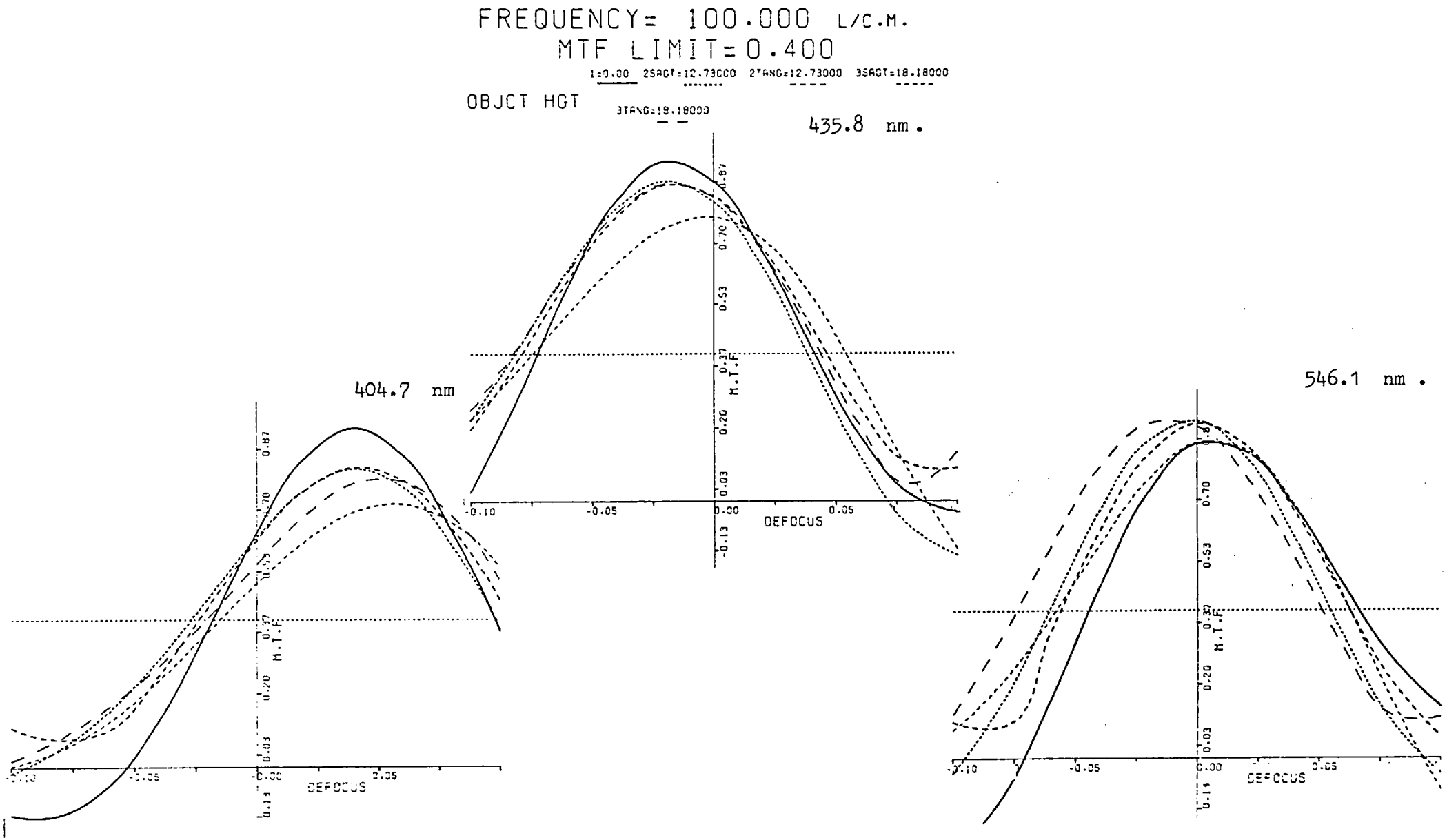

7.d Monochromatic DOF determination at 404.7, 435.8 and 546.1 nm

design, for a white object, was 0.057 cm, as shown in figure 7.e below.

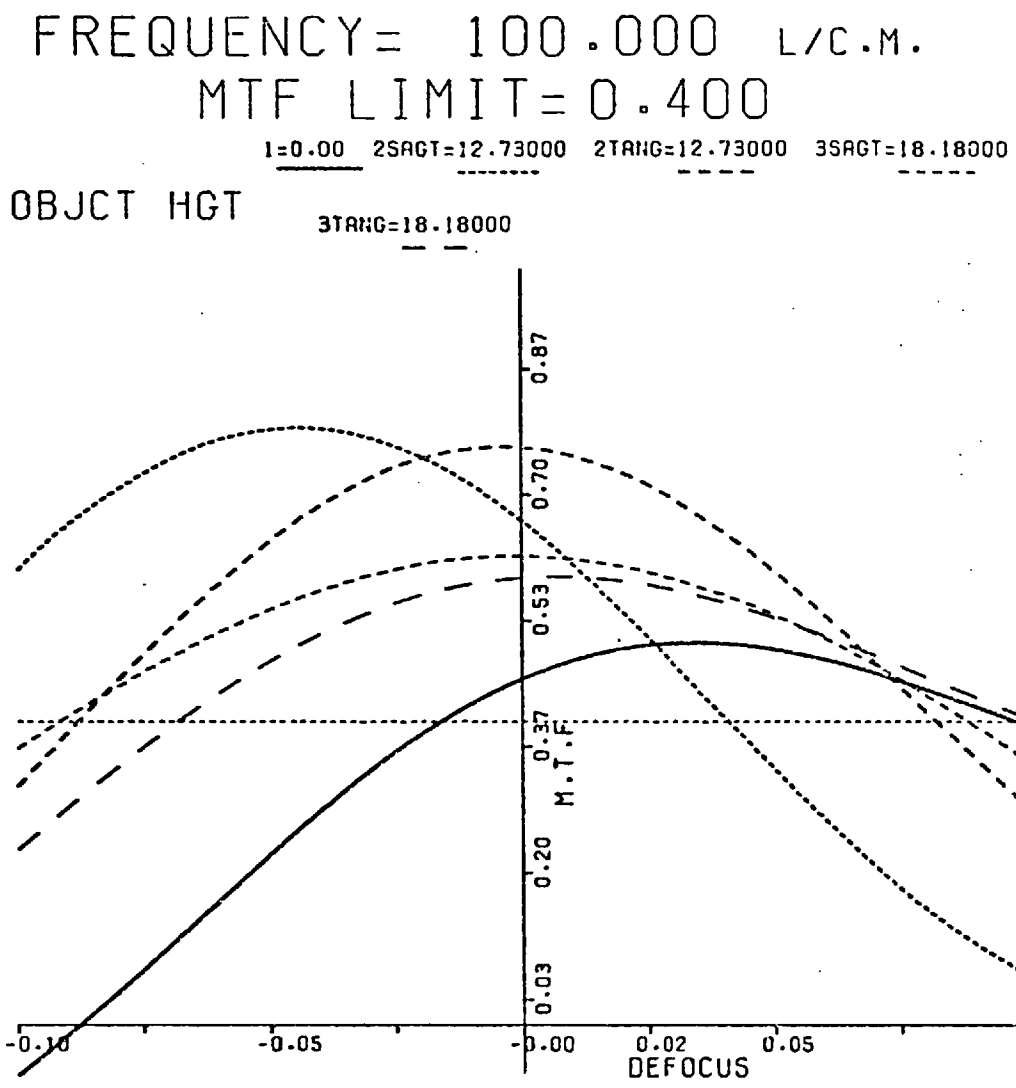

7.e DOF Determination

As in the monochromatic cases, the intermediate field position in the sagittal azimuth limits the focal depth range. For the same reasons as explained in Chapter 5, this field position was chosen for the primary target and its weighting factors were varied whilst maintaining the ratios between the various wavelengths. For each skew ray six weighting factors were used, two for each wavelength (for the two

azimuths). As explained above the ratios between the weighting factors in the three optimisation wavelengths were equal to the square roots of the corresponding relative spectral sensitivities, and the weighting factors for the three field positions were initially equal for any one wavelength. All the weighting factors in the second field position sagittal azimuth were multiplied by a single factor which took values up to 8, the DOF took an optimum value of 0.785 mm with a factor of 2.2. Figure 7.f below, shows the DOF variations throughout this sequence, against the weighting factor which was applied to the second object position in the sagittal azimuth. The optimum system from the above technique increased the DOF value by 38%.

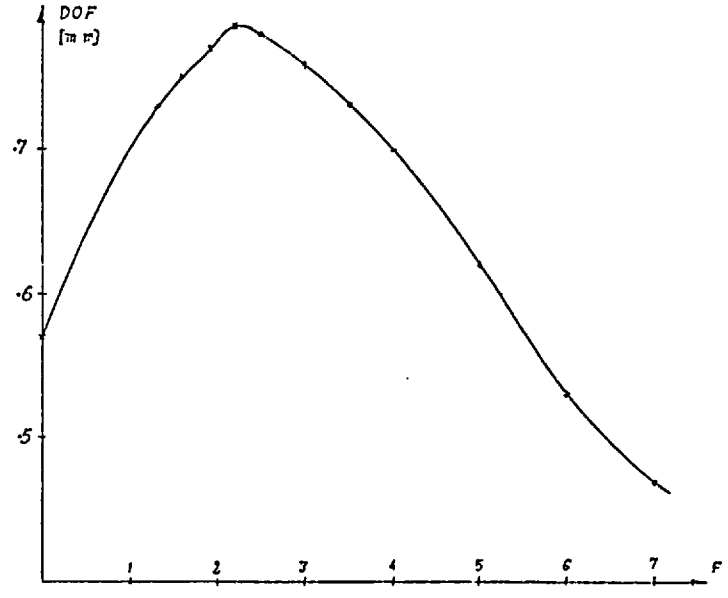

7.f DOF vs. the weighting factor of the second object position sagittal azimuth

7.4 DOF Optimisation Based on the VDOF Program

The VDOF program, which had not proved successful in the case of the monochromatic copying lens, was applied to this design. The optimisation defocus distance, which is equal to half the separation between the optimisation image planes, was increased up to .04 cm. It resulted in an optimum focal depth of 0.58 cm for an optimisation defocus of .0287 cm. This series proved most sensitive to optimisation defocus and at its optimum value improved the DOF by 1.7% which was a poor achievement considering the sophisticated procedure involved.

A detailed study of this sequence showed that the aberrations at the limiting object position and azimuth, for the h mercury lines, were at their "lowest possible" value. The structure of the merit function and the choice of the weighting factors caused the transverse ray aberrations at the h wavelength to dominate the optimisation steering the system to a region where further improvement at this wavelength and object position was not possible by a small finite change of parameters. Naturally, the corresponding aberrations at the e and g spectral lines were much higher than those at the h line. The finite changes in the parameters of the optical system did not improve the merit function due to the choice of weighting factors and also due to the suppression of small improvements in aberrations of certain magnitude caused by the 'sine square' function which had been used in the merit function, as explained in Chapter 4. Therefore, to get the system out of this parameter region, the aberrations in

the h line for the second field position and sagittal azimuth were no longer controlled. This was done, practically, by applying a weighting factor of zero to the h line and increasing the weighting factors for the e ang g lines at this critical azimuth and field position. Because of the nature of the optimisation program, finite changes in the parameters of the system followed which resulted in improved aberrations for the e and g wavelengths but some deterioration at the h spectral line. Since the system was near the "local optimum" of the h wavelength, a finite change in parameters caused minute deterioration in the MTF at this colour. For the other colours, the system was not near the optimum position, hence, finite parameter changes improved the MTF significantly.

The relaxation of the emphasis on the h spectral line was tried in a sequence where the weighting factors at the intermediate object position sagittal azimuth took the values We, Wg, Wh for the aberrations in the corresponding wavelengths, where Wh = 0.

This sequence required extra precautions and the results at the end of each iteration were carefully analysed. As expected, on the basis of the theory explained above, the "white object" MTF in the target field angle improved slightly from iteration to iteration whilst the monochromatic MTF at the same object position in the h wavelength deteriorated slightly. At the same time the general DOF for a "white object" kept improving. The deterioration in the MTF at the h line, reached a breaking point beyond which the MTF

deterioration limits the DOF range, also the MTF values at other field angles started to deteriorate and affected the DOF range too. In other words, the DOF for a "white object" improved for a finite number of iterations in the optimisation procedure, reaching an optimum value. Any additional iteration will reduce the DOF value and the optimisation process must terminate at this stage. The SLAMS programs used lacked a facility to terminate the optimisation at this stage, but it might be quite easily included. Ouring this sequence the program was terminated by the designer.

The optimum was found with the following weighting factors: Wg = 108, We = 45 and Wh = 0, at the critical object position and azimuth; for the other azimuths and field angles the weighting factors were: Wg = 43, Wh = 50 and We = 28. The optimum design from this technique had DOF of .1055 cm and was found by an optimisation defocus of 0.232 cm. This optimum optical system and its DOF determination are shown in figure 7.g below, the transverse ray aberrations for the intermediate field angle in the sagittal azimuth are given in figure 7.h, and the wavefront aberrations for the same object position are illustrated in figure 7.i.

This sequence improved the OOF of the system by 85%, techniques of the type tried in Chapter 5, failed to improve the focal depth further.

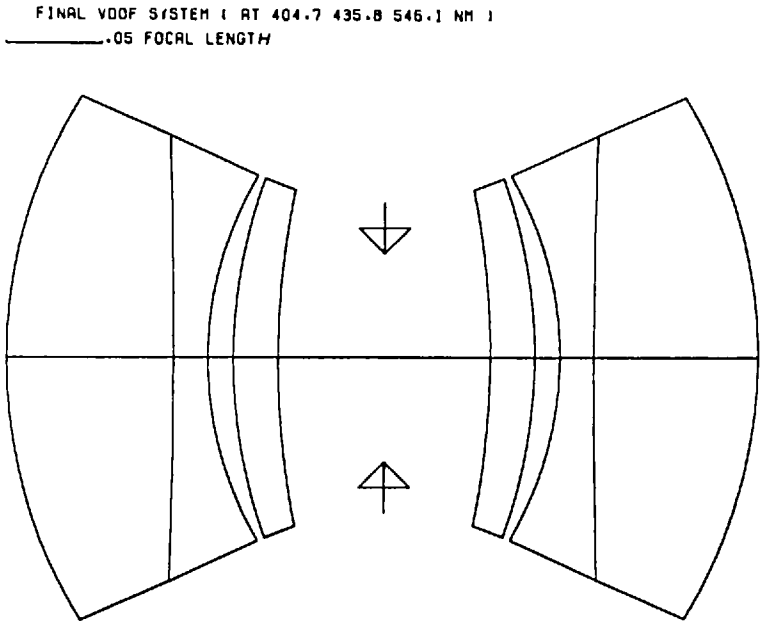

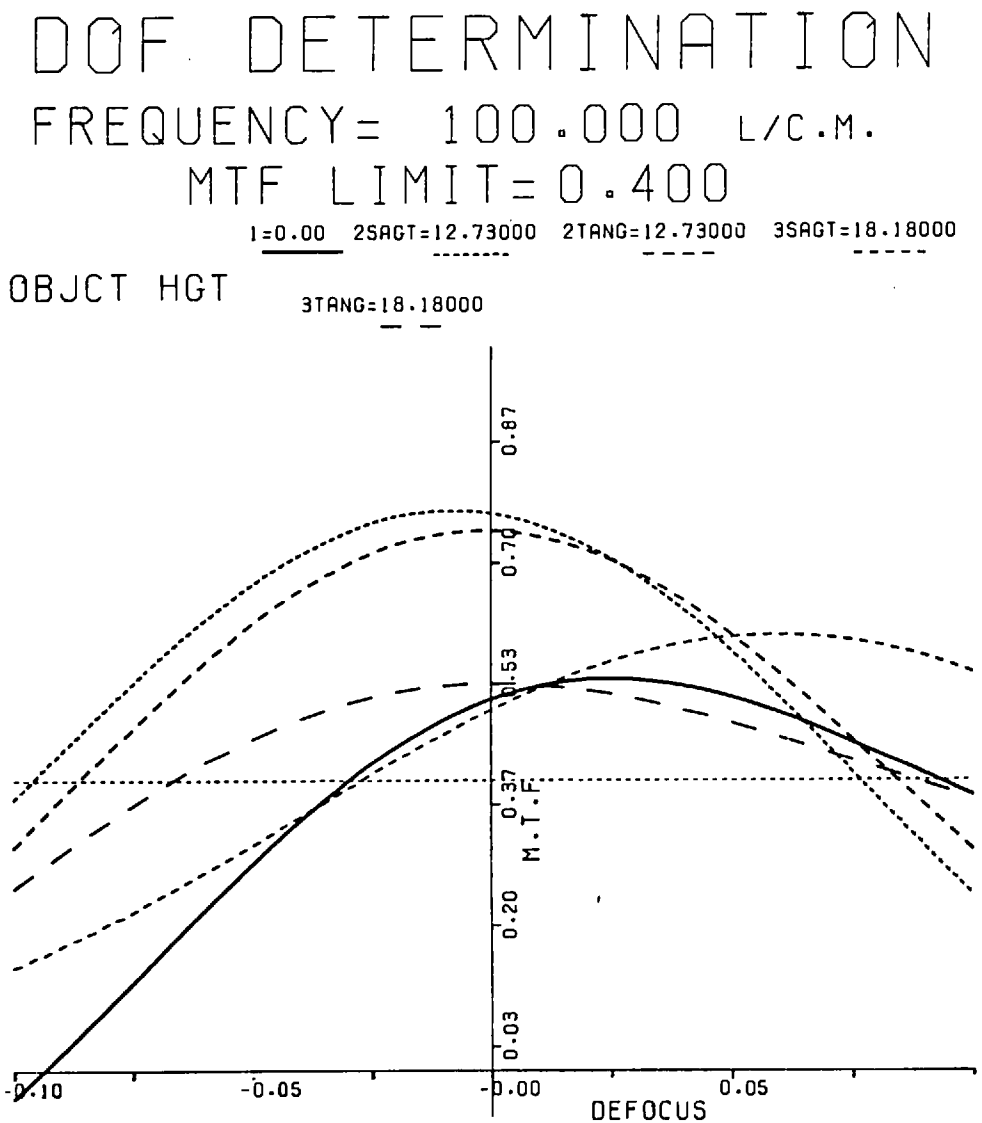

CURVE	SEPN	INDX/DIS
0.151320	0.000000	1.000000
-0.01021	2.205770	1.706670
0.210148	0.457260	1.630480
0.143218	0.336340	1.000000
0.088985	0.595280	1.598010
0.000010	1.412640	1.000000
-0.08899	1.412640	1.000000
-0.14322	0.595280	1.598010
-0.21015	0.336340	1.000000
0.010211	0.457260	1.630480
-0.15132	2.205770	1.706670
0.000010	-0.278020	1.000000

7.g The optimum system and its DOF range

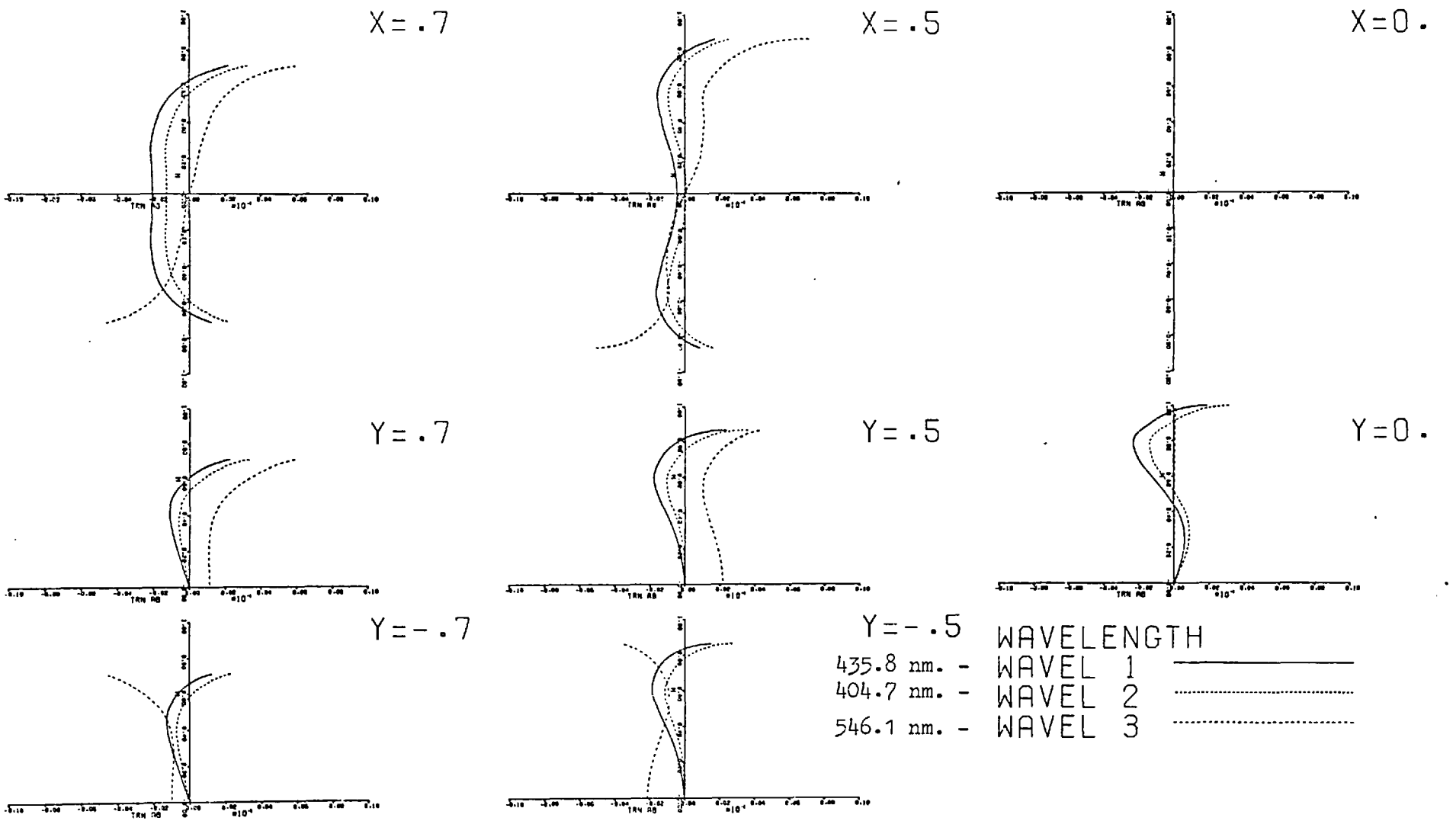

7.h Transverse ray aberrations in the second field angle sagittal azimuth

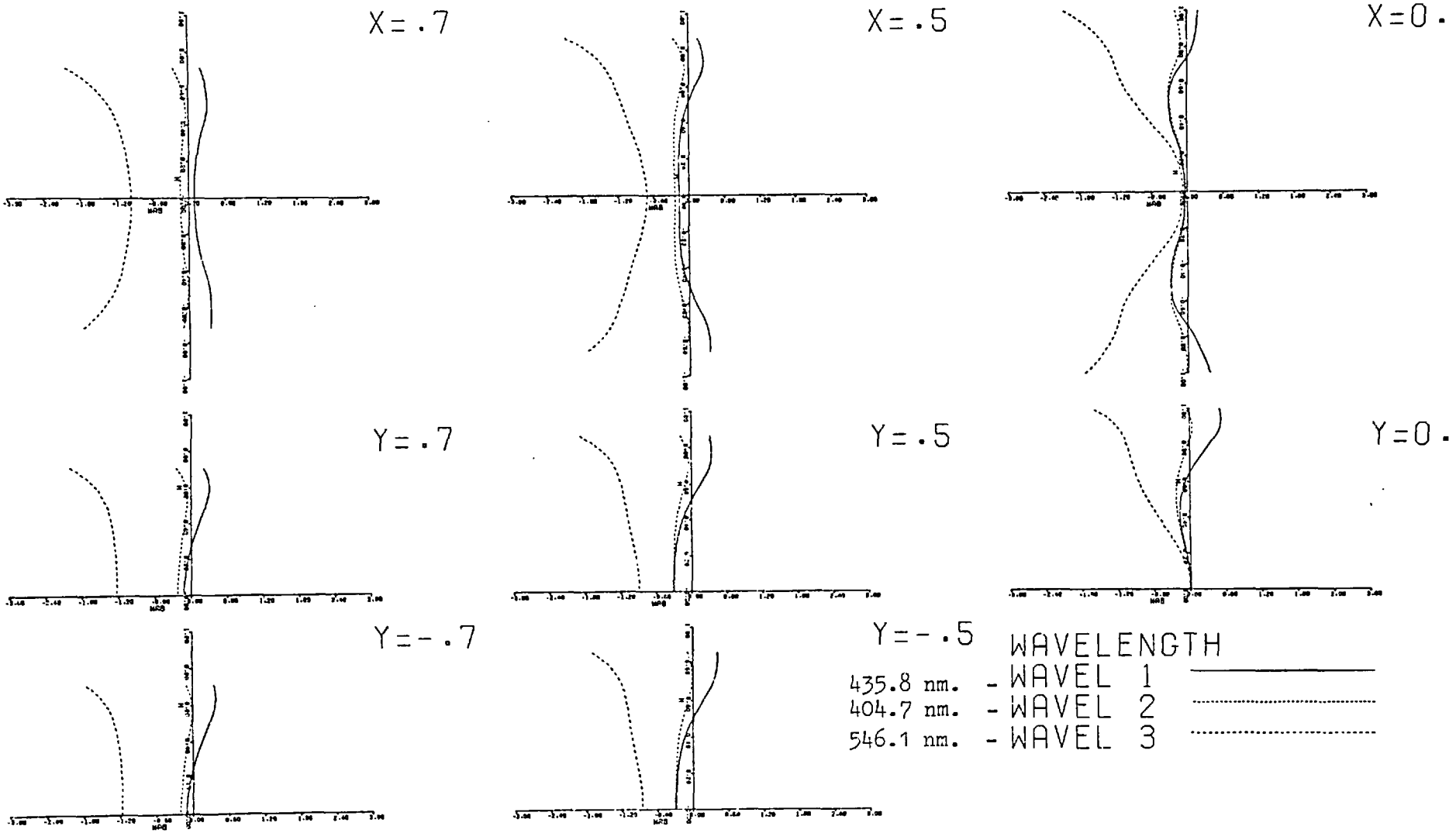

7.i Wavefront aberrations in the second field angle

CHAPTER 8

THE DESIGN OF A SIX ELEMENTS REDUCING LENS FOR POLYCHROMATIC WORK

8.1 The Design of a Six Elements Polychromatic Reducing Lens

The monochromatic reducing lens was used as the initial system for this design, the LF2 glass being replaced by the Kz FS1 glass from the Schott catalogue. The numerical aperture was .067, the same as in the monochromatic case described in chapter 6, and the total glass thickness was reduced to 8. cm. The design was initiated by using the V14 program, changing to the VGOTF program when the aberration magnitude was appropriate. The VGOTF optimisation was carried out in steps, increasing the optimisation frequency up to the value of 100. cycles/cm. The three final image planes, in the three optimisation wavelengths, were separated by 0.74 cm. This design is shown in figure 8.a, the MTF characteristics for a white object are given in figure 8.b in the optimisation field positions. The focal depth of this system was 0.9865 mm and its limits are illustrated in figure 8c.

8.2 DOF Optimisation Based On The VGOTF Program

The system shown in figure 8.a was used as input to a VGOTF optimisation sequence. For similar reasons to those in the monochromatic case, the second field position in the sagittal azimuth was chosen as the target for this technique. The weighting factors at the target field position and azimuth were multiplied by a single factor, so as to maintain the ratio between the weighting factors in the optimisation wavelengths at the target field position, in a similar way to that explained in chapter 7. The DOF values are shown as a function of this single factor

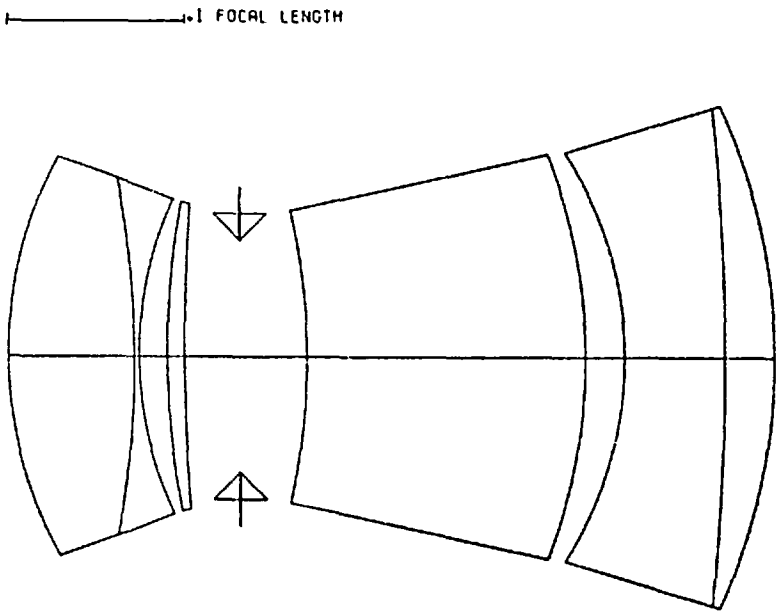

CURVE	SEPN	INDX/DIS
0.173125	0.000000	1.000000
-0.07460	1.770930	1.706670
0.195918	0.067810	1.630480
0.089636	0.397270	1.000000
0.036507	0.245390	1.706670
0.000010	0.782910	1.000000
-0.10970	0.943610	1.000000
-0.13087	3.962850	1.706670
-0.19233	0.557890	1.000000
-0.03012	1.434360	1.630480
-0.12144	0.708680	1.706670
0.000010	-0.060450	1.000000

8.a Final VGOTF design

FIELD ANGLE = 9.89°

ON AXIS

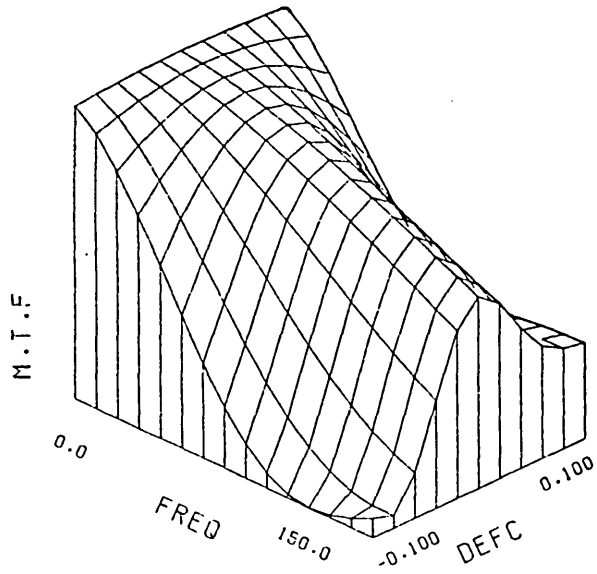

SAGITTAL MTF

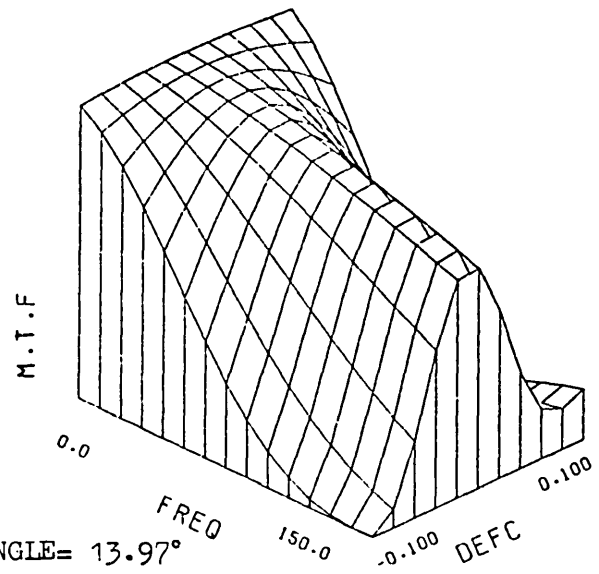

TANGENTIAL MTF

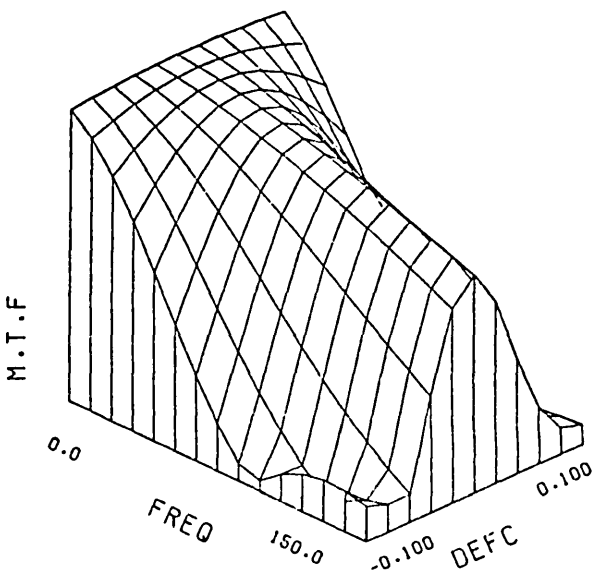

FIELD ANGLE= 13.97°

SAGITTAL MTF

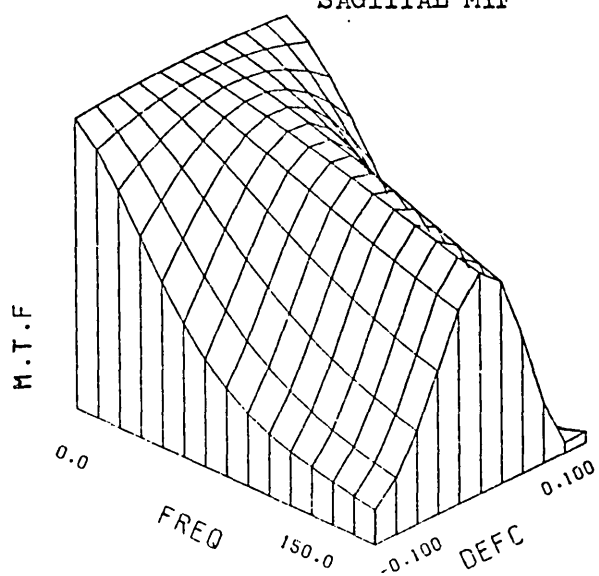

TANGENTIAL MTF

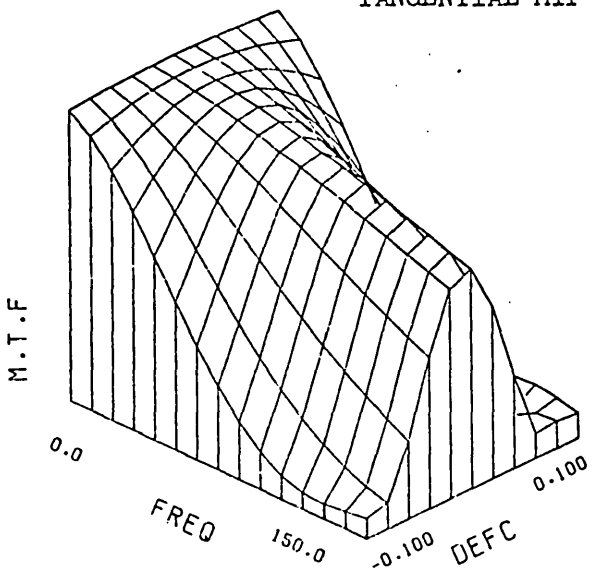

8.b MTF characteristics for white object at the optimisation field positions for the final VGOTF design

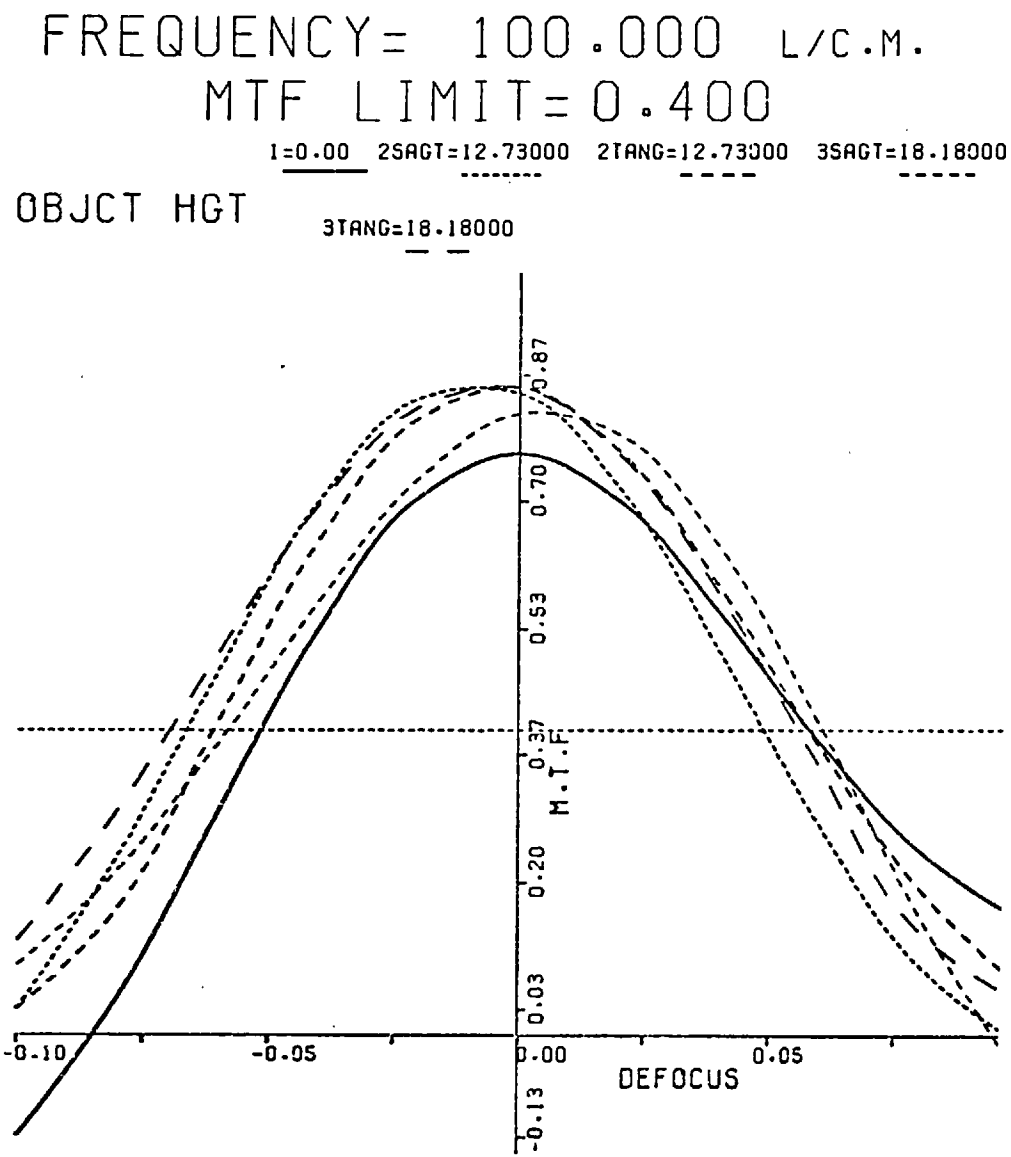

8.c DOF for the final VGOTF system

in figure 8.d. The best result was obtained with a factor of 1.7 which resulted in a focal depth of 1.0016 mm which is a 1.5% improvement on the DOF of the initial system. The optimum design for the above sequence is illustrated in figure 8.e and its DOF determination in figure 8.f.

Further attempts were made to extend the DOF, in the same way as for the copying lens described in chapter 7, but these failed to improve the focal depth significantly.

8.3 DOF Optimisation Based On The VDOF Program

The system shown in figure 8.a was then used as input in a VDOF optimisation sequence in which the optimisation defocus distance was increased up to .06 cm. Further defocus was not practical since the aberration product given by equation 4-11 was violated. The DOF values for this sequence are shown in figure 8.g as a function of the optimisation defocus. The optimum focal depth, found with a defocus of .040 cm, was 1.0323 mm which was a 4.5% improvement on the initial value. This best design is illustrated in figure 8.h, its MTF characteristics are shown in figure 8.i and the DOF determination is given in figure 8.j. The Seidel coefficients for the systems produced throughout this sequence are illustrated in figure 8.k plotted against the optimisation defocus.

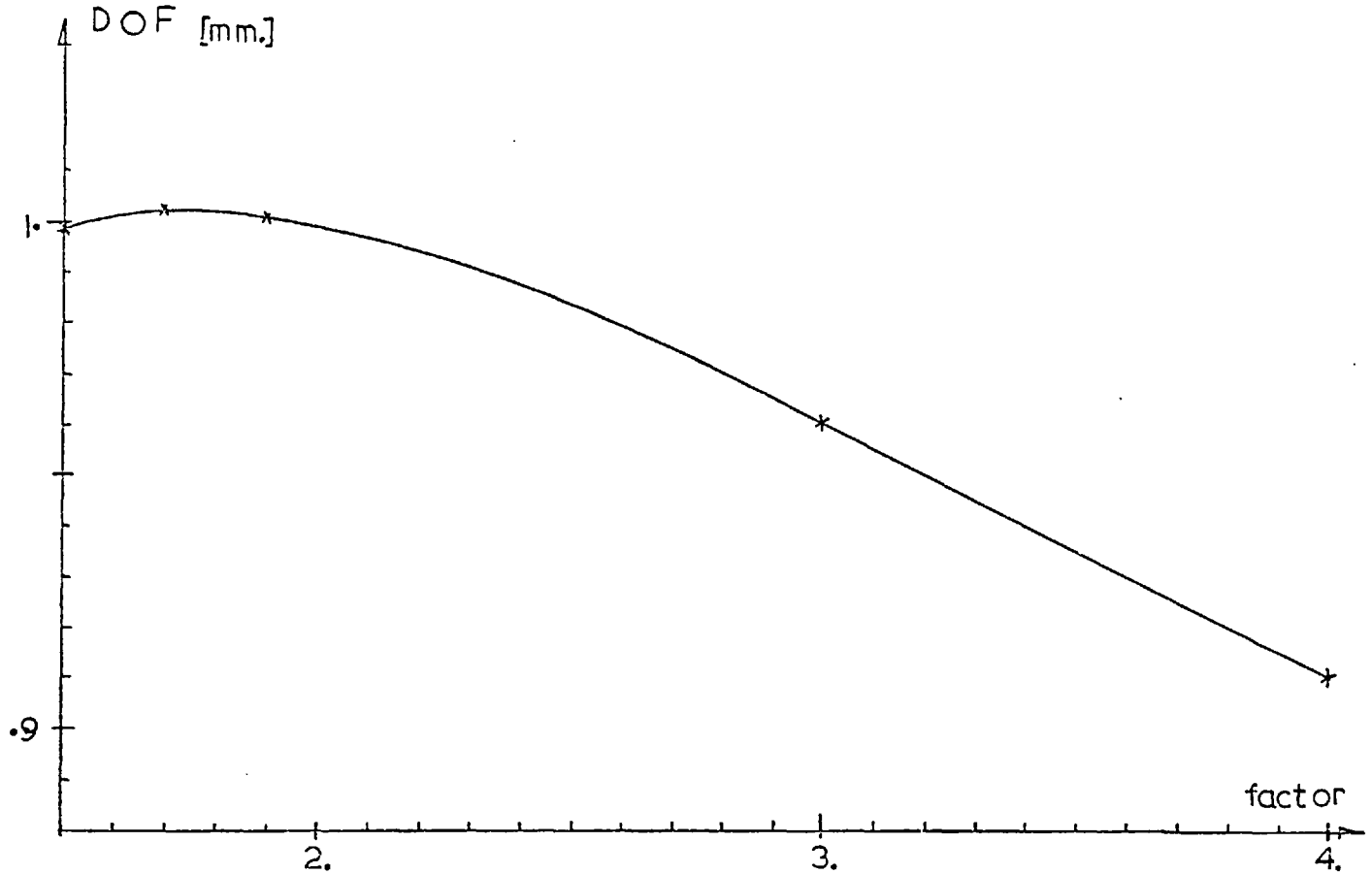

8.d DOF vs. factor of target field position through VGOTF sequence.

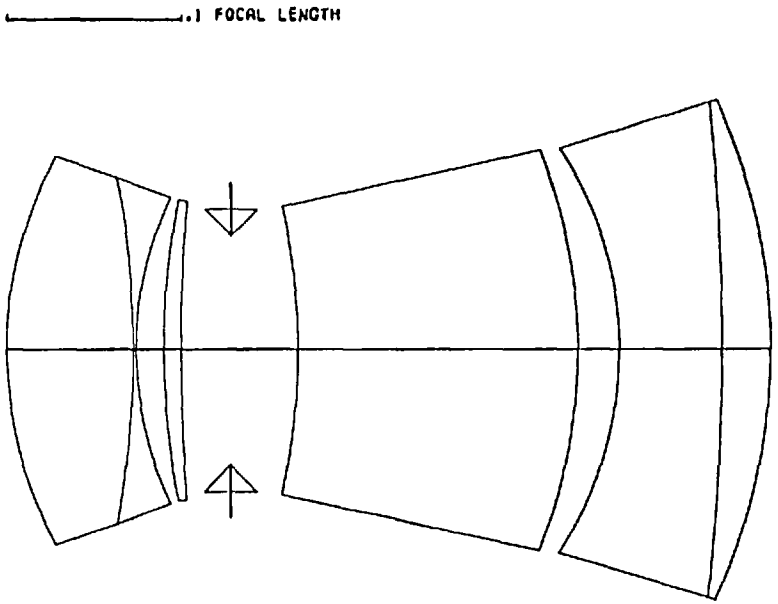

CURVE	SEPN	INDX/DIS
0.173539	0.000000	1.000000
-0.07690	1.786930	1.706670
0.196462	0.043020	1.630480
0.089751	0.391170	1.000000
0.035539	0.245510	1.706670
0.000010	0.704970	1.000000
-0.11003	0.961210	1.000000
-0.13104	3.996780	1.706670
-0.19214	0.595990	1.000000
-0.03133	1.471750	1.630480
-0.12032	0.695760	1.706670
0.000010	-0.057820	1.000000

8.e. Best VGOTF design.

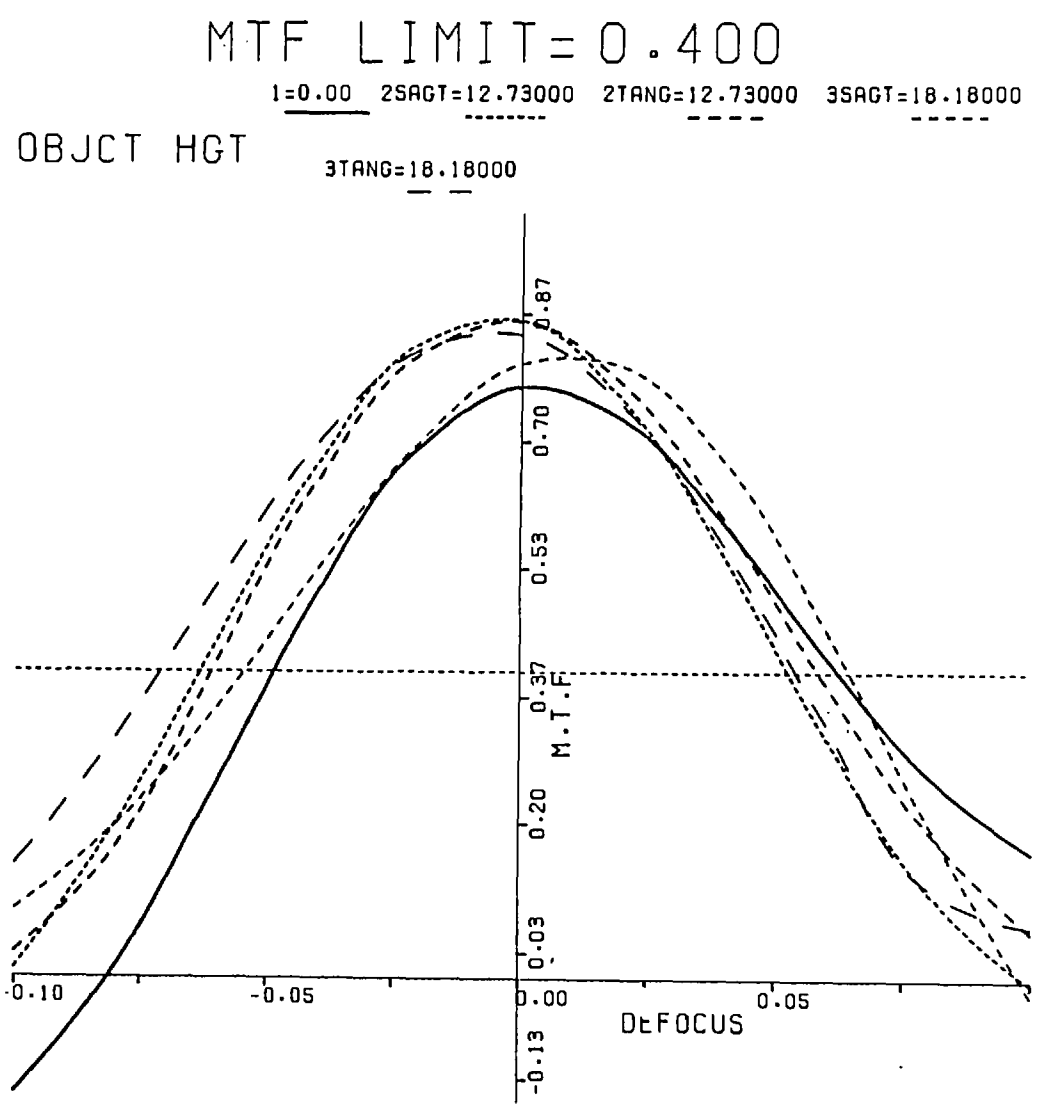

8.f. DOF for best VGOTF design.

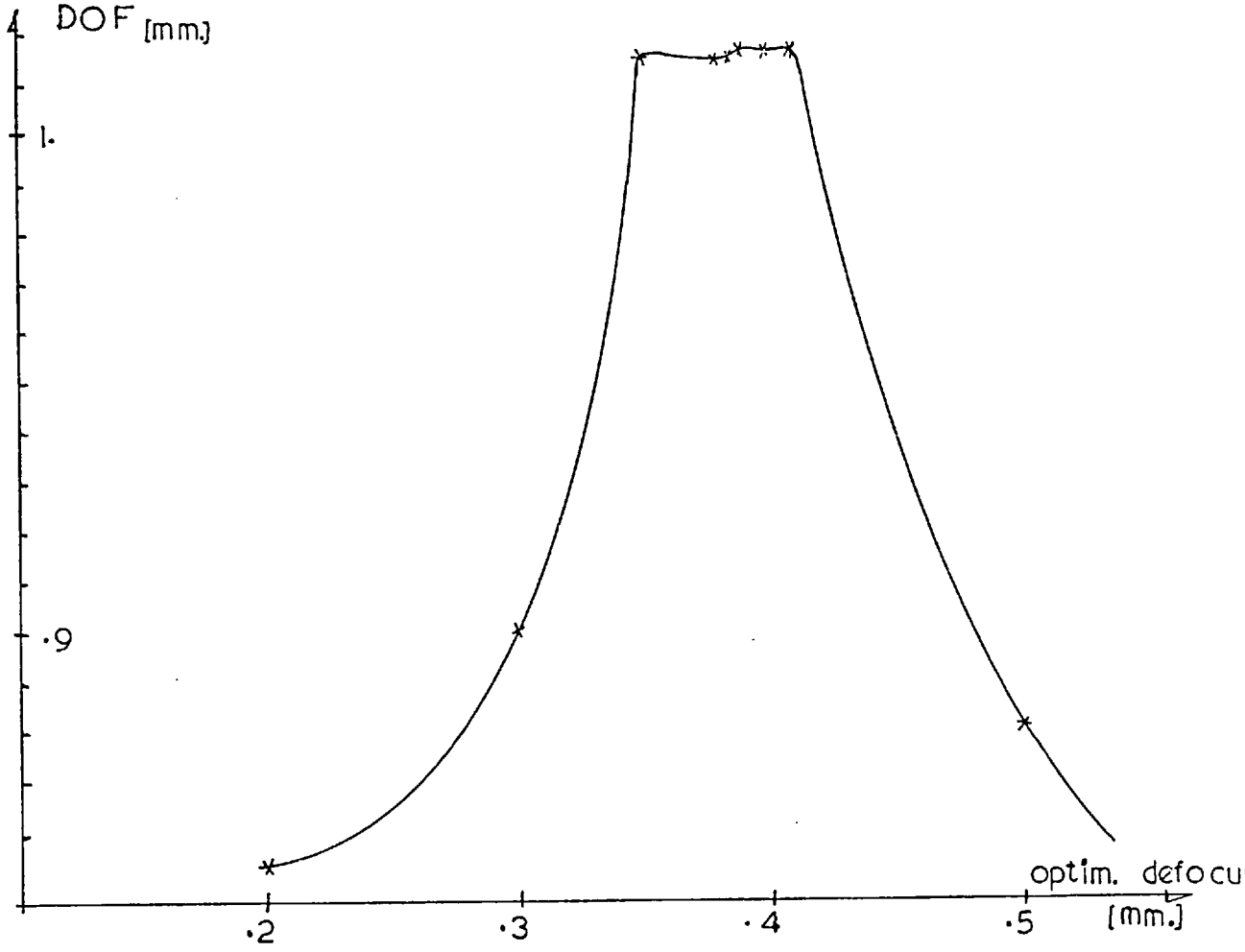

8.g

DOF vs. optimisation defocus for the VDOF sequence

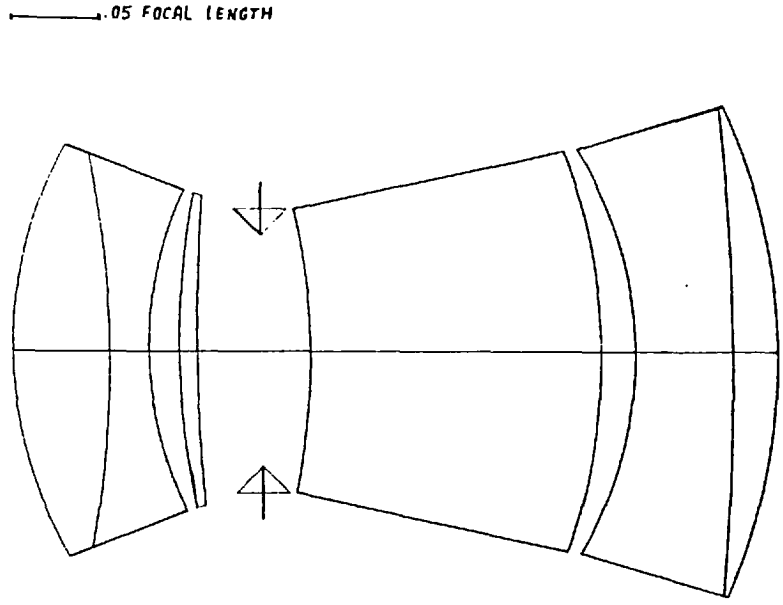

CURVE	SEPN	INDX/DIS
0.173051	0.000000	1.000000
-0.07427	1.344160	1.706670
0.195806	0.545990	1.630480
0.089674	0.423550	1.000000
0.036566	0.244690	1.706670
0.000010	0.880510	1.000000
-0.10990	0.678220	1.000000
-0.13077	4.073360	1.706670
-0.19260	0.489510	1.000000
-0.02991	1.382470	1.630480
-0.12143	0.622230	1.706670
0.000010	-0.049240	1.000000

8.h. Best VDOF design

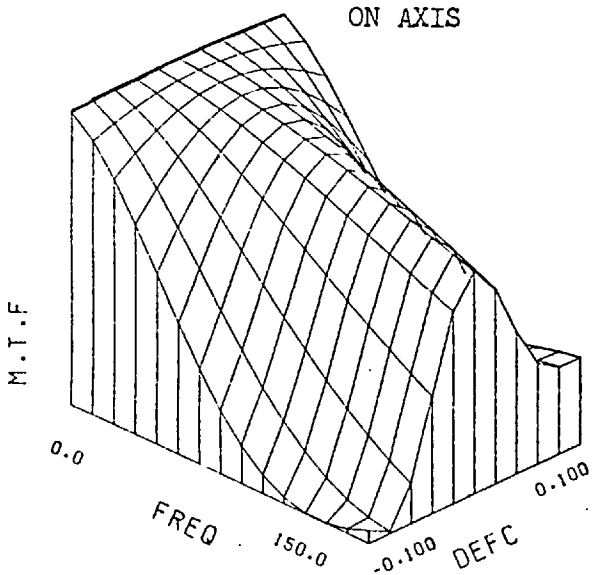

FIELD ANGLE = 9.82°

SAGITTAL MTF

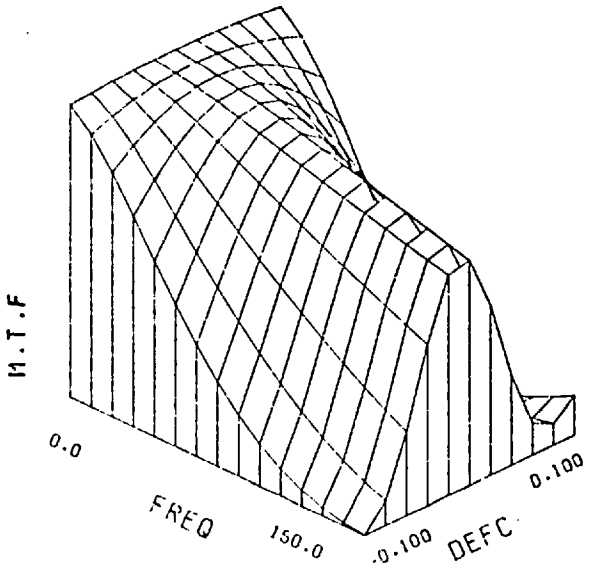

TANGENTIAL MTF

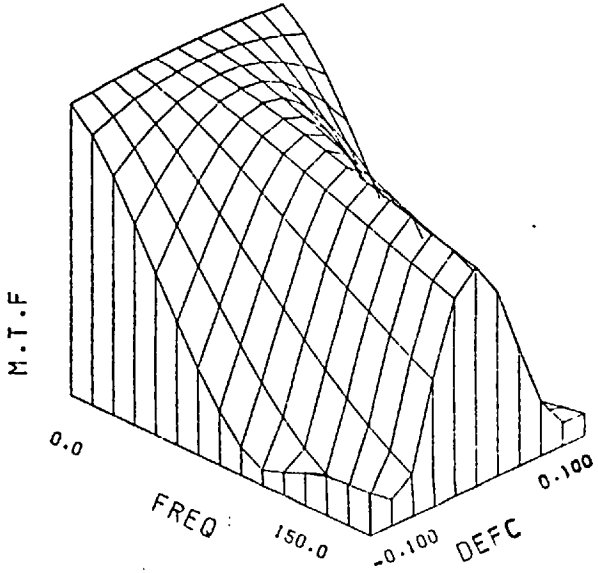

FIELD ANGLE = 13.88°

SAGITTAL MTF

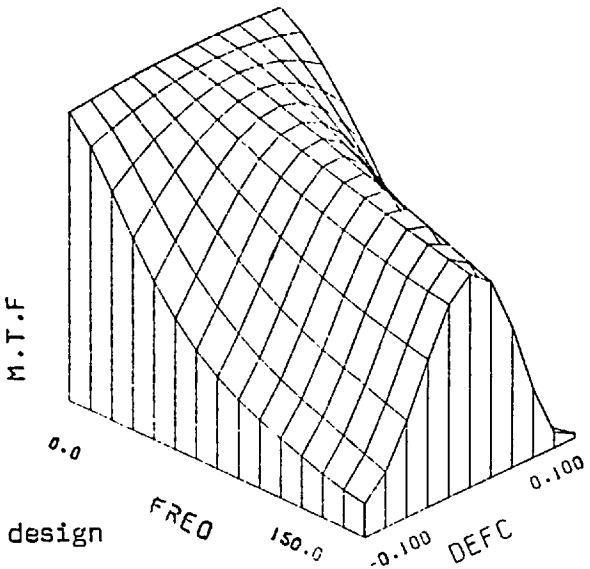

TANGENTIAL MTF

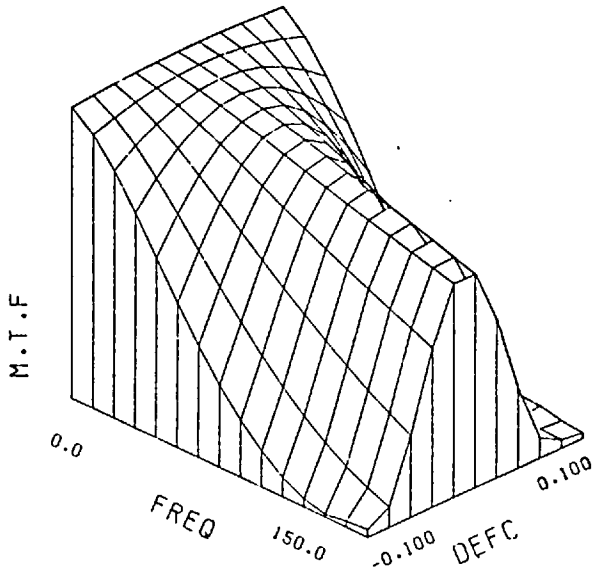

8.i. MTF characteristics for best VOOF design

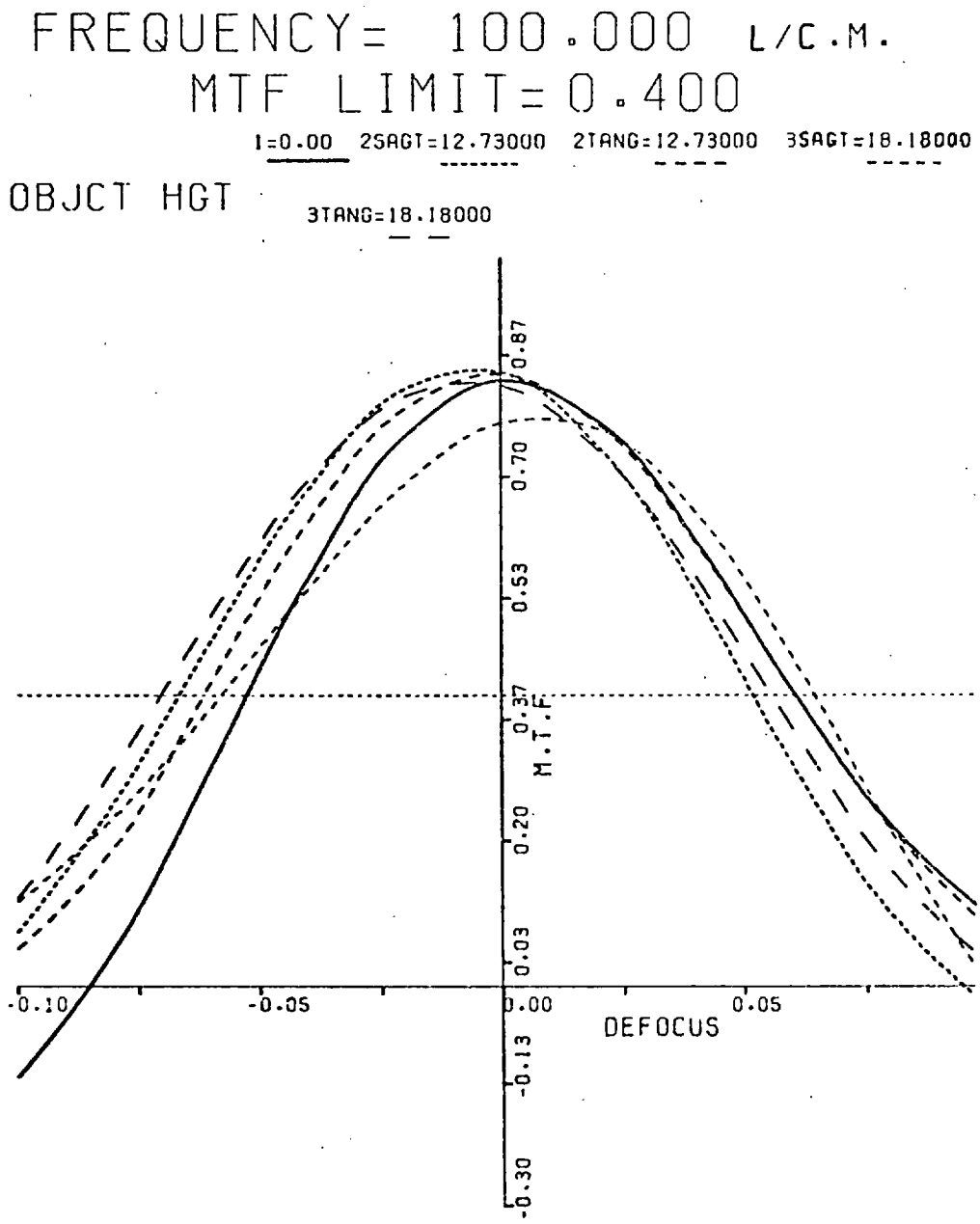

8.j DOF of best VDOF system.

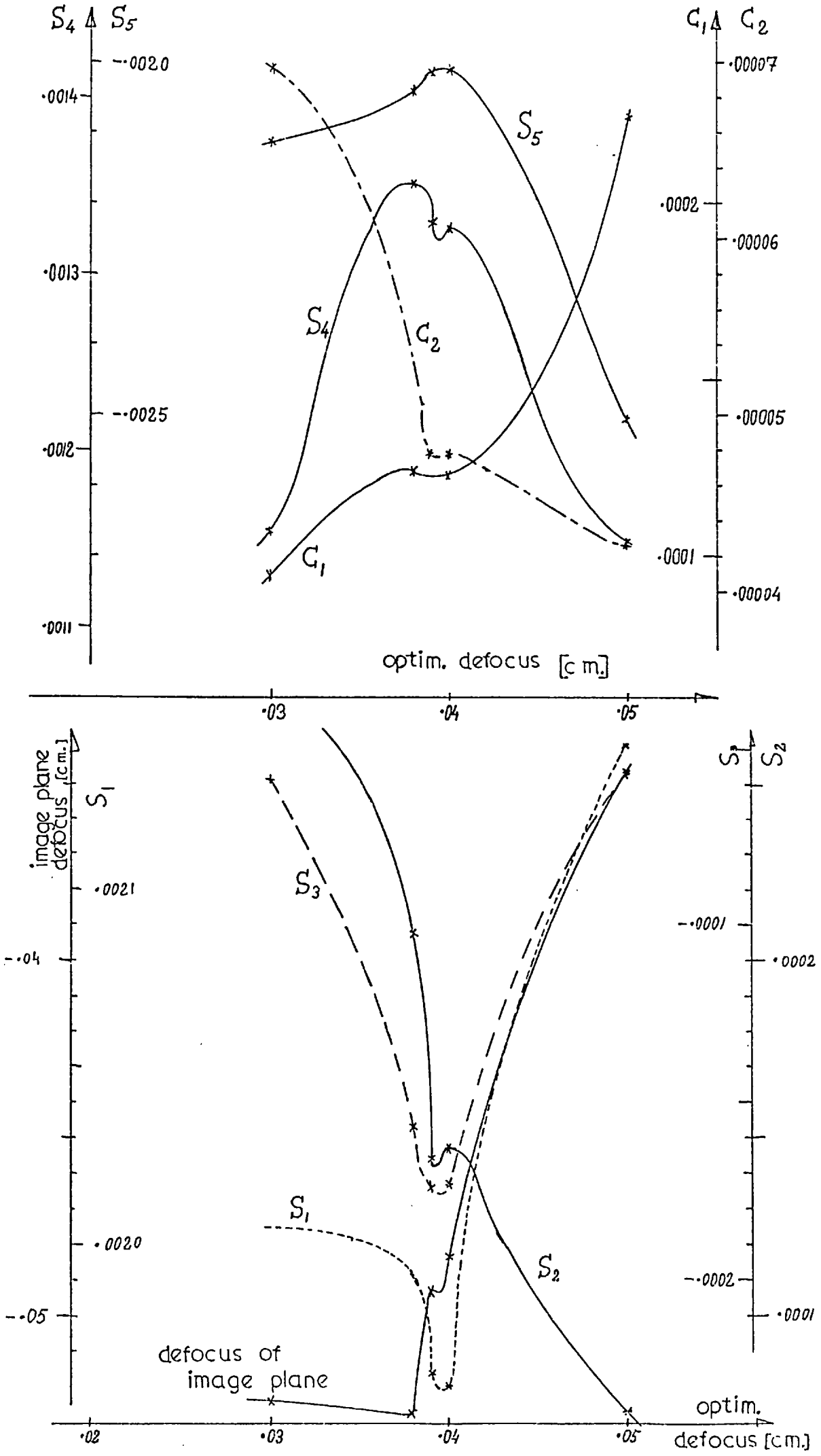

8.k Seidel coefficients for VOOF sequence, against optimisation defocus.

CHAPTER 9

DISCUSSION OF THE RESULTS

9.1 DOF Optimisation Techniques

Optimisation techniques for extended depth of focus have been demonstrated in Chapters 5,6,7 and 8 by considering the design of four derivatives of a six elements lens and these techniques can be classified into the main groups according to the program used : the VGOTF technique and the VDOF technique. Both of these programs use geometrical MTF components in the merit function instead of the transverse ray aberrations of V14; the same number of rays are traced in each case.

In the VDOF program which considers the MTF in two defocused image planes, the number of terms in the merit function is doubled, this of course requires more computing time and a larger storage space in the computer, both of which will increase the cost of an optimisation run, and one may ask whether the results obtained justify this extra expense. A brief answer to this can be given in the form of a table where the DOF values for the systems developed in this work are compared with theoretical values for an aberration-free system. The focal depth of an ideal optical system working at the same numerical aperture and in the same wavelength was calculated using the method described earlier in section 3.2 . On the basis of these results, the VDOF program is seen to be useful and if at 500 nm the polychromatic copying lens is used instead of the monochromatic design, the VDOF designs are superior in all cases. The rest of this chapter contains a more detailed comparative analysis of all the results and some comments concerning the VDOF program and its performance.

Lens Type	Ideal DDF	DDF of The Initial System (% of ideal DDF)	DDF Of Best "VGDTF" System (% of ideal DDF)	DDF For Best "VDOF" System (% of ideal DOF)
Copying lens f/5.6 operating at 500 nm	.1920 cm	.0840 cm (43.7%)	.1120 cm (58.3%)	.1010 cm (52.6%)
Reducing lens f/5 operating at 500 nm	.1330 cm	.1016 cm (76.4%)	.1040 cm (78.2%)	.1120 cm (84.2%)
Copying lens f/5.6 operating in the e,g,h Hg lines	.1860 cm	.0570 cm (30.6%)	.0785 cm (42.2%)	.1055 cm (56.7%)
Reducing lens f/5 operating in the e,g,h Hg lines	.1240 cm	.0986 cm (79.5%)	.1002 cm (80.8%)	.1032 cm (83.2%)

9.2 The Performance of the VDOF Program

The concept of an optimisation in two image planes is new and has not been published before, thus a brief evaluation of its performance throughout this work is given. Because of the nature of the problem to be solved the "direct MTF" optimisation method was used, for a more detailed evaluation of this method, a comparison run with the same system data should be made using a similar program, with a merit function consisting of transverse ray aberrations in two image planes.

The number of terms summed in the merit function was increased without increasing the number of rays that were traced, this resulted in a slightly longer computation time for the VDOF program compared with the VGDTF version. The increased storage required to run the

VDDF was minute when compared with the 45K of store required by VGDTF. The conversion of the VGDTF program to perform VDDF was a relatively simple task; the original program was stored on the computer using the CDC "Update" system, which allows text modification of a source program by altering, deleting or adding statements, and it required a relatively short and simple correction file to effect this conversion. The tests included in the program, such as the aberration product test (equ.4-11), proved to be most useful and enabled parameters to be changed throughout the optimisation procedure.

When considering the results of the polychromatic copying lens, it is clear that the magnitude of the aberrations is critical. If the range of values of the aberrations is large, then the merit function may contain terms which, when finite changes are applied to the system, are of the wrong magnitude because of the "sine squared" function. This phenonemon must be well controlled by the careful choice of weighting factors and optimisation defocus distance, in order to improve the performance of the system. If this control over the magnitude of the aberrations is lost, the VDDF stops performing in the desired direction and produces a system which is worse than the initial lens.

For effective DDF optimisation, it is necessary that the curves of MTF plotted against defocus in the chosen frequency for the initial system should peak in a relatively narrow defocus range, for all field angles and azimuths considered. If this condition is not satisfied, the aberrations in the defocused image planes will vary in size to such an extent that a proper optimisation will not be possible. A substantial decrease in the optimisation defocus may reduce the variation in aberration size, but will result,

practically, in a single image plane optimisation which may be of no use in extending the DOF. In cases of this kind, as described in Chapter 5, the most obvious change to the system is a defocus from the Gaussian image plane which may oscillate between successive iterations and thereby prevent any real improvement.

The VDOF program is therefore not suitable for systems which do not satisfy the condition stated above, and further optimisation by other methods is required first in order to steer the system into a region suitable fo the two image-plane technique. The system described in Chapter 5 is an example of a case for which the VDOF program does not work.

9.3 The Monochromatic Systems

The optimisation of monochromatic systems described in Chapter 5 and 6 adds to the understanding of the procedure because of the simplicity of the DOF determination. A comparison of the results of the V14 and VGOTF programs indicates quite clearly the advantage of optimisation with a "direct" criterion such as the MTF, this is emphasised by figures 5.b, 5.c and 5.d. A careful study of the DOF sequence, though not very effective in this case, shows that elementary techniques, such as those based on Seidel coefficients, are incapable of improving the DOF. This is clearly seen in figure 5.f in which S_3 or S_4 do not peak anywhere near the optimum value which is a defocus of .062 cm and the extremum point for the S_1 curve is merely due to the defocus of the "best image plane" as explained above.

The VGOTF-based techniques, which proved superior in this case, is less sensitive to change of weighting factors. This is demonstrated by comparing figure 5.e with 5.j, and suggests that the

optimum weighting factor is easier to find than the optimum defocus distance. Also sensitivity to the weighting factor is lower than that to the optimisation defocus which suggests that any result in the region of the optimum will be satisfactory.

The study of the Seidel coefficients shown on figure 5.k emphasises again that a simple technique based on third order aberrations can not improve the DOF of an optical system. Examination of higher order aberrations and the corresponding coefficients, for example the wavefront expansion coefficients, shows that these are also insufficient for improving the DOF; as an example the coefficients for the VGDTF series given in section 5.3, and shown in figure 9.a, verify this result.

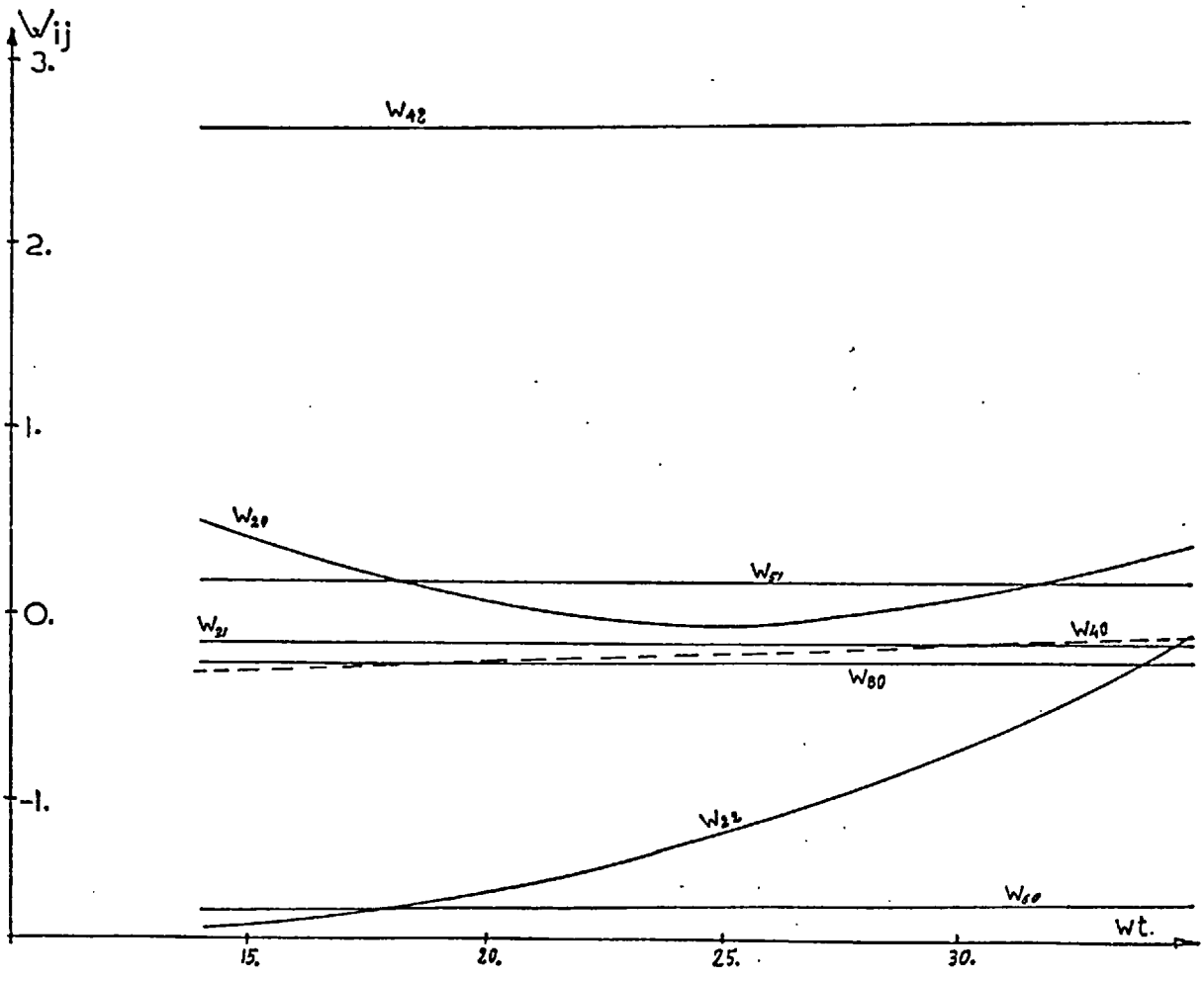

Fig 9.a, Wavefront aberration coefficients against the weighting factor in a VGOTF optimisation series described in Chapter 5.

The results for the reducing lens, described in Chapter 6, emphasise strongly the sensitivity of the VDOF method to the defocus distance, this is illustrated by figure 6.d. The VGOTF sequence is less sensitive to weighting factor choice and this is clearly shown in figure 6.i. The study of the Seidel coefficients throughout the VDOF sequence, as illustrated in figure 6.h does not show outstanding extremums around a defocus distance of .6 mm. The large scaling used in this diagram shows that the initial values are of similar magnitude. The most dramatic change is noticed in S_3 but this sequence may suggest on the other hand a connection between the optimum and the turning point in the Seidel curves. However, this is not practical since sequences throughout a large defocus range will be required, which is very expensive on computer usage.

The study of the optimisation of the reducing lens confirms some of the conclusions put forward in previous publications. As mentioned in Chapters 2 and 3, the aberration balance plays a critical role in the OOF characteristics of a system and this explains why a small change in the aberration coefficients may improve the focal depth, since it will effect the aberration ratio mentioned in Chapter 3. The introduction into the merit function of aberrations such as coma, which do not appear in symmetrical designs, enables an optimum aberration balance to be obtained. This again confirms the results predicted in Chapter 3, and explains why with the reducing lenses the OOF optimisation is more effective although more aberrations are present. Increasing the number of aberrations whilst maintaining the same balance may not limit the focal depth, but will make the system inadequate for most practical purposes and this is why the necessity to maintain "low" aberration values, imposed by the aberration product criterion (equ. 4-11), is not a restriction.

The complex combination of techniques, which could be combined into any optimisation procedure for extended focal depth, is demonstrated in figure 5.q. The results of this work show clearly that the first stage of the optimisation procedure is the crucial one and any following attempts to improve the results will be less effective.

Tests of the techniques used in the optimisation procedure are described in section 5.4 and the geometrical approximation to the real part of the OTF as used in this work has proved to be sufficiently accurate. In the Gaussian image plane, this geometrical MTF value differs from the diffraction MTF by 2%, as shown in figure 5.m for the copying lens. The same degree of accuracy is detected when considering the limiting field angles and azimuths. This is shown, clearly, by the variation in the DOF range for the geometrical and diffraction calculations illustrated in figure 5.n. The 1.5% disagreement is well within the numerical error of the complex algorithms involved in the computation. Tests on other systems optimised in this work showed similar results.

The limitation to three field angles only in the optimisation program was not found very restricting. Correct choice of field positions and maintenance of these values throughout the entire optimisation sequence has successful results. The DOF measured in these field angles deviates from the "real" value calculated with the results of 12 intermediate object positions, by only 2%. The accuracy in the case of the reducing lens was even higher. On the basis of the above investigation it may be concluded that the DOF value for the optimisation techniques used lies within 5% from its "real" value. This result seems satisfactory for most practical cases.

9.4 The Polychromatic Systems

The advantage of the VDOF technique is even more obvious in the case of polychromatic systems, the simplest of which are systems working in a finite number of spectral lines, such a those described in Chapters 7 and 8. The DOF determination is governed by the colour of the "object" considered as explained in Chapter 7. Even in the simplest case of "white object", when the system is optimised at three field angles (one of which is the axial case) and in two azimuths considering three wavelengths, the DOF determination is based on a complex formula which takes into account fifteen MTF against defocus curves. This degree of complexity requires a technique where the weighting factor choice is simplified. The VDOF proved less sensitive to variation in weighting factors for the various field angles and, therefore, is easily applied in this case. The only "variable" being the optimisation defocus.

In cases of large aberration spread, such as that experienced with the copying lens described in Chapter 7, extra precautions are required. The large variations are easy to detect since the MTF components, which are used by the merit function, are printed by the program together with the violations of the aberration product, and thus enable the designer to stop the program and change the weighting factors or optimisation defocus when appropriate. In this rather complex situation, the more rapidly the DOF varies with the optimisation defocus, the easier the optimum is found. This fact is demonstrated by comparing figure 8.d with 8.g.

The sensitivity of this optimisation technique to optimsation defocus variations in the region of the optimum system

may be reduced and may even result in curves with flat horizontal regions near the optimum, as seen in figure 8.g. This can be easily understood if one considers the optimum result as being a weighting sum of three curves, for the three colours considered. In this particular case the MTF in all the colours peak in the same region which results in a flat peak region.

The effect of this sequence on the Seidel coefficients is clearly seen from figure 8.k. The S_4 and S_5 reach their maximum near the optimum defocus, which gives a further emphasis to the idea that the optimum system is not essentially the one with the minimum aberrations. The idea about detecting the optimum from extremums in the derivatives of the Seidel coefficients curve (turning points) is proved again to be right, though unpractical as far as computer time is concerned. The peculiar shapes, near the turning points and the number of extremum points, is again explained by the fact that for each wavelength used there is a different extremum point.

9.5 Conclusions

The idea of optimisation in two image planes was found useful and applicable to optical optimisation for extended focal depth maintaining a target MTF value. The VDDF program, though slightly more expensive on time and storage as far as computers are concerned, is capable of improving the focal depth. During the work described earlier, the VDDF program improved the focal depth by up to 14.5% more than the VGDTF program. This technique is not very successful when the initial system is very poor in the sense that MTF against defocus curves, in various field angles

and azimuths at the frequency of interest, do not peak in a narrow focal range. In such cases further optimisation should be carried out before trying to extend the focal depth, alternatively a method which does not involve the VDOF program should be applied. In the cases of relatively good MTF curves which peak in the same image plane in the optimisation object positions and azimuth for a given frequency, large extension of the DOF is most unlikely. But, if the DOF image is cruical to the system and even small improvements are an advantage, the VDOF program will produce the largest focal depth as proved by the examples in Chapters 6 and 8.

Some of the techniques described above were also tried on a nine element lens, with a stop on the central element. This enabled the introduction of slight asymmetry in cases with magnification close to unity, by varying the radius of curvature on both surfaces of the central element, which in turn increased the number of aberrations present and made it easier to achieve an optimum balance resulting in extended focal depth. Generally, the results from the nine elements designs confirmed the results described in this work and similar improvements to DOF were experienced.

This work suggests a direct involvement of the optical designer in the modifications of his optimisation program to perform in accordance with his specific requirements and to emphasise his specialised criteria. By this method, a quick optimisation might be achieved, which does not involve a long empirical process to find the right weighting factors and other control quantities.

The final systems obtained in this work may be regarded as practical,being in the region of 60-80% of the ideal, aberration-

free case. In certain circumstances one may attempt to push the limits even further, some suggestions as to possible techniques follow:

The polychromatic copying lens has a larger DOF than the monochromatic version, which is due to a more sophisticated design involving additional, expensive, glass. Careful observation of the DOF determination curves for those lenses shows that the MTF values inside the useful focal depth range for the polychromatic system are lower than those of the monochromatic lens. It may be regarded as trivial that for an extended DOF the MTF should not peak high above the target MTF value, which is the reason why the VGDTF program is less suitable for this work. An attempt to decrease the MTF value in the middle of the DOF range might be included in the optimisation, it could be added, for example by including a third optimisation image plane. The merit function would then consist of the MTF components in two defocused image planes, as in the VDOF program, but also incorporate target values at a central image plane which would bring the MTF value closer to the limiting MTF specified. The nature of such target values must be studied since their choice is not obvious. The increased number of aberrations can be controlled in a similar way to the case of the additional optimisation wavelengths, discussed in Chapter 4.

One may increase the number of defocused planes involved by adding MTF values in several defocused planes to the merit function. This involves again, an increase in the storage required to run the program and also requires careful study and consideration of the weighting factors emphasising the various defocus MTF values according to their contribution to the DOF.

The programs used in the course of this work as well as the modifications suggested above, assume that the same weighting factors and target values are applied to all the MTF components in a certain field angle azimuth and wavelength. Variation of those values, within the field angle in question can emphasise various regions of the pupil and therefore steer the system to a new direction. It is likely that a correct choice of these weighting factor and target values may extend the DOF.

The defocused image planes throughout this work, were chosen symmetrically on both sides of the Gaussian image plane. The weighting factors and target values for both image planes are multiplied by a single scaling factor, as given by equations 4-9 and 4-10. Changing of this symmetry, about the Gaussian image plane, can complicate the program by requiring more input data and by including few more statements, but provides a better program for extending the DOF.

These suggestions point out possible modifications to the merit function, weighting factors and target values which can lead to new versions of the VDOF program providing new tools to the optical designers and to designers with special interest in extended depth of focus in particular.

APPENDIX A

PROGRAMS USED THROUGHOUT THIS WORK

In this appendix a short description of the programs which have been used in this work is given. This information is not intended to be comprehensive nor sufficient as a users manual, and it is given mainly to represent the general structure of the programs concerned. This structure is critical for some of the decisions taken throughout this work at various stages of the optimisation. It also may explain why some data were prepared and used in certain ways and the format of some of the output.

Some of the programs described below were not developed through this work and were obtained from the optical design group of Imperial College, examples of such programs are V14 and VGOTF. Other programs were slightly modified to accept different input data which enable the use of complex procedure files, they were also altered to be suitable for compilation on recent compilers with higher efficiency, examples for such programs are the diffraction and geometrical OTF programs. The rest of the programs were developed throughout this work, sometimes using routines or procedures previously available at the design group.

Though some of these programs are for specialised purposes it is thought that they could be combined into a useful general optical program library. The idea is that an optical designer should be familiar with his programs and capable of modifying any program in use to his specialised needs.

THE 'SLAMS' OPTIMISATION PROGRAMS

All SLAMS optimisation programs are based on the damped least squares method and are described in more detail throughout this work. In this work 'V14' (version 14) and 'VGOTF' (geometrical OTF version) were used and 'VDOF' (geometrical OTF optimisation in two image planes was developed. Chapter 4 details the main differences between the three versions. A very general flow diagram of the optimisation procedure is illustrated below.

Version 14 classifies the system into one of the following;

a) systems with object at infinity

b) systems with finite object with controlled throw or image magnification.

c) Afocal systems

d) symmetrical systems

e) telecentric systems

f) systems with linked parameters

The controlled parameters may be curvatures, separations and glass types. Rays can be specified by normal or relative data, chromatic aberrations may be calculated using the Conrady formula or as transverse ray aberrations in each wavelength. Surfaces may be spherical or aspherical but rotational symmetry of the system about the optical axis is assumed.

Version 14 allows for up to 50 surfaces with up to 75 variable parameters, a maximum of 50 rays can be used which may result in up to 150 aberrations, only 100 of which may be controlled. The boundary condition controls include the effective focal length, magnification

or throw, back focal distance, overall length, lens thickness, total thickness of glass elements, maximum diameter of beam at any given surfaces, height of final principal ray at the stop, asphericity, glass violations, axial thickness violations and edge thickness violations for separate elements.

These limits are increased in the VGOTF and VOOF programs and are described to a certain extent in Chapter 4. Each of the optimisation programs will produce on request a file called 'PUNCH' which contains the data of the final system produced by the last iteration.

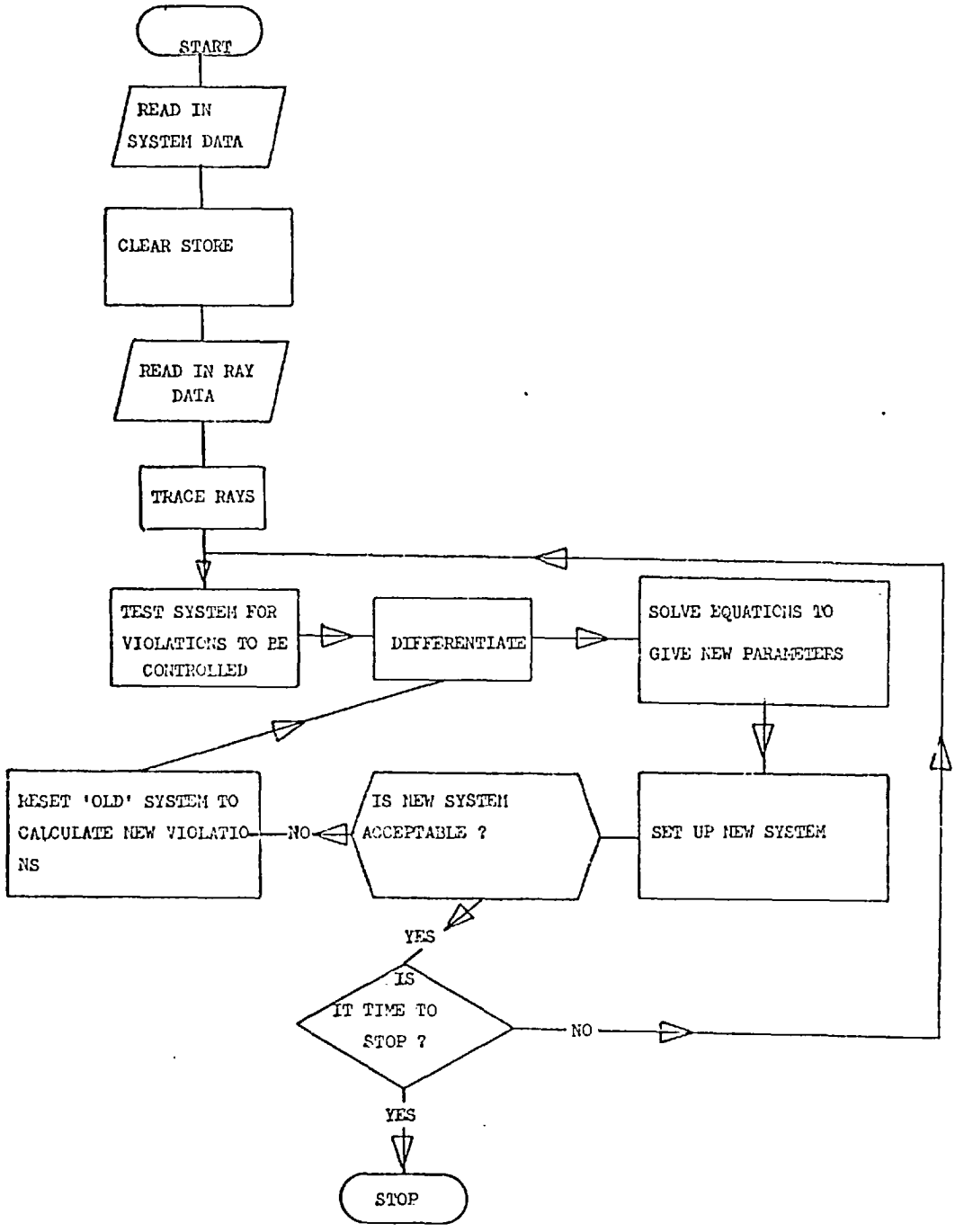
START
READ IN SYSTEM DATA
CLEAR STORE
READ IN RAY DATA
TRACE RAYS
TEST SYSTEM FOR VIOLATIONS TO BE CONTROLLED
DIFFERENTIATE
SOLVE EQUATIONS TO GIVE NEW PARAMETERS
RESET 'OLD' SYSTEM TO CALCULATE NEW VIOLATIONS
NO
IS NEW SYSTEM ACCEPTABLE ?
SET UP NEW SYSTEM
YES
IS IT TIME TO STOP ?
NO
YES
STOP

GEOMETRICAL OTF PROGRAM

This program uses as input data the file PUNCH, which is produced on request by the optimisation program, and generates a mesh of ray co-ordinates through which rays are traced. The vignetting of the system can be estimated by the number of rays which fail to pass through the system. Transversed ray aberrations are used to calculate the geometrical MTF of the system at each field angle. In the case of polychromatic systems the "mean wavelength OTF" is calculated by a weighted sum of the monochromatic OTF values, where the user specifies the weight for each wavelength. The maximum frequency required and the defocusing distance steps are also included in the input file. resulting in the MTF being calculated for the sagittal and tangential azimuths for 15 frequencies at equal intervals, from 0. to the specified maximum. These MTF values are calculated in 5 different focal planes, one at the Gaussian image plane and two defocused image planes on either side. Oue to the specific interest in through focus MTF in this work, the number of defocused planes was increased to 11,5 defocused planes on each side of the focal plane. The following flow diagram illustrates the structure of the program;

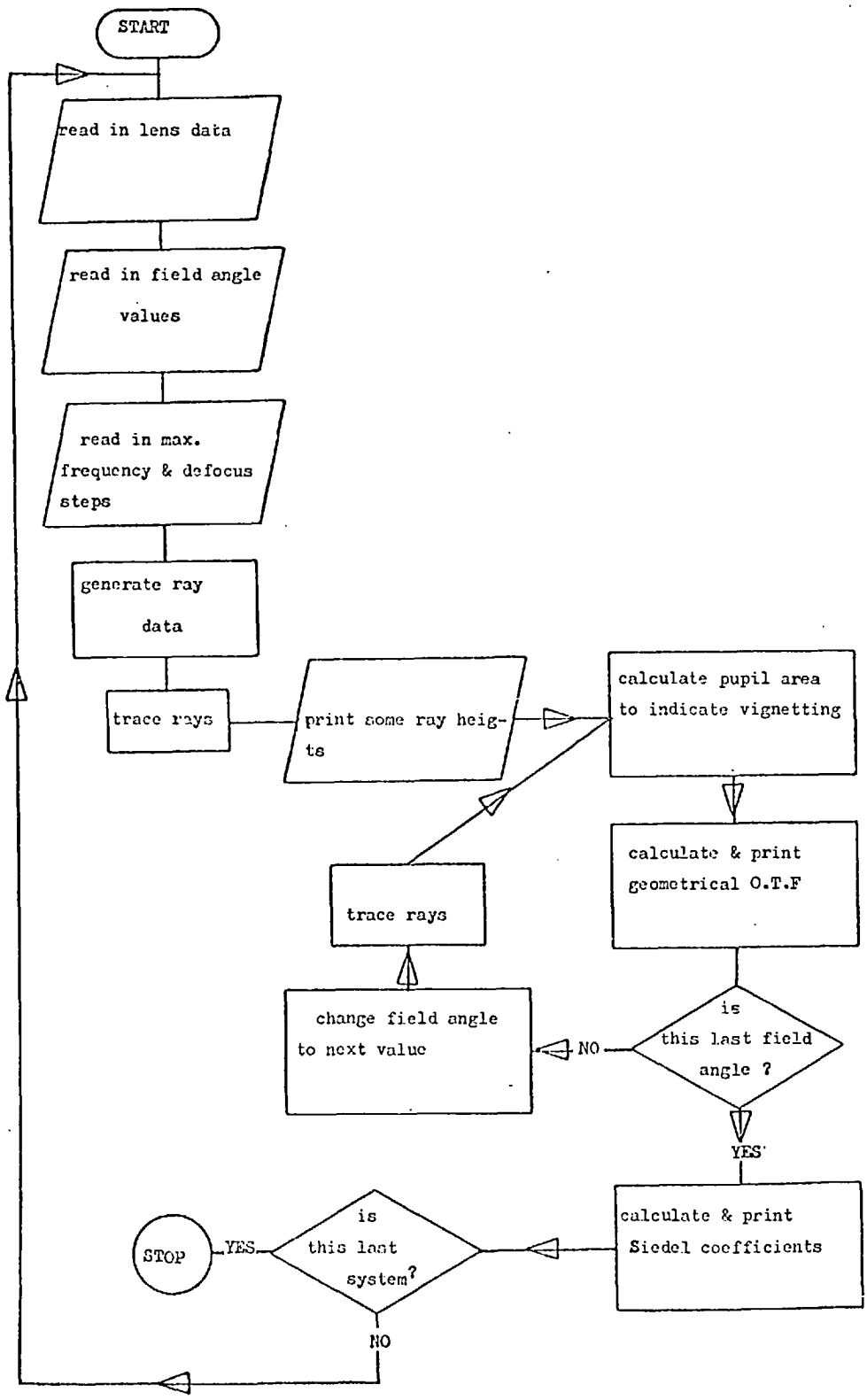
START
read in lens data
read in field angle values
read in max. frequency & defocus steps
generate ray data
trace rays
print some ray heig-ts
calculate pupil area to indicate vignetting
calculate & print geometrical O.T.F
trace rays
change field angle to next value
NO
is this last field angle ?
YES
calculate & print Siedel coefficients
is this last system?
YES
STOP
NO

DIFFRACTION OTF PROGRAM

The diffraction OTF program, written by M.J. Kidger, was also modified to read the file Punch as input. The program does a polynomial fitting to the wavefront function and calculates the OTF by shearing the pupil function. In the case of polychromatic system the OTF is a weighted sum of monochromatic OTF values. For highest efficiency without losing accuracy the integration part is repeated with an increased number of Lagrange coefficients until two successive calculations agree to within a given "error limit". For reference, this difference is printed as "error" in the output. The wavefront aberration coefficients which were calculated in the fitting routine, are printed in the form of Wjk values. The structure of the program is illustrated below.

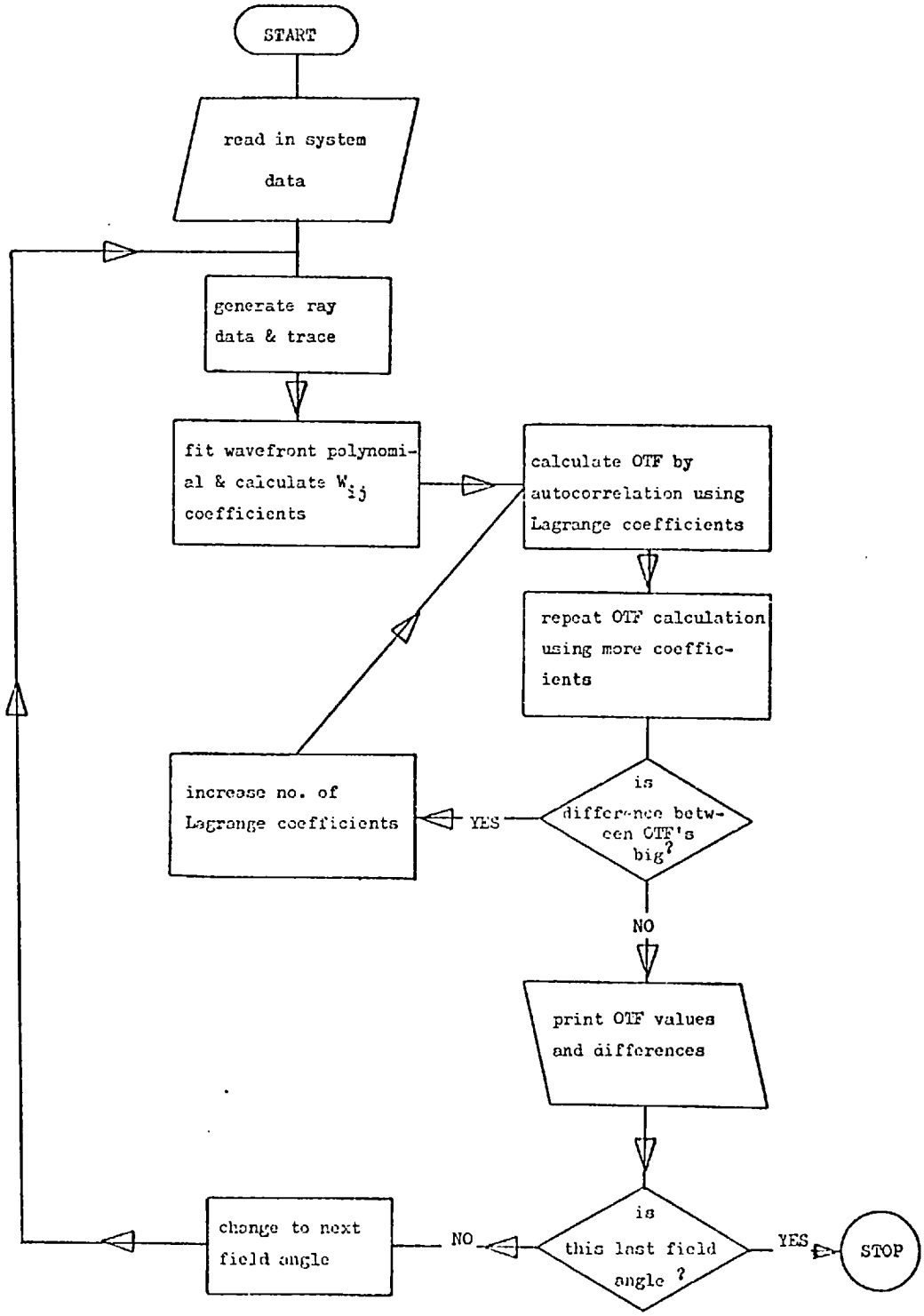
START
read in system data
generate ray data & trace
fit wavefront polynomial & calculate W_{ij} coefficients
calculate OTF by autocorrelation using Lagrange coefficients
repeat OTF calculation using more coefficients
is difference between OTF's big?
YES
increase no. of Lagrange coefficients
NO
print OTF values and differences
is this last field angle ?
YES
STOP
NO
change to next field angle

GRAPHICAL PACKAGE (PARTS A-D)

This is a graphical package for the evaluation and display of the optical system qualities, which has been found useful at various stages of the designing process. This package uses the "Imperial College Computer Centre" graphical library to produce 35 mm microfilm plots and is compatible for use with the kingmatic table plotter. Therefore use of these programs is restricted to sites which have ICCC libraries, if they are to be transferred to other sites a compatible (or translation) graphical routines must be added. Part A will draw the lens and scale it in terms of focal length and then will produce sets of MTF vs. frequency curves at certain defocus planes or MTF vs. defocus curves at fixed frequency, as specified by an input file SENSE. The system data is read from the file PUNCH produced by the geometrical OTF program. The MTF values are written in the form of matrixes on to an output file RESULT which can be used by PART B to produce 3-D bodies of MTF as a function of frequency and defocus. Those solids (e.g. fig 5.b) can be used for studies of the nature of the MTF, but for numerical evulation the appropriate cross section produced by PART A, should be used.

File PUNCH can be used by PART C to produce cross sections of the aberration function in the various field angles, another input file ABERTYP determines whether transverse ray aberrations (e.g fig 7h) or wavefront aberrations (e.g. - fig 7i) should be produced. PART D will use PUNCH as input to produce a lens drawing (fig 7a) with the system data in cases of up to 40 surfaces.

The DOF of the system is determined graphically and analytically (e.g. fig 7.c) where the frequency of interest, the units and the MTF limit are on data statement, rather than on input file.
The way in which those programs work oan be better understood from the following flow diagrams which give the general structure of the programs;

PART A

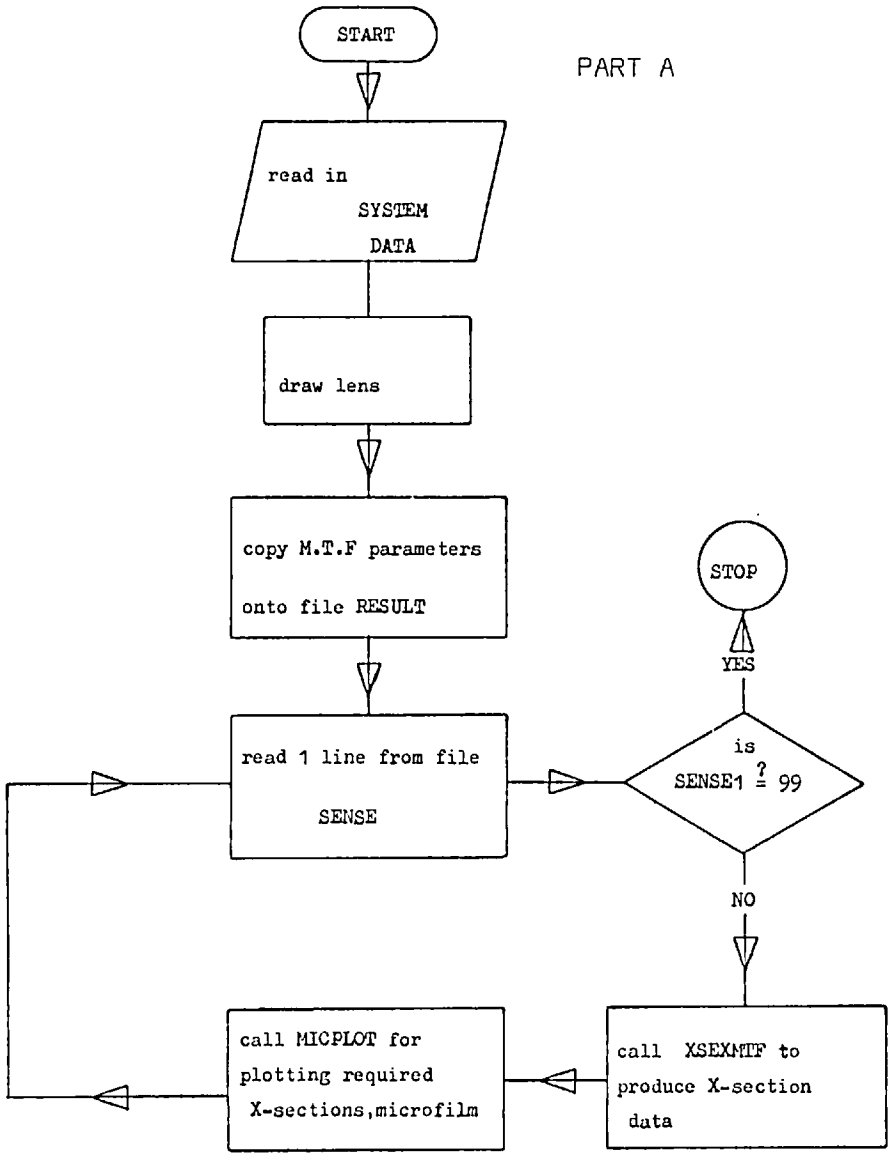
START
read in SYSTEM DATA
draw lens
copy M.T.F parameters onto file RESULT
read 1 line from file SENSE
is SENSE1 = ? 99
YES
STOP
NO
call XSEXMTF to produce X-section data
call MICPLOT for plotting required X-sections,microfilm

PART B

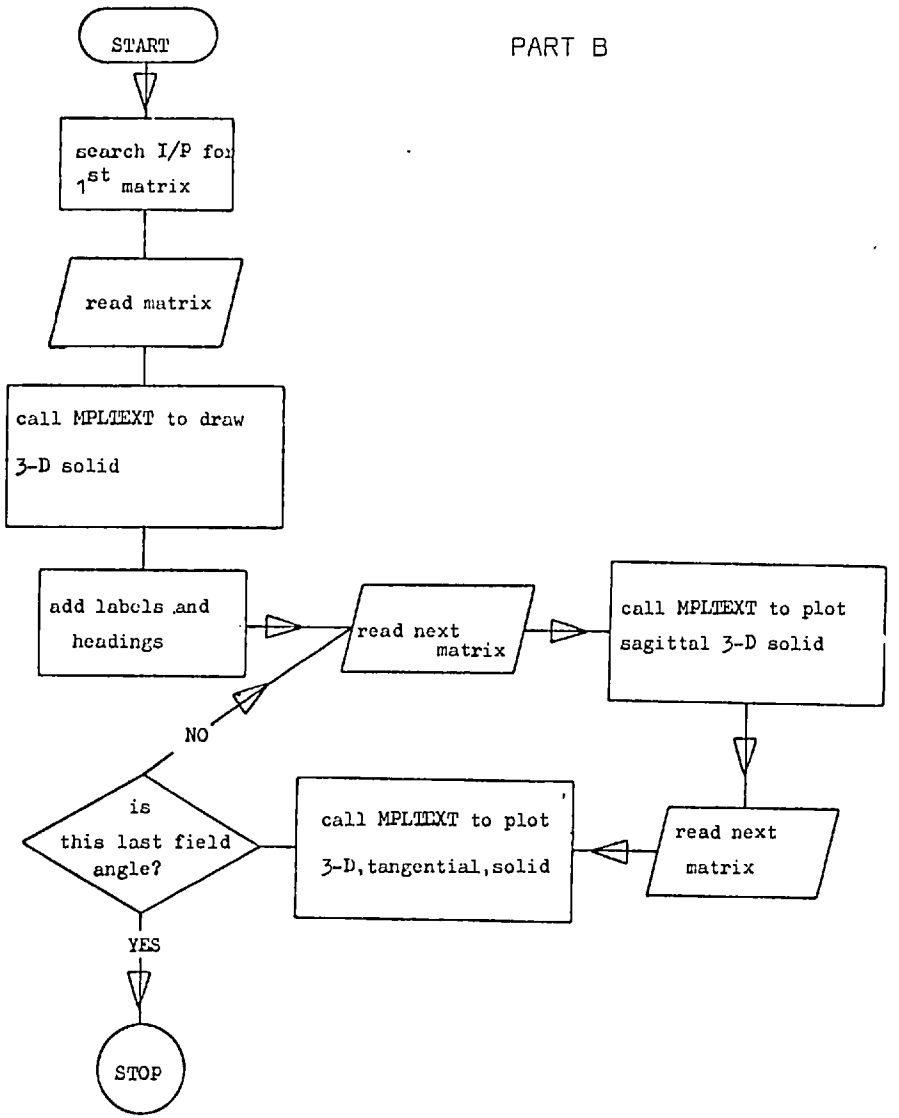
START
search I/P for 1st matrix
read matrix
call MPLTEXT to draw 3-D solid
add labels and headings
read next matrix
call MPLTEXT to plot sagittal 3-D solid
NO
is this last field angle?
call MPLTEXT to plot 3-D,tangential,solid
read next matrix
YES
STOP

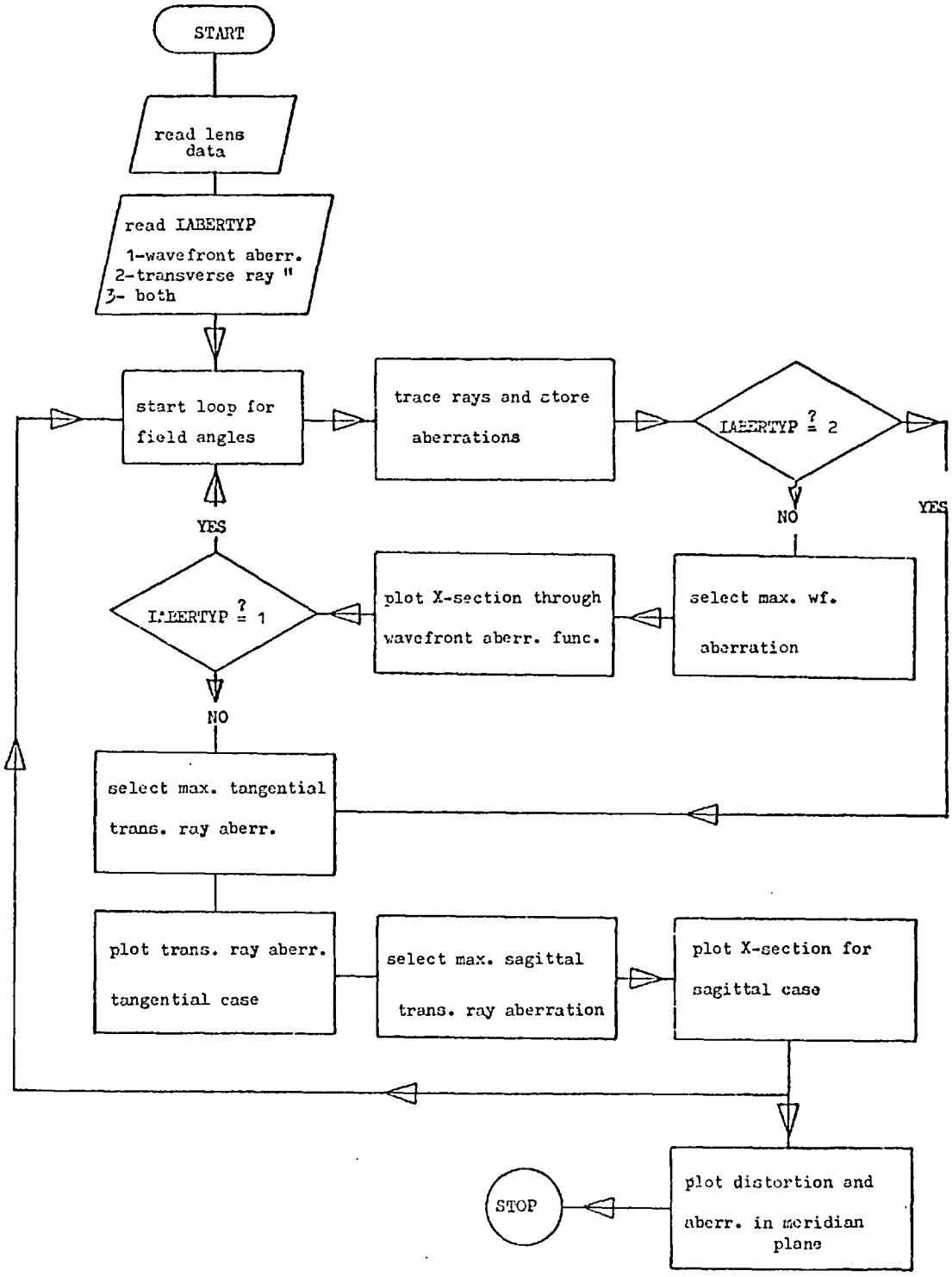
START
read lens data
read IABERTYP
1-wavefront aberr.
2-transverse ray "
3- both
start loop for field angles
trace rays and store aberrations
IABERTYP ? = 2
NO
YES
YES
IABERTYP ? = 1
plot X-section through wavefront aberr. func.
select max. wf. aberration
NO
select max. tangential trans. ray aberr.
plot trans. ray aberr. tangential case
select max. sagittal trans. ray aberration
plot X-section for sagittal case
plot distortion and aberr. in meridian plane
STOP

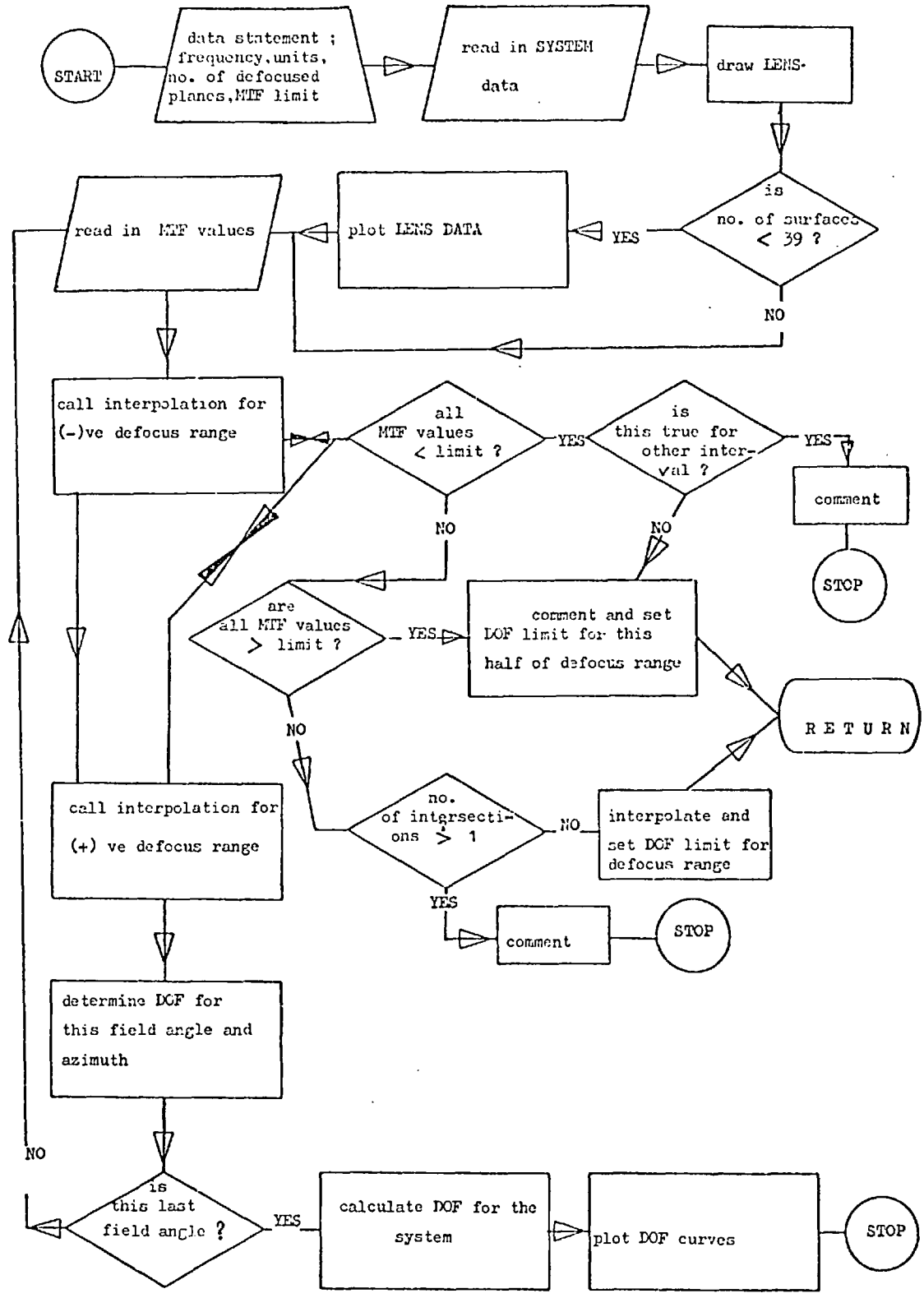
START
data statement ; frequency, units, no. of defocused planes, MTF limit
read in SYSTEM data
draw LENS-
is no. of surfaces < 39 ?
YES
NO
plot LENS DATA
read in MTF values
call interpolation for (-)ve defocus range
all MTF values < limit ?
YES
NO
is this true for other interval ?
YES
NO
comment
STOP
are all MTF values > limit ?
YES
NO
comment and set DOF limit for this half of defocus range
RETURN
no. of intersections > 1
NO
YES
interpolate and set DOF limit for defocus range
comment
STOP
call interpolation for (+) ve defocus range
determine DOF for this field angle and azimuth
is this last field angle ?
NO
YES
calculate DOF for the system
plot DOF curves
STOP

It follows that it is possible to use any combination of PARTS A,C or D with the O/P of the geometrical OTF program. If PART B is to be used, PART A must be used earlier for the preparation of I/P data.

APPENDIX B

NINE ELEMENT LENSES

This appendix illustrates the basic designs for a nine element f/5.6 copying lens and a f/2.8 reducing lens optimised by V14 and VGOTF in the course of this work. The specifications for these lenses were similar to those of the six element lenses described in this work.

A DOF optimisation carried out on those designs confirmed the results detailed in Chapters 5, 6, 7 and 8.

NINE ELEMENTS COPYING LENS (600 NM.)

.1 FOCAL LENGTH

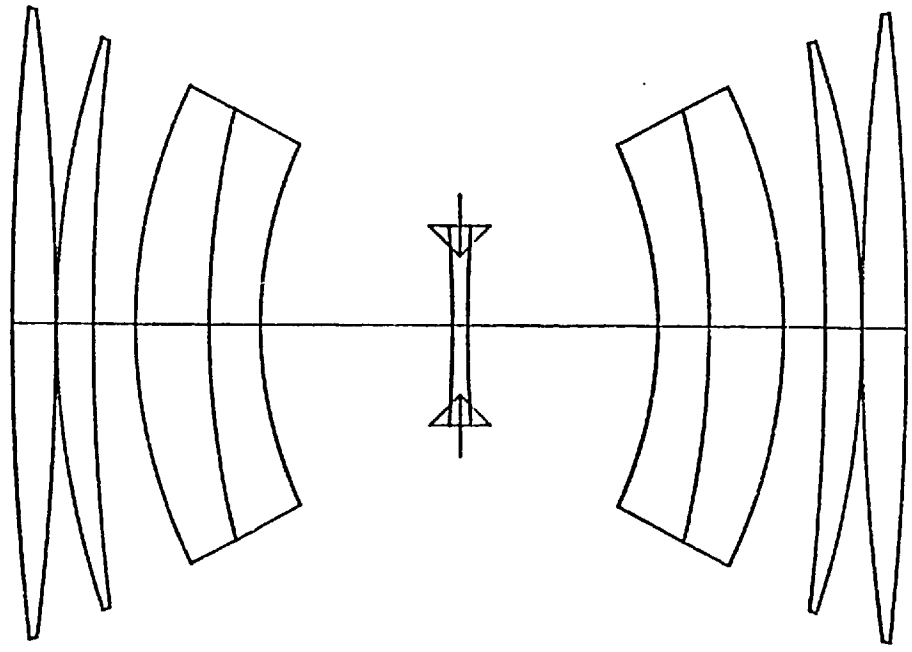

CURVE	SEPN	INDX/DIS
0.020430	0.000000	1.000000
-0.02396	0.706450	1.486560
0.066660	0.005000	1.000000
0.024800	0.593370	1.486560
0.112360	0.676810	1.000000
0.067250	1.202480	1.691000
0.141110	0.829170	1.581440
-0.03984	3.097750	1.000000
0.000010	0.125000	1.581440
0.039840	0.125000	1.581440
-0.14111	3.097750	1.000000
-0.06725	0.829170	1.581440
-0.11236	1.202480	1.691000
-0.02480	0.676810	1.000000
-0.06666	0.593370	1.486560
0.023960	0.005000	1.000000
-0.02043	0.706450	1.486560
0.000010	-0.079370	1.000000

NINE ELEMENTS REDUCING LENS (600 NM.)

.1 FOCAL LENGTH

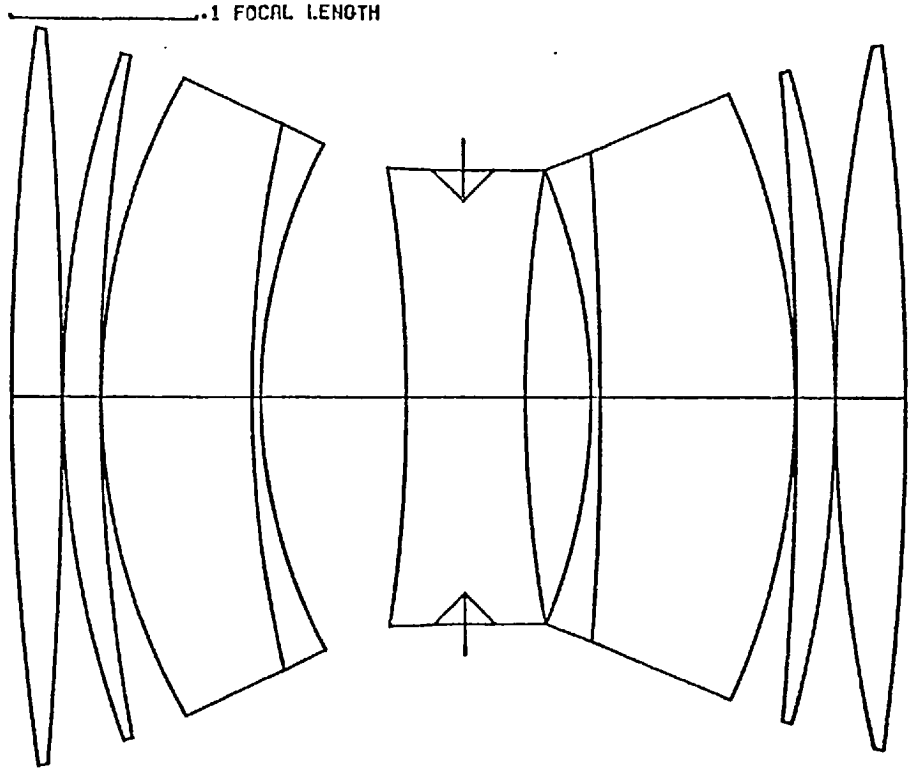

CURVE	SEPN	INDX/DIS
0.027480	0.000000	1.000000
-0.01673	0.672200	1.487940
0.072640	0.010000	1.000000
0.039010	0.507130	1.487940
0.113610	0.010000	1.000000
0.061110	2.040990	1.694000
0.137970	0.125000	1.549820
-0.04838	1.943160	1.000000
0.000010	0.768060	1.699180
0.055750	0.831330	1.699180
-0.12822	0.898240	1.000000
-0.02217	0.125000	1.549820
-0.10041	2.602180	1.694000
-0.02009	0.010000	1.000000
-0.05920	0.510850	1.487940
0.043120	0.010000	1.000000
-0.02684	0.918320	1.487940
0.000010	-0.071160	1.000000

REFERENCES.

BLACK G. (1975)	PROC.ROY.SOC.	B	68 729
BLACK G & LINFOOT E.H. (1956)	PROC.ROY.SOC.	A	239 522
BROMILOW N.S. (1958)	PROC.PHY.SOC.		71 231
DE M. (1955)	PROC.ROY.SOC.	A	233 91
DE M. & NATH B.K. (1958)	OPTIK		15 732
DUFFIEUX P.M. (1946)	L'INTEGRALE DE FOURIER ET SES APPLICATIONS A' L'OPTIQUE BESCANGON PRIVATELY PRINTED		
FEDER D.P. (1957)	J.O.S.A		47 902
FEDER D.P. (1962)	J.O.S.A		52 178
FINKLER R. (1975)	THESIS IMPERIAL COLLEGE, UNIVERSITY OF LONDON		
GIRRARD A. (1958)	REVUE D'OPTIQUE		37,225,397
GLATZEL E. (1961)	OPTIK		18 577
GLATZEL E. & WILSON R. (1968)	APP. OPTICS		7 265
GOODBODY A.M. (1958)	PROC.PHY.SOC.		71 231
GOODBODY A.M. (1959)	PROC.PHY.SOC.		72 411
GOSTICK R.W. (1974)	THESIS, IMPERIAL COLLEGE, UNIVERSITY OF LONDON		
HOPKINS H.H. (1950)	WAVE THEORY OF ABERRATIONS, OXFORD, CLARENDON PRESS		
HOPKINS H.H. (1953)	PROC.ROY.SOC.	A	217 408
HOPKINS H.H. (1955)	PROC.ROY.SOC.	A	231 91
HOPKINS H.H. & McCARTHY (1955)	J.O.S.A		45 363
HOPKINS H.H. (1957)	IBID		70 449
HOPKINS R.E. (1961)	PRO.CONF. OPTICAL INSTRUMENTS AND TECHNIQUES, LONDON		
KAZUO SAYANAGI (1961)	PRO.CONF. OPTICAL INSTRUMENTS AND TECHNIQUES, LONDON		

KIDGER M.J. (1971)	THESIS, IMPERIAL COLLEGE, UNIVERSITY OF LONDON	
KING W.B. (1968)	J.O.S.A.	58 655
LEVENBERG K. (1944)	QUART. APP. MATH	2 1944
McDONALD D.E. (1951)	SYMPOSION "OPTICAL IMAGE EVALUATION" U.S. BUREAU OF STANDAROS CIRCULAR (1954)	526 62
ROSEN S. & ELDERT (1954)	J.O.S.A.	44 250
SPENSER G. (1963)	THESIS, UNIVERSITY OF ROCHESTER	
WYNNE C.G. (1959)	PROC.ROY.SOC.	73 777
WYNNE C.G. & WORMELL P.M.J.H. (1963)	APP. OPTICS	2 1233
WYNNE C.G. & NUNN M. (1959)	PROC.PHY.SOC.	74 316